FEDERAL UNIVERSITY OF ITAJUBA
MECHANICAL ENGINEERING INSTITUTE

MECHANICAL CHARACTERIZATION OF COMPOSITES BASED ON A NOVEL VACUUM-INFUSED THERMOPLASTIC MATRIX

LORENA CRISTINA MIRANDA BARBOSA

Itajuba – MG
2020

FEDERAL UNIVERSITY OF ITAJUBA
MECHANICAL ENGINEERING INSTITUTE

MECHANICAL CHARACTERIZATION OF COMPOSITES BASED ON A NOVEL VACUUM-INFUSED THERMOPLASTIC MATRIX

Lorena Cristina Miranda Barbosa

A thesis presented to the Postgraduate Program of Mechanical Engineering, from Mechanical Engineering Institute of the Federal University of Itajuba, as a requirement to obtain the title of Ph.D. in Mechanical Engineering.

Main advisor: Dr.Antonio Carlos Ancelotti Junior

Itajuba – MG
2020

This work is dedicated to my friends and especially to my family because there are no words that describe what they do for me.

ACKNOWLEDGMENTS

I thank God for making possible one more of my plans and dreams. To my parents, Sônia and Celso, who have always supported me and allowed me to follow the paths that have brought me here. Without your support, it would be impossible to get to where I am. Thank you for every word of encouragement, for all investissement, for every concern, for patience, for everything! I love you unconditionally.

This thesis work which was carried out during four years does not only concern my effort but that of an entire team.

I am proud to have worked with Antonio Ancelotti, my thesis advisor who shared interesting ideas and his scientific knowledge with me that developed me during that period. I would also like to thank all the collaborating professors at UNIFEI for the partnership and for all the time spent in the development of my work.

I would also like to thank the friends I made at NTC for the funny moments we spent together in the lab.

I would like to especially thank the trio Olivia, Paloma, and Barbara, my great friends, who showed me the strength of women's empowerment in Brazilian research. I am enormously proud of just the way you are and looking forward to following you in everything to come.

It is also worthwhile to thank the friends I made during my stay in Itajuba and especially Gui, Nathalia, and Vini who proved to be true friends even in difficult times. Thanks for the friendship.

“ Plus je lis, plus j'obtiens, plus je suis certain de ne rien savoir.”

Voltaire

ABSTRACT

This study is focused on the assessment of the mechanical performance and the failure mechanisms of composites based on a liquid thermoplastic resin under several loading conditions compared to epoxy-based composites. Composite laminates reinforced by carbon fibers were manufactured by VARTM (Vacuum-assisted resin transfer molding). The composites were subjected to mode II loading conditions in order to verify its damage tolerance. In this case, the thermoplastic composites presented 40 % more resistance to interlaminar fracture in comparison to epoxy composites. These materials obtained superior performance in crack propagation resistance because it tends to absorb the energy associated with crack propagation in the form of plastic deformation in comparison to epoxy composites. Tensile strength and in-plane shear tests were also performed to evaluate both materials response in non-conditioned and conditioned samples. The thermoplastic composites presented 30 % more tensile resistance in comparison to epoxy composites. For conditioned specimens, this difference was 14%. These results were related to plasticization which tends to favor the polymer softening providing a greater matrix plastic deformation, promoting a ductile fracture of the composite. On the other hand, the in-plane shear properties were 30 % higher for the thermosetting laminates for both conditions. In this case, moisture may have favored the formation of surface cracks and weakened the fiber/matrix interfacial adhesion. Additional analysis based on the design of experiments has shown that the Elium® 150 resin significantly affects all responses and presented in fact a better behavior in comparison to epoxy resin. While the conditioning effects have featured a statistically noticeable contribution to the tensile strength, the presence of the moisture did not provide a significant enhancement to the in-plane shear strength. The analysis based on accelerated test methodology of Carbon Fiber/Elium® 150 composites shows that the high frequencies increase the glass transition (Tg) to higher values probably favored by polymer chains movement. The artificial neural network evidenced an excellent agreement between the trained and experimental values. The long-term life prediction using master curves confirms that this new material can be considered to acoustic or vibrational damping purposes, considering its use in temperatures below Tg.

Keywords: Liquid thermoplastic resin, Fracture toughness in Mode II, Fractography, Conditioning effects, Artificial neural networks

RESUMO

Este estudo está focado na avaliação do desempenho mecânico e dos mecanismos de falha de compósitos à base de uma resina termoplástica líquida sob várias condições de carregamento em comparação com compósitos à base de epóxi. Os laminados compostos reforçados por fibras de carbono foram fabricados pela VARTM (Moldagem por transferência de resina assistida a vácuo). Os compósitos foram submetidos às condições de carregamento do modo II, a fim de verificar sua tolerância a danos. Nesse caso, os compósitos termoplásticos apresentaram 40% mais resistência à fratura interlaminar em comparação aos compósitos epóxi. Esses materiais obtiveram desempenho superior na resistência à propagação de trincas, pois tendem a absorver a energia associada à propagação de trincas na forma de deformação plástica em comparação aos compósitos epóxi. Também foram realizados testes de resistência à tração e cisalhamento no plano para avaliar a resposta de ambos os materiais em amostras não condicionadas e condicionadas. Os compósitos termoplásticos apresentaram 30% mais resistência à tração em comparação aos compósitos epóxi. Para amostras condicionadas, essa diferença foi de 14%. Esses resultados foram relacionados à plastificação, que tende a favorecer o amolecimento do polímero, proporcionando maior deformação plástica da matriz, promovendo uma fratura dúctil do compósito. Por outro lado, as propriedades de cisalhamento no plano foram 30% maiores para os laminados termoendurecíveis em ambas as condições. Nesse caso, a umidade pode ter favorecido a formação de rachaduras na superfície e enfraquecido a adesão interfacial fibra / matriz. Análises adicionais baseadas no projeto de experimentos mostraram que a resina Elium® 150 afeta significativamente todas as respostas e apresentou, de fato, um melhor comportamento em comparação à resina epóxi. Embora os efeitos do condicionamento tenham apresentado uma contribuição estatisticamente perceptível à resistência à tração, a presença da umidade não proporcionou um aprimoramento significativo da resistência ao cisalhamento no plano. A análise baseada na metodologia de teste acelerado de compósitos Carbon Fiber / Elium® 150 mostra que as altas frequências aumentam a transição vítrea (Tg) para valores mais altos, provavelmente favorecidos pelo movimento das cadeias poliméricas. A rede neural artificial evidenciou uma excelente concordância entre os valores treinados e experimentais. A previsão de vida útil em longo prazo usando curvas mestres confirma que este novo material pode ser considerado para fins de amortecimento acústico ou vibracional, considerando seu uso em temperaturas abaixo de Tg.

Palavras-chave: Resina termoplástica liquida, Resistência ao cisalhamento interlaminar em Modo II, Fractografia, Efeitos do condicionamento, Redes neurais artificiais

TABLE OF CONTENTS

LIST OF FIGURES

LIST OF TABLES

LIST OF ABBREVIATIONS

ANOVA	Analysis of variance
ANN	Artificial neural networks
ASTM	American Society for Testing and Materials
AVE	Advanced Video Extensometer
CF	Carbon fibers
DAFFs	Directly attributable fiber failures
DIC	Digital Image Correlation
DMA	Dynamic-mechanical analysis
DOE	Design of Experiments
FFD	Full Factorial Designs
GF	Glass Fibers
MMA	Methyl methacrylate
NPC	Non-precracked
PA-12	Polyamide-12
PA-6	Polyamide-6
PBT	Polybutylene terephthalate
PC	Precracked
PEEK	Polyether ether ketone
PMMA	Polymethyl methacrylate
PTFE	Teflon
SEM	Scanning Electron Microscope
VARTM	Vacuum-assisted resin transfer molding
WLF	Williams–Landel–Ferry

LIST OF SYMBOLS

E’	Storage modulus
E”	Loss modulus
G_{IIC}	Mode II interlaminar fracture toughness
Tanδ	Loss factor
T_f	Reference temperature
Tg	Glass Transition Temperature
V_f	Free volume
Vr	Resin volume
Vv	Voids contents
Vf	Fiber volume
Wi	Mass obtained before exposure
Wb	Mass after exposure
G	Shear modulus
τ	Shear Strength
γ	Shear strain

CHAPTER 1 : INTRODUCTION

The insertion of polymeric composite materials in various engineering segments combined with the technological evolution of its raw materials and processing techniques has enabled new material alternatives in reducing structural weight and consequently the costs of the process. In general, this class of materials has gained strength thanks to applied engineering in the development of components used in the aeronautical and aerospace industries. Thus allowing, a reduction in weight combined with high mechanical properties and rigidity when compared to other conventionally used materials. Besides that, composite materials present superior life in fatigue which allows the reduction in the maintenance frequency and structure lifespan. They also allow the manufacturing of complex shapes, reducing part counts and consequently saving weight by diminishing the number of fasteners [1-5].

The composite materials consist in a multiple fabric layers stacked and embedded in a typically brittle matrix. A 2D arrangement of reinforcement fibers makes each layer free from the adjacent ply and consequently, causes the connection between the layers given by the matrix only. The interlaminar region (between fabric plies and matrix) is, therefore, subjected to damages due to the lower fracture toughness of the matrix. Delamination is one of the significant damages in conventional composite laminates which can considerably reduce the load-bearing capacity of a structure and may be induced by out-of-plane loading (static and impact) and typically combined with stress concentrations (related with structure geometry) or discontinuities such as manufacturing defects, ply drops or free edges [6,7].

Although the sector of structural polymeric composites is dominated by the use of thermosetting matrices, with emphasis on epoxy and phenolic resins, engineering

thermoplastics have been used progressively and presented as an alternative for structural applications. Thermosetting polymers form dense three-dimensional, cross-linked networks upon polymerization and are not thermo-softening materials. As a result, they cannot be reshaped, joined and readily recycled like their thermoplastic counterparts. Consequently, from an ecological point of view, thermoplastic matrices are more desirable for applications [2, 8-10]. Once rather than being cross-linked, thermoplastic composites consist of entangled chains. It is this architecture that allows thermoplastics to be thermally remolded or dissolved and these techniques are not available to thermosets. [11,12].

While thermoplastics are able to flow with sufficient heat, these polymers are usually too viscous to effectively infuse using vacuum-assisted resin transfer molding (VARTM), which is the technique used to manufacture several structural components[13]. They typically require high-cost processing techniques where elevated temperatures and pressures are used to ensure infiltration viscosities and optimal consolidation. Thermosetting matrices possess inherently low viscosities, making them ideal for low-cost processing [14].

In the VARTM process, a flexible vacuum bag is placed over fibers, breather cloth, and flow media. Vacuum and inlet ports are strategically positioned to fill the part during infusion. Generally, the vacuum is pulled through port(s) at one side of the part and a reactive monomeric liquid is pulled through the inlet port(s). Once filled, the part cures into a solid composite material [15]. Figure 1.1 shows a test panel in the middle of the VARTM infusion and a 13m wind turbine blade being prepared for VARTM infusion. Since resin must be pulled through a thick mat of fibers, resin viscosity control is of critical importance for this process to be carried out effectively.

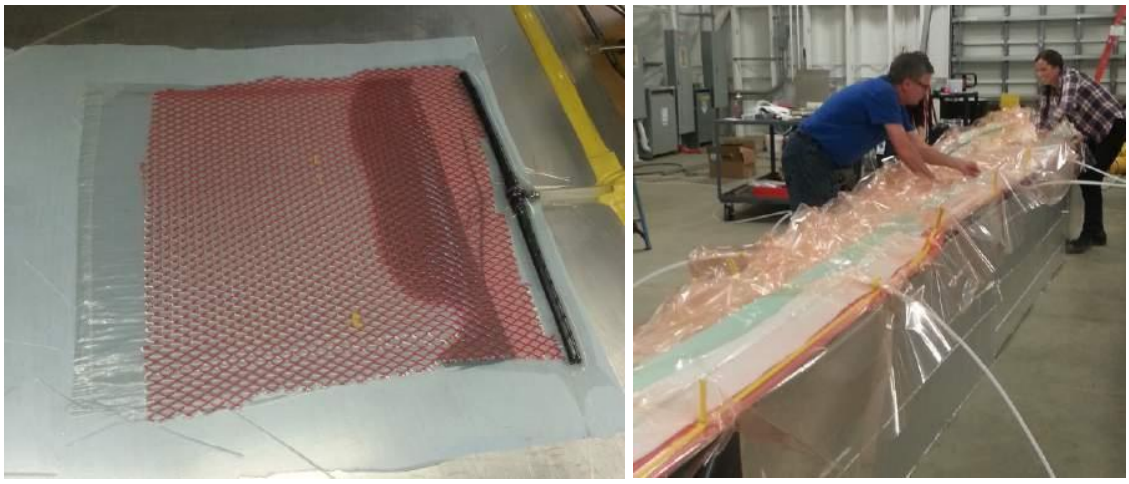

Fig 1.1 - VARTM of a composite test panel (left) and setup of VARTM for infusion of a 13 m prototypical thermoplastic wind turbine blade [15]

Previous researches have focused on infusion and in-situ polymerization of engineering thermoplastic polymers such as polyamide-12 (PA-12) [16], polyamide-6 (PA-6 [17,18]) and polybutylene terephthalate using cyclic oligomer precursors (PBT) [19,20]. In each of these cases, however, elevated mold temperatures are required in order to polymerize the matrix system. Temperatures above 150 °C in the case of the PA-6 and PA-12 systems, and as high as 180 °C for the PBT are required. This can add a significant expense in terms of high-temperature mold tooling, especially for large structures such as wind turbine blades [21-24].

In this context, a notable advancement in this area has been the recent development of novel reactive thermoplastic resins such as Arkema's acrylic-based Elium®. Combining the requirements of the composite materials industry with the proposal to reduce manufacturing costs, the Elim resin's family is based on based on MMA (methyl methacrylate) monomers and acrylic copolymers, activated by peroxide. These resins are low-viscosity liquids (100–200 mPa.s) at room temperature and are resins developed and suitable for infusion processes such as VARTM and which have mechanical properties comparable to those of composites with epoxy matrix [25].

Unlike unsaturated polyester, Elium resins do not contain styrene. In this type of thermoplastic material, once the polymerization process is completed, the final component obtained can be easily thermoformed and potentially recycled. Currently, this material has been applied in the automotive, sports, wind energy and marine industries, among others. In addition, it also has a good structural response with natural fiber reinforcements, showing itself as an innovative solution in the production of more sustainable materials [25,26].

Many authors have been studied the properties of this acrylic resin and its composites. These works have effectively established the knowledge base on the material's mechanical characteristics, with extensive efforts in characterizing tensile, compressive, shear, impact, and fracture toughness [27-41]. Much applied research has been conducted on understanding the material's fatigue [34, 42, 43]; moisture diffusivity and marine aging [44-48]; interfacial adhesion [49,50]; damage evolution and fracture behavior [34,47,51-54]; and even the effects of processing on final properties [36,55]. Moreover, the thermomechanical properties of this acrylic family and their composites have also been studied by a number of researchers [40,51,56,57].

Several authors have published works on the comparative behavior of the composites based on acrylic liquid resin with respect to comparable thermoset composites. An overview of existing literature by characterization and reinforcement type is presented in Table 1.1.

Chilali *et al.*[35] reported comparable tensile and shear performance in both acrylic-based and epoxy-based composites. They also observed superior damage resistance in flax-acrylic composites with respect to a comparable flax-epoxy material, no differences in the extent of damage and residual performance were reported between their glass-reinforced counterparts. Their findings on the tensile performance of the glass-reinforced composites are in agreement with published work by Lorriot *et al.* [58].

However, Baley *et al*[27] reported significantly lower (−40%) tensile strength in glass-reinforced acrylic than glass-reinforced epoxy. Kinvi-Dossou *et al*. [39] reported superior impact performance in glass-acrylic composites than their thermoset counterpart. In the meantime, Obande *et al*.[40] found that despite exhibiting more energy dissipative behavior, glass-acrylic composites were less impact damage resistant than their epoxy counterparts.

Tab. 1.1 - Summary of published literature on the mechanical behavior of acrylic composites

Autor	Reinforcement	Test
Chiali *et al* [35,47,48]	Flax fibers Carbon fibers	Tensile Shear Damage and fractographic study Moisture diffusivity & aging
Obande *et al* [40]	Glass fibers	Impact Damage and viscoelasticity
Davies *et al*.[44,45]	Carbon fibers Glass fibers Flax fibers	Tensile Moisture diffusivity & aging Fatigue Flexural Shear
Bhudolia *et al*.[41]	Carbon fibers	Fracture toughness Impact Shear Damage and viscoelasticity Damage and fractographic study
Kinvi-Dossou *et al*.[39]	Glass fibers	Impact
Baley *et al*.[27]	Flax fibers Jute fibers	Tensile Compressive
Freund *et al.*[46]	Flax fibers Glass fibers	Moisture diffusivity & aging
Lorriot *et al*.[58]	Glass fibers	Tensile Shear
Murray *et al*.[59]	Glass fibers	flexural

Although in the course of time more research focusing on the characterization of composites based on the acrylic resin is published, there is still a lot of space for the development of research that analyzes the mechanical properties of this type of material. As shown in Table 1, there is a lack of studies evaluating that evaluates general mechanical properties, fracture toughness, damage behavior and thermomechanical characteristics in a complementary fashion. This clearly highlights the need for rigorous benchmarking to develop the robustness of the material performance database on acrylic matrices in composites, which despite attracting considerable research interest is not as well understood as traditional matrix systems such as epoxies. Such benchmarking analyses will serve to improve the understanding of areas in which acrylic composites may be most effectively applied.

Thus, because it is a new material under developement to be used as a matrix for composite materials, its properties are still little known, which favours the study of its behavior. In this context, this present work aims to investigate the mechanical properties of a carbon fiber composite based on acrylic resin and benchmark against a traditional thermosetting epoxy-based composite. The manufacturing of the various composite specimens molded by the VARTM process was also used to evaluate the mechanical properties of the composites. They were subjected to different loading conditions (in and out-of-plane loading) to understanding the behavior of the matrix in their interlaminar fracture toughness and damage tolerance, as well as on the in-plane properties.

Considering the different loadings to which composites are submitted, in Chapter 1, a fractographic study was conducted using scanning electron microscopy to assess all the fracture modes and characterize the fracture surfaces of the interlaminar fracture toughness tests.

Moreover, a statistical approach to compare the structural health of the thermoplastic and thermosetting composites summited to moisture is proposed in chapter 2 in order to provide supplementary comprehension of the tufts in the structure.

In chapter 3 this thesis presents the initial development of an artificial neural networks model for the thermoplastic composites.

Finally, chapter 5 gives a final conclusion of this work and analyzes each characterization test used and contributes to the validation of this novel resin system.

1.1 Research objective

To gain a deeper knowledge on the mechanical behavior of the composites based on liquid thermoplastic resin and to extend its application in several structures, we need to answer this question: What are the specific properties and how do they influence the mechanical properties of this type of thermoplastic composites at the micro-level/material level and macro-level/process-level?

Even though a lot of effort has been done into understanding and characterizing the quality of well-known thermoplastic composites, there are still gaps in our knowledge in the case of composites based on Elium resin.

Therefore, the objective of the research work presented here was to:

- ✓ Gain an in-depth understanding of how specific properties of thermoplastic can influence in the toughness fracture behavior;
- ✓ Establish a comparison based on the influence of moisture on tensile and in-plane shear properties;
- ✓ Provide documentation that promotes the dissemination of knowledge by means complementary analyzes to prove the efficiency of the application of Elium resin;

- ✓ Analyze in a micro-level study, the specific properties that can influence the properties, such as the thermal reactions;
- ✓ Provide a detailed study of fracture surfaces, in order to analyze the effect of this type of matrix on the final properties of the composite.

1.2 Thesis outline

The flowchart in Figure 1.1 presents the methodology used in the development of this work, thus the following Ph.D. thesis is organized into four chapters with a final chapter with the general conclusions.

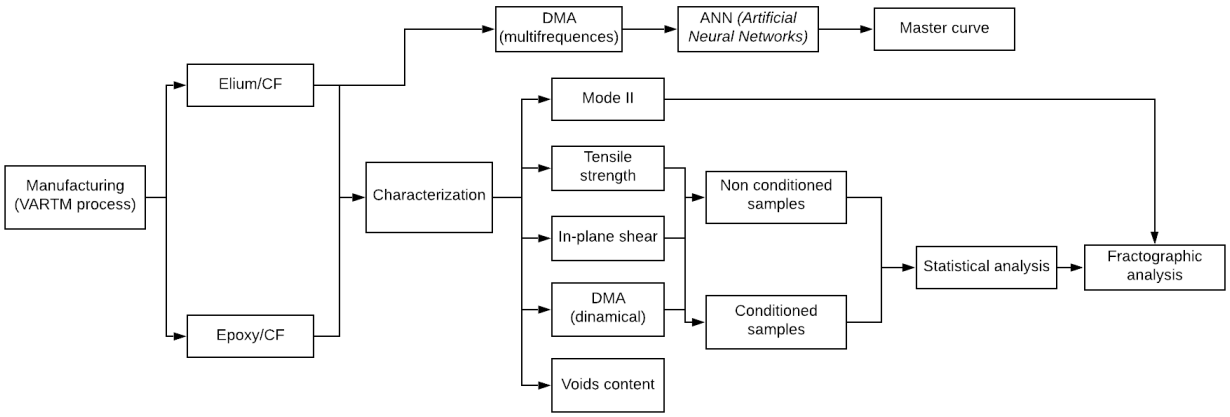

Fig 1.2 - Methodology applied in the development of this work

- ✓ In Chapter 2, an experimental study was conducted in order to understand the behavior in Mode II interlaminar fracture;
- ✓ In Chapter 3, the influence of the moisture was investigated, and its effects were analyzed statistically ;
- ✓ In Chapter 4, the evaluation of the multiplexed frequencies and long-term life prediction was discussed and ANN (artificial neural networks) technique was

used to model the temperature-frequency dependence of dynamic mechanical properties over the wide range of temperatures and frequencies;

- ✓ In Chapter 5, the thesis terminates with an overview of the main conclusions obtained for each covered subject and, the perspectives for the future works.

CHAPTER 2 : ANALYSIS OF FRACTURE TOUGHNESS IN MODE II AND FRACTOGRAPHIC STUDY

One of the major challenges of composite materials is to increase their properties related to interlaminar fracture toughness and consequently delamination. This chapter shows a composite system based on a new thermoplastic Elium® 150 resin developed to be a competitive solution for the composites traditionally based on epoxy resins. Based on Figure 1.1 both composites were fabricated via VARTM using a 0 / 90° plain weave carbon fiber fabric and tested in Mode II interlaminar fracture toughness. The unknown fractographic aspects of the fracture surfaces of the thermoplastic laminate was used as a complementary tool for the mechanical characterization.

2.1 Introduction

Delamination is an important issue to consider when dealing with fiber-reinforced composites materials. Generally, the origin of the failure is influenced by the excessive three-dimensional state of interlaminar stresses, which are developed at the interface between layers due to the existence of resin-rich regions [60]. In fracture mechanics, interlaminar fracture toughness is a parameter used to characterize the material's capacity to resist delamination growth under various modes of deformation [61-69]. In this way, interlaminar fracture characterization under mode II loading is extensively used as a fundamental tool to accurately predict the susceptibility of the material to delamination.

Delamination is typically characterized based on linear elastic fracture mechanics using the strain release rate, G, which quantifies the material’s resistance to delamination [70,71]. It can be initiated from low-velocity impacts, fatigue, shear and

free-edge stresses resulting in significant loss of mechanical properties, including compressive strength and in-plane stiffness [69,72-74]. Therefore, enhancing the interlaminar fracture toughness of laminates becomes an important topic for promoting damage tolerance of composites [75].

Composites materials based on thermoplastic matrices offer superior out-of-plane response when compared to thermoset based systems. This occurs because the individual chains of thermoplastic polymers are held together by van der Waals forces, which are weaker in polymers oriented randomly (amorphous), whereas thermosetting matrices have a strong covalent linkage (cross-linking) between polymer chains. In this context, during the fracture process, there is a breakdown of the bonds of the polymer chains and the fracture energy of thermoplastic composites is related from the process of restricted plastic deformation at the crack. On the other hand, in thermosetting composites, the high density of crosslinks leads to much more rigid materials. Thus, when subjected to shearing, the propagation of microcracks tends to generate more delamination in this class of polymers [76,77].

Friedrich *et al*. compared the Mode I and Mode II fracture performance of composites made from carbon fiber and thermoplastic PEEK (Polyether ether ketone) matrix. It was highlighted that G_{Ic} and G_{IIc} were ten times higher in the case of CF/PEEK compared to CF/ Epoxy composite [78]. Hunston *et al.* carried out a detailed investigation between toughened-thermoset, and thermoplastic composites and showed that toughened resin matrices in general offer the composites increased interlaminar fracture toughness by 1 kJ/m^2 compared to the neat resin composite laminates [19]. However, despite all the advantages related to the properties offered by thermoplastics, their processing is a drawback [79].

Another subject of extremely importance to the fracture toughness properties is related to the fiber/matrix adhesion and has been also the subject of attention as found in the literature [79,80]. Besides the matrix materials, considerable research has been carried out on the effect of fiber architecture in improving the delamination properties. One of these topics is related to the structurally stitched composites. It offers out of plane properties improvement when there is through-the-thickness reinforcement (z-direction)[82].

In this context, thanks to its capability to be molded by infusion into large and stiff structural parts, with excellent toughness, Elium® 150 new liquid thermoplastic resin's family from ARKEMA, based on MMA, came out as a breakthrough in this scenario[23]. This material shall be acceptable for manufacturing composite parts while matching the mechanical performance of its counterpart thermoset resins. Another important point to highlight about these materials is that they make possible to use the same well-established processing techniques which are already widely used in the manufacture of thermosetting composites, besides that the composites manufactured with Elium® 150 resin are recyclable, thermoformable and weldable. According to Bhudolia et al, the liquid MMA was found to be 27% more efficient in improving the structural damping compared to the epoxy resin [84].

In another study of Bhudolia *et al.* on the evaluation of fracture toughness of thin and thick ply Elium acrylic composite systems, was evidenced a 30% and 70% interlaminar fracture toughness for thin ply/ liquid MMA composite, compared to thick ply/liquid MMA and thin ply/epoxy composites respectively. This effect was attributed to both strong fibers-matrix interfaces and to the plastic deformation of the matrix. The strong adhesion between fibers and matrix in composites is essential to avoid a severe loss of mechanical properties along the thickness direction [85].

In his study, Pini analyzed two types of novel acrylic thermoplastic resins, one neat (Elium) and one toughened (Elium impact - Elium filled with acrylic block copolymers at a nanometer scale), were used as matrices for composite materials in order to study its fracture behavior. It was found that the Elium impact matrices depicted an intralaminar fracture toughness much higher than the one of neat Elium resin. The dependence of the fracture toughness of such composites on crack propagation speed was observed to be slightly different from that of the relevant matrices [86].

The present work is focused on evaluating the out of plane properties of the composite based on Elium® 150 by comparison with a well-known epoxy system. This paper highlights the improvement that this novel composite system offers in Mode II fracture toughness and also shows a study of fracture surfaces as the baseline for a qualitative evaluation of the correlation between material-processing-property.

2.2 Experimental

2.2.1 Materials

Carbon fiber laminates were manufactured using a 0/90° *plain weave* fabric provided by SIGRATEX, SKDL 8051 model, with Grafil/Pyrofil TR50S and 6000 filaments (6k) per weft and warp mesh for multi-purpose applications.

The resin used is a low viscosity thermoplastic liquid acrylic resin commercially known by ELIUM® 150 supplied by ARKEMA. Its polymerization reaction is initiated by 0.8% - 1.6% peroxide called LUPEROX® 75, s established by the supplier's established based on the supplier's datasheet suggestion. All the laminates used in this work were fabricated using 1.6% of the peroxide.

The thermosetting composites were manufactured using Araldite® LY 5052/ Aradur® 5052 supplied by Huntsman. This resin was chosen due to its low viscosity, remarkable wettability and impregnation, compatibility with carbon fiber and excellent mechanical properties after curing, both at room temperature and at high temperatures.

2.2.2 Manufacturing

The manufactured thermoplastic and thermosetting composites laminates are composed of 12 stacked layers of carbon fiber fabric. A Teflon (PTFE) release film, with a length of approximately 45 mm, was placed in the mid-section of the laminate in order to induce and start the delamination. The number of layers was chosen so as to obtain plates with a thickness of ~4mm. As the ELIUM® 150 and epoxy resin have low viscosity to be infused, both laminates were prepared by the VARTM process, as shown in Figure 2.1.

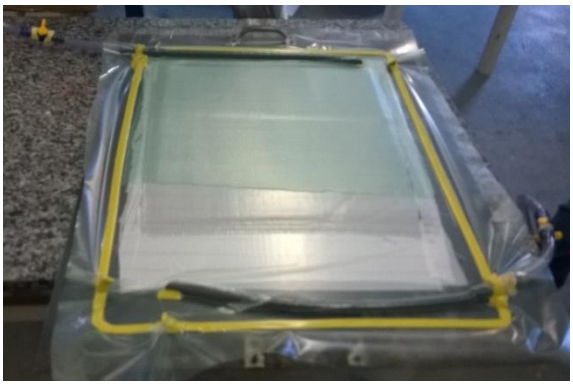

Fig 2.1 - VARTM manufacturing set-up

The technique basically consists of placing the dry reinforcement layers on the rigid mold, one by one. Then, access points are placed for the infusion of the resin and the system is sealed by a flexible bag. The resin is then injected through one end of the part simultaneously with the application of vacuum at the other. During the process, the vacuum has the function of directing the resin front, in addition to eliminating possible porosities caused by air and volatiles released during the curing reaction of the part.

2.2.3 Mode II fracture toughness test (ENF test)

Mode II fracture toughness tests were conducted according to the ASTM D7905M-14 Test Standard. All tests were carried out in an EMIC test machine using end-notched flexure (ENF) specimens with 165 mm long and 19 mm wide, as shown in Figure 2.2. The ENF specimens were painted in white on the side and compliance calibration (CC) markings were made.

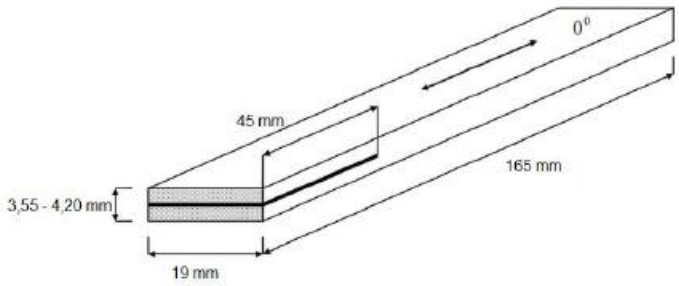

Fig 2.2 - Specimens dimensions [1]

The calibration marks were made from the tip of the Teflon insert (a = 40 mm, a= 30 mm and a = 20 mm), as shown in Figure 2.3. All the specimens contained an initial 45 mm long mid-plane pre-crack at one end to initiate the crack.

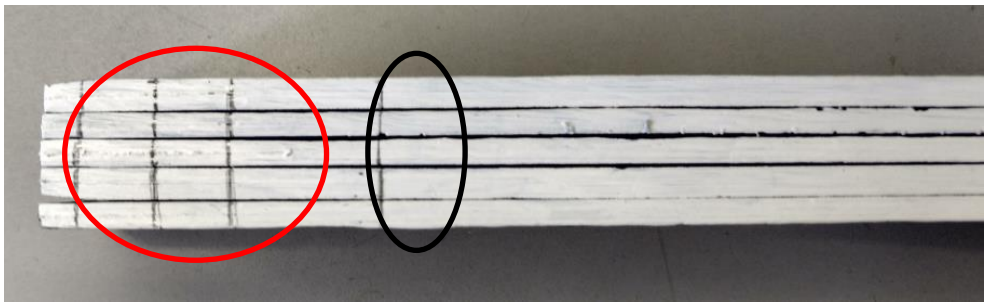

Fig 2.3 - Specimens with compliance calibration marks at a0 = 40 mm, a0 = 30 mm and a0 = 20 mm (red circle) and the marks of the end of Teflon inserts (black circle)

This standard test consisted of non-precracked (NPC) and precracked (PC) fracture tests and proposes to determine G_{IIc_NPC} and G_{IIc_PC} from specimen compliance equation for both NPC and PC test specimens. The NPC, which would be to start the delamination from the end of the insert polymeric and determine the values of the critical energy release rate (G_{IIc}), and the PC that will also determine the G_{IIc} after delamination starts.

To determine the CC coefficients of the NPC and PC tests, it is necessary to have three tests, one for each slit length. The first test (at NPC test) was performed for the a_0 = 20 mm and the distance between the supports is 100 mm (for all tests). The specimens were positioned on the 3-point test device and the mark was supported in the center of the left side of the device. When the force reaches a predetermined value, which does not initiate the delamination, it is necessary that the test is ended and the specimen was withdrawn and repositioned at the device for another a_0 position. The same procedure was adopted for the a_0 = 40 mm. For the third test, it was used a_0= 30mm. At this stage, the assay was performed until the test specimen began delamination. The test was interrupted when the force value reached the maximum value.

After completing the NPC fracture test, which created a shear precrack, the specimen was removed from the test machine and reused to conduct PC test with the crack length measure. The new delamination tip location was marked and PC fracture tests were conducted using the new crack length as shown in Figure 2.4 with the same procedure as for the NPC test, but the force and displacement values were different.

(Intentionally left blank)

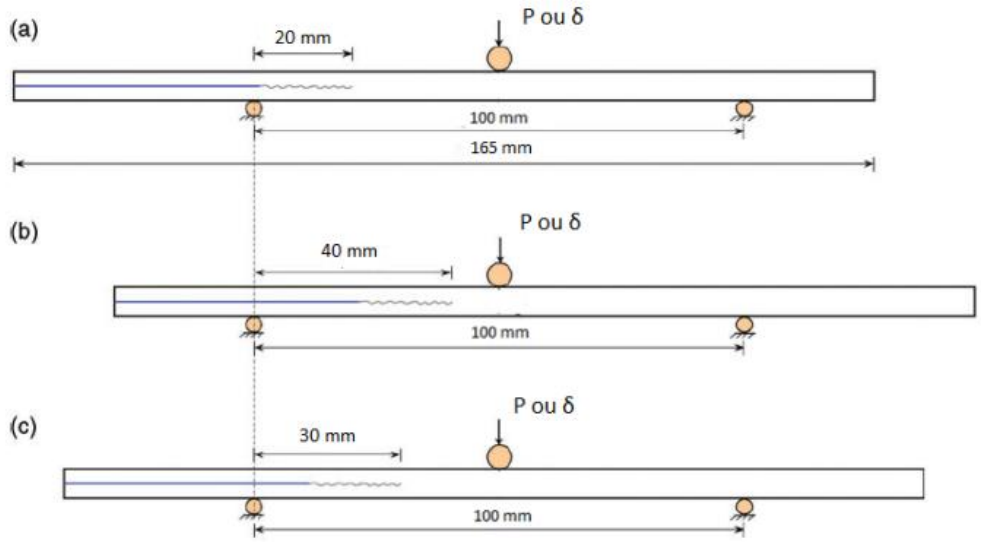

Fig 2.4 - New crack lengths from the end of the crack[82]

The compliance equation (Equation 1) was established by experiment to predict crack length as needed. The coefficients (CC) *A* and *m* are determined from the linear regression data of the C curve as function obtained by Equation 1.

$$C = A + ma^3 \qquad (1)$$

where, (C) is the compliance, (a^3) is crack length cubed, (A) is the intercept and (m) the slope of the linear regression.

From these results, using the constant m from the compliance equation, the values of load and displacement are measured to obtain the mode II interlaminar fracture toughness, $G_{IIC,}$ according to equation 2.

$$G_{IIc} = \frac{3mP_{max}^2 a_0^2}{2B} \qquad (2)$$

where, (P_{max}) the maximum force that initiates the cracking/delamination, (a_0) the crack length to start the delamination (30 mm) and B the specimen width.

2.2.4 Fractographic study

Fractography is a complementary analysis of the composite's mechanical characterization and provides an important contribution to the processing optimization of the materials. In composites, it is known that in order to achieve a better mechanical performance a strong fiber/matrix interfacial adhesion is required.

Most of the fractographic studies are traditionally reported for thermoset composites. Due to its complexity, fractographic studies involving thermoplastic matrices are still less exploited. During the mechanical loading of thermoplastic composites, the matrix presents deformation followed by the generation of stresses at the fiber surface, which can produce interfacial stresses. These stresses are mainly produced because of the difference between the elastic properties of fiber and polymeric matrix [27-29]. Thus, the plastic deformation observed during loading may modify the

fracture surface by hiding or masking the fractographic aspects hindering the detailed analysis of the failure causes in this class of materials [86].

The samples were metalized with a gold coating by a sputtering process (Quorum Q150RS plus model), making them conductive for Scanning Electron Microscope (SEM) analyses. This study was performed in a microscope model FEI INSPECT S50. The sputtering technique uses low-temperature enhanced-plasma magnetrons optimized for the rotary pump pressures, combined with low current and deposition control, which ensures the sample is protected and uniformly coated. The fractographic modes were identified under the composite's failure surfaces to understand the evidence presented in the fracture region.

2.3Results and discussions

2.3.1 End Notched Flexure test

In order to understand the differences in the mechanical properties between Elium ® 150 /CF and Epoxy/CF composites, mode II interlaminar fracture toughness was investigated.

Tables 2.1, 2.2, 2.3 and 2.4 summarize the calculated values of the compliance C for *NPC* and *PC* tests, and the CC coefficients m and A. These coefficients were determined using a linear least-squares linear regression analysis of the compliance, *C*, versus crack length cubed, a^3, data from the equation (1). Figures 2.5 and 2.6 show a linear fit to the average data points of NPC and PC tests for Elium and Epoxy resins, respectively. From these results, and according to equation (2) was possible to obtain the G_{IIc} values.

Tab. 2.1 - Interlaminar fracture parameters for epoxy/CF composites in NPC tests under ASTM 7905 standard

Test	Specimen	C (mm/N)			CC Coefficients	
		a_0= 20mm	a_0 = 30mm	a_0 = 40mm	m	A
Epoxy - NPC	EP-1	4.80E-03	5.80E-03	7.50E-03	4.80E-08	4.50E-03
	EP-2	4.70E-03	5.50E-03	7.30E-03	4.67E-08	4.30E-03
	EP-3	4.60E-03	5.50E-03	7.40E-03	5.02E-08	4.20E-03
	EP-4	4.50E-03	5.60E-03	7.70E-03	5.71E-08	4.00E-03
	EP-5	4.50E-03	5.40E-03	7.20E-03	4.82E-08	4.10E-03
	Average	4.62E-03	5.56E-03	7.42E-03	5.00E-08	4.22E-03
	Standard Deviation	1.30E-04	1.52E-04	1.92E-04	4.13E-09	1.92E-04

Tab. 2.2 - Interlaminar fracture parameters for epoxy/CF composites in PC tests under ASTM 7905 standard

Test	Specimen	C (mm/N)			CC Coefficients	
		a_0= 20mm	a_0 = 30mm	a_0 = 40mm	m	A
Epoxy - PC	EP-1	5.80E-03	7.40E-03	1.03E-02	8.10E-08	5.20E-03
	EP-2	5.20E-03	6.70E-03	7.60E-03	4.03E-08	5.20E-03
	EP-3	4.70E-03	5.60E-03	7.60E-03	5.21E-08	4.20E-03
	EP-4	4.80E-03	6.00E-03	8.50E-03	6.63E-08	4.20E-03
	EP-5	4.90E-03	6.30E-03	8.80E-03	6.94E-08	4.40E-03
	Average	5.08E-03	6.40E-03	8.56E-03	6.18E-08	4.64E-03
	Standard Deviation	4.44E-04	6.89E-04	1.11E-03	1.58E-08	5.18E-04

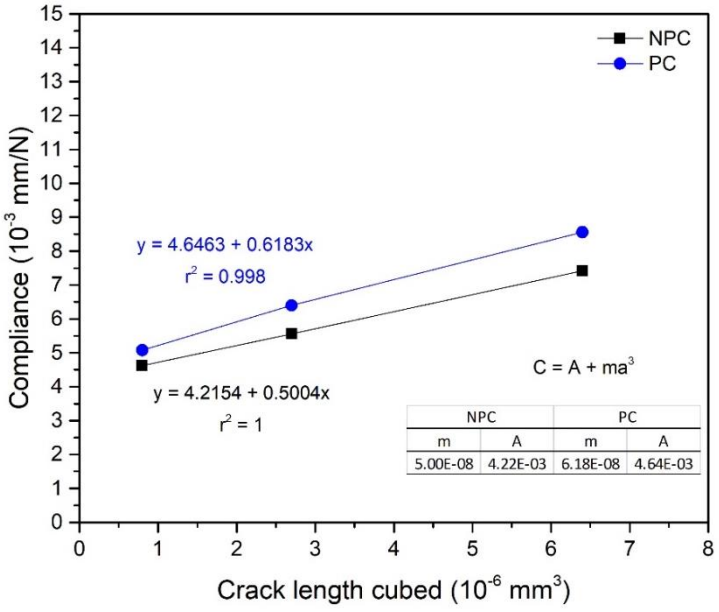

Fig 2.5 - Compliance versus crack cubed length for Epoxy CF composites in NPC and PC tests

Tab. 2.3 - Interlaminar fracture parameters for Elium® 150/CF composites in NPC tests under ASTM 7905 standard

Test	Specimen	C (mm/N)			CC Coefficients	
		a_0= 20mm	a_0 = 30mm	a_0 = 40mm	m	A
Elium - NPC	EL-1	5.20E-03	5.90E-03	7.50E-03	4.14E-08	4.80E-03
	EL-2	5.20E-03	5.80E-03	7.40E-03	3.98E-08	4.80E-03
	EL-3	5.20E-03	5.70E-03	7.40E-03	4.02E-08	4.80E-03
	EL-4	5.30E-03	5.90E-03	7.30E-03	3.60E-08	5.00E-03
	EL-5	4.90E-03	5.70E-03	7.50E-03	4.67E-08	4.50E-03
	Average	5.16E-03	5.77E-03	7.42E-03	4.08E-08	4.78E-03
	Standard Deviation	1.52E-04	9.57E-05	8.37E-05	3.86E-09	1.79E-04

Tab. 2.4 - Interlaminar fracture parameters for Elium® 150/CF composites in PC tests under ASTM 7905 standard

Test	Specimen	C (mm/N)			CC Coefficients	
		a_0= 20mm	a_0 = 30mm	a_0 = 40mm	m	A
Elium - PC	EL-1	7.20E-03	9.80E-03	1.36E-02	1.13E-07	6.50E-03
	EL-2	6.30E-03	8.10E-03	1.18E-02	9.85E-08	5.50E-03
	EL-3	6.30E-03	8.10E-03	1.23E-02	1.08E-07	5.30E-03
	EL-4	5.80E-03	8.10E-03	9.30E-03	6.00E-08	5.80E-03
	EL-5	6.80E-03	9.60E-03	1.40E-02	1.27E-07	5.90E-03
	Average	6.48E-03	8.74E-03	1.22E-02	1.01E-07	5.80E-03
	Standard Deviation	5.36E-04	8.79E-04	1.86E-03	2.53E-08	4.58E-04

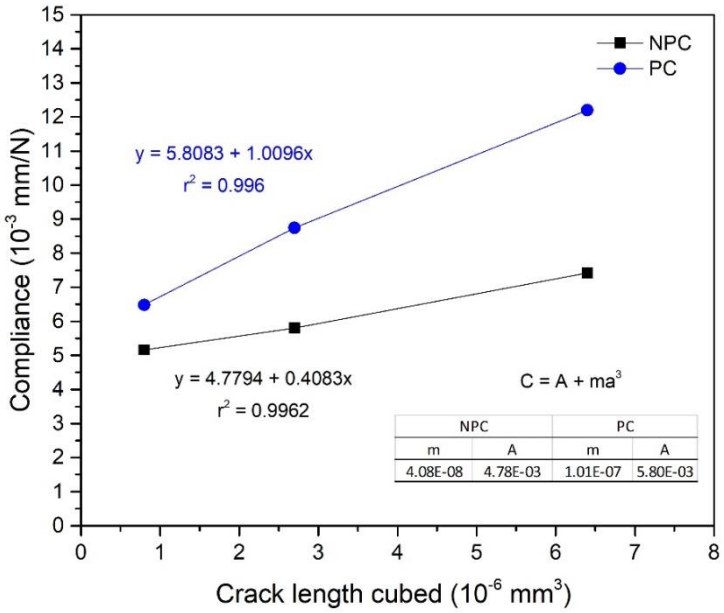

Fig 2.6 - Compliance versus crack cubed length for Elium/ CF composites in NPC and PC tests

2.3.2 Load-displacement curve

The load-displacement curves for the two composites types are evidenced in Figure 2.7 and 2.8. As seen in the Figures and values presented in table 2.5, peak load for both PC and NPC tests for the Elium ® 150 and Epoxy composites are constantly high. The curve representing the NPC test for both composites is initially linear, showing the brittle nature of the matrix. On the other hand, for the PC test, after the linear growth of the curve, there is an immediate sharp load drop, indicating that the unstable crack propagation occurs. However, for the Elium ® 150 composites (Fig.2.7), an apparent non-linear segment is observed after the linear portion. This fact is attributed to the thermoplastic resin plastic deformation and the unstable crack propagation is then delayed to a higher displacement value.

Another point to be observed is that although the magnitude of peak load for the Epoxy composite is higher than than Elium ® 150 composites, the load-displacement

curves show that thermoplastic resin can effectively control the magnitude of load drop and stoped unstable crack propagation. Thus, is possible to state that peak load is related to the capability to suppress the delamination occurrence, whereas the magnitude of load drop is related to the capability to arrest delamination.

Tab. 2.5- Values for Pmax

Specimens	**P_{Max} (N)**
NPC test	
Epoxy	737,80 ± 30,92
Elium® 150	672,16 ± 30,45
PC test	
Epoxy	672,60 ± 53,86
Elium® 150	531,20 ± 42,34

(Intentionally left blank)

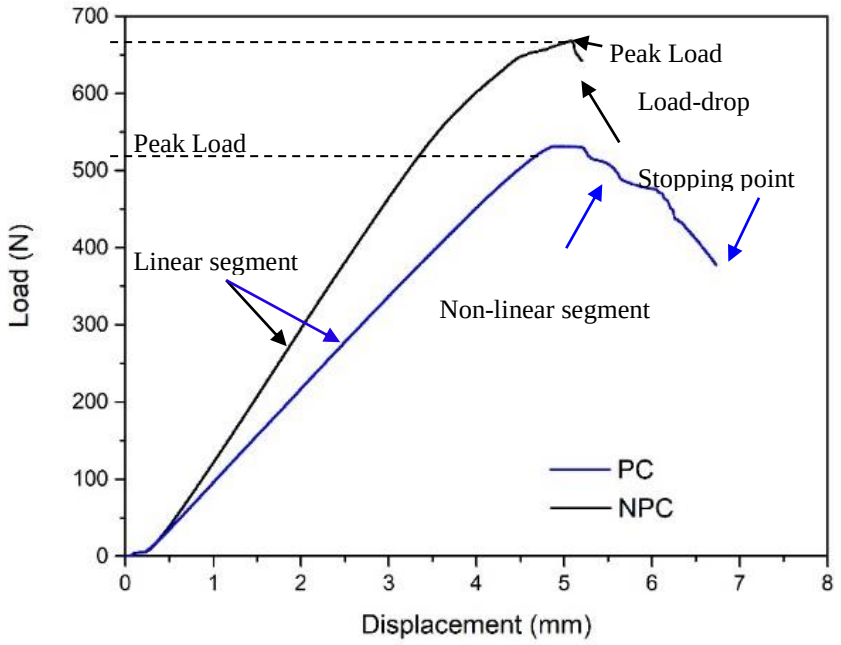

Fig 2.7 - Load-displacement curves for precracked (PC) and non precracked (NPC) tests for the CF/ Elium ® 150 composites

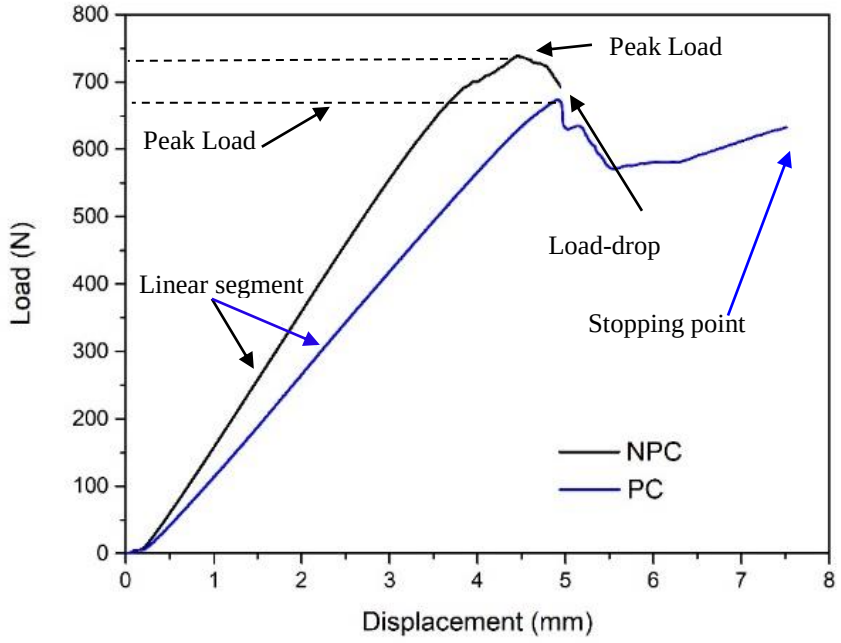

Fig 2.8 -Load-displacement curves for precracked (PC) and non precracked (NPC) tests for the CF/ Epoxy composites

Tables 2.6 and 2.7 depicts the Mode II interlaminar fracture toughness values for the composites types and their coefficient of variations based on the values from

tables 2.1,2.2,2.3 and 2.4. Moreover, the average values of the 5 specimens are indicated using the error bars in figure 2.8.

Tab. 2.6 - Mode II interlaminar fracture toughness GIIc values for non-precracked (NPC) test.

ENF Especimens – NPC test	G_{IIc} (J/m^2)
Epoxy	195.10 ± 24.69
Elium ® 150	125.25 ± 11.46

Tab. 2.7 - Mode II interlaminar fracture toughness GIIc values for precracked (PC) test

ENF Especimens – PC test	G_{IIc} (J/m^2)
Epoxy	201.22 ± 58.47
Elium ® 150	214.22 ± 29.97

As in the NPC phase, the test is interrupted before the delamination propagation, the matrices presented different behaviors in the G_{IIc} values. According to Table 6 and Figure 2.9 it is possible to notice that the average G_{IIc} values for the Elium® 150 / carbon fiber composites in the NPC test were 36% lower than the values found for the thermosetting composites. This difference may be related to the interfacial adhesion between the resin and the fibers. Although the carbon fibers used in the development of this work have superficial treatments for multi-purpose applications, a specific treatment for acrylic polymers could perhaps increase the interfacial fiber/matrix adhesion and consequently improve their fracture toughness mainly in NPC test.

On the other hand, comparing the values of both composites in the pre-cracked samples, in Table 2.7, it is possible to notice an increase in G_{IIc} values in general. For the epoxy-based composite, a small change (3%) in the GIIc was observed between the

non precracked (NPC) sample and the precracked (PC). In the Elium® 150 composites, this variation was 41%. These results confirm that the thermoplastic laminate fails at lower energies compared to thermosetting laminate (NPC test), but during the crack propagation (PC test), the thermoplastic matrix exhibits a higher resistance.

In other words, thermoplastic matrices have weaker intermolecular bonds, which favors premature material failure, however, a large free volume between the polymer chains, tends to absorb the energy associated with crack propagation in the form of plastic deformation. On the other hand, the thermosetting resins are highly cross-linked and provide high strength, but the crosslinking of the molecular chains causes extreme brittleness, i.e., low fracture toughness. Thus, although the Elium® 150 resin fails at low energies, but more energy is needed to propagate the crack, due to the additional energy related to the high deformation rate constituted in the surface energy [77,85].

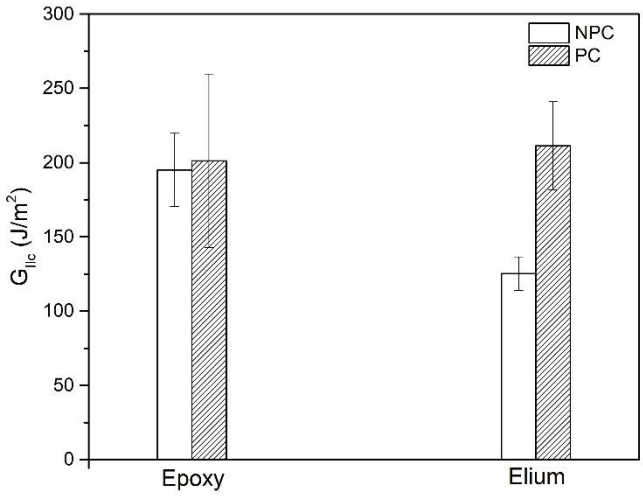

Fig 2.9 - Mode II fracture test results for the composite systems.

The images of Figures 2.10 and 2.111 represent the macroscopic growth of the crack during the ENF tests. The first images (a and b) are representative of the NPC test and shows the beginning of crack propagation in both materials. The images c and d represent the beginning of the PC test and shows the crack growth and resistance during the delamination process. These images are in agreement with the results presented in

this work, where it is possible to notice that the Elium® 150 -based composite has a higher resistance to crack propagation. Although both tests had the same duration, the CF/epoxy composites propagated 15mm during the PC test, the Elium® 150 resin composites showed propagation of only 5mm.

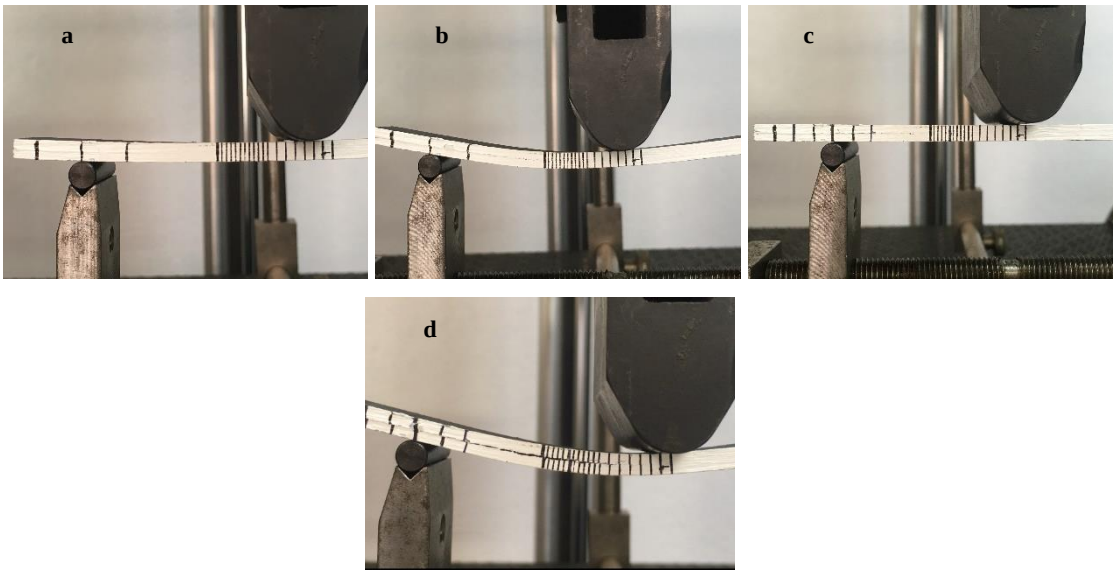

Fig 2.10 - Macroscopic photographs of ENF test for Epoxy composite. (a) beginning of the (non-precracked) NPC test, t=0s. (b) end of the NPC test t= 400s. (c) beginning of the PC test t=0. (d) end of the PC test t=600.

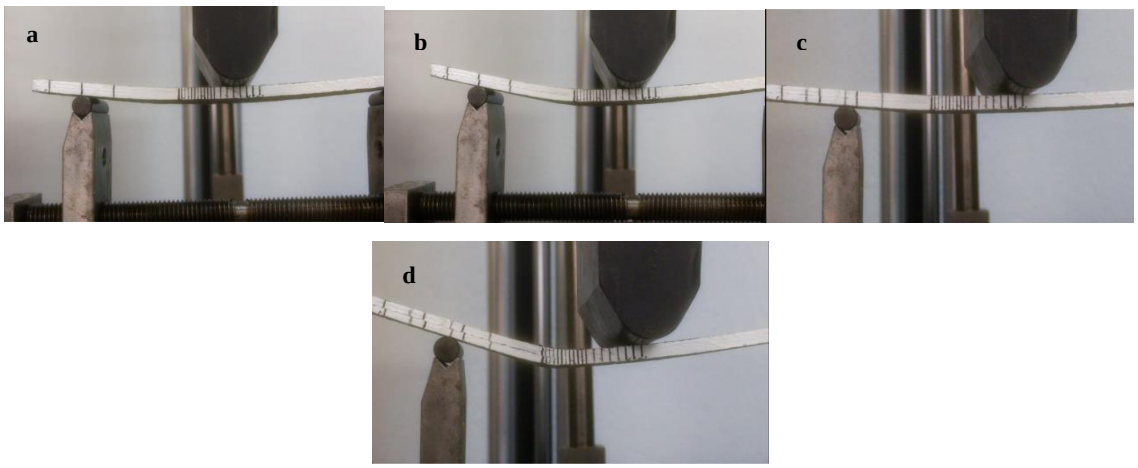

Fig 2.11 - Macroscopic photographs of ENF test for Elium ® 150 composite. (a) beginning of the (non-precracked) NPC test t=0. (b) end of the NPC test t=360s. (c) beginning of the (precracked) PC test t=0.. (d) end of the PC test t=600.

2.4 Fractographic evaluation

The images of Figures 2.12 and 2.13 are representative of the fractographic aspects observed in the fracture laminates surfaces. In general, the most common

fractographic features that characterized the mode II loading are the shear cusps, identified in both materials. The dimensions and distribution of this fractographic aspect are affected by matrix volume and by the distance between the fibers, both parameters defined during the consolidation stage of the composite material. The presence of shear cusps is related to the development of inclined platelets in the spaces between fibers. This aspect occurs because, during the ENF test, the applied loads to the fiber surface causes interlaminar shear at the fiber/matrix interface and is attributed to the relative movement of surfaces and also to high loading rates, which may cause the cleavage of matrix [60, 87]. Besides that, the cusps inclination indicates the direction of failure propagation, so when inclined to the left, the movement moves from left to right [86].

As the Elium® 150 resin is an amorphous thermoplastic polymer, the aspects identified in the fracture of this material are very similar to those observed for composites based on epoxy resin, but presenting a ductile failure morphology in some regions. Although many aspects can be representative of fragile failure, it is clear from the SEM images in Figure 2.12, that the matrix thermoplastic property enhanced the resistance to crack initiation and growth through plastic deformation and debonding of the CF fibers from the matrix.

(Intentionally left blank)

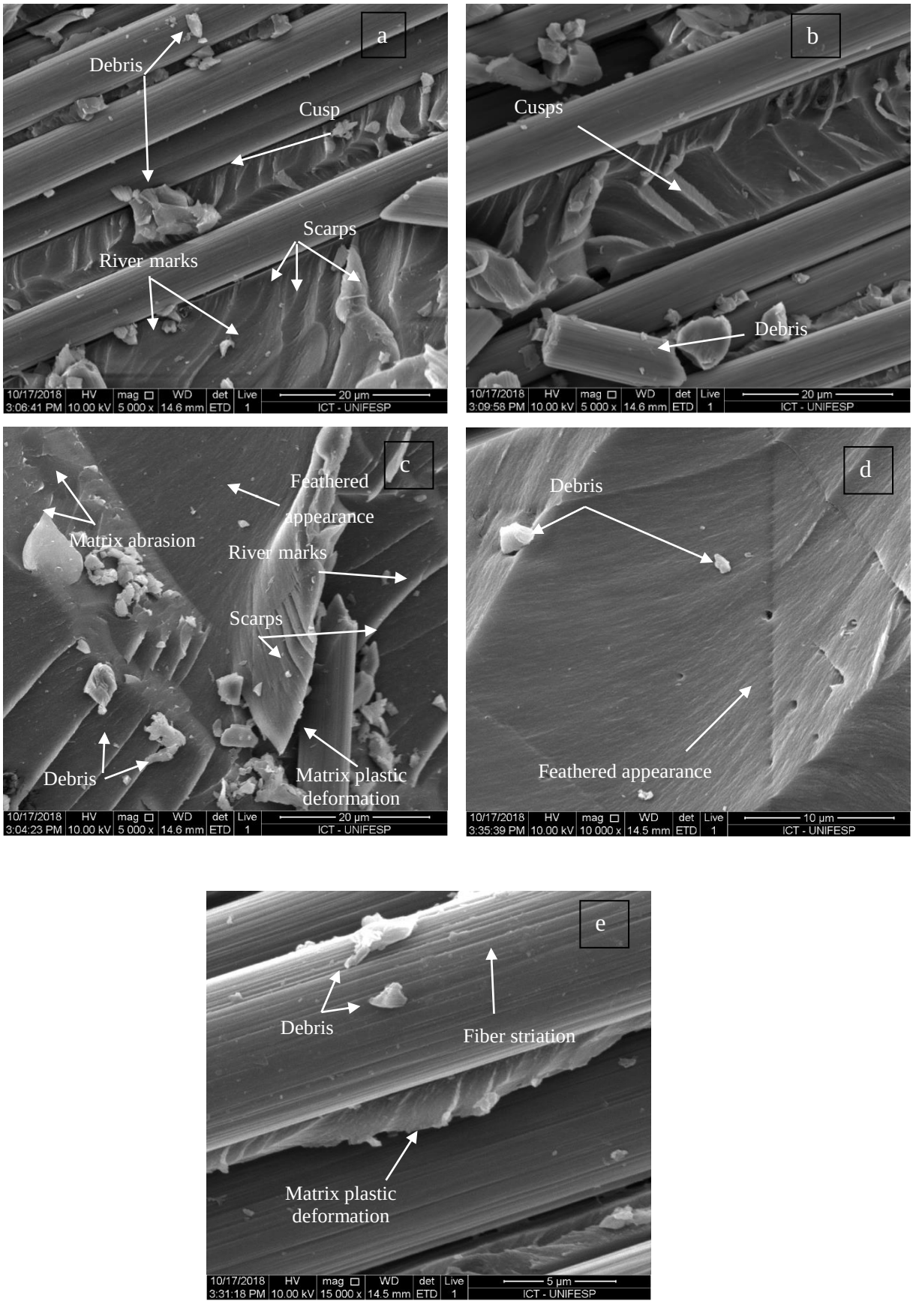

Fig 2.12 -SEM of fracture surfaces of CF/Elium® 150 composites

It is possible to notice that the fracture surfaces are rich in fractographic aspects with the presence of typical aspects representatives of shear failures mainly located at the matrix rich regions with the presence of interfacial failures (Figure 2.12 and 2.13). Moreover, it is also possible to identify fractographic aspects that suggest shell shape presence in Figure 2.13. These aspects originate from cusps separation on the opposite face of the fracture surface and are always present in shear failures and provide little information about the origin and failure direction [88]

The fragile fracture aspects characterized by the matrix abrasion region are shown in Figure 2.12c. According to Purslow (1987), these aspects are attributed to high loading rates and also the relative countermovements of surfaces, which may cause the cleavage of matrix [89]. Another aspect observed in the resin fracture of the thermoplastic composite is the feathered appearance, which occurred due to the beginning and propagation of a very thin and flat texture forming continuous and curved flow lines [60,87-89]. Still, with respect to the thermoplastic matrix characteristics, it is possible to notice the matrix plastic deformation (Figure 2.12d). This latter aspect occurs due to thermoplastic matrix viscoelastic characteristics allowing the extension of the fracture plane by matrix deformation [60,86].

Another characteristic aspect observed in the fractographic analysis of both materials is also aspects such as river line marks. The river line marks are formed by several peers of unequal crack planes, which are directed to a single crack plane during the failure propagation. The crack growth is the direction in which the river line marks converge to form the aspect of scarps [86].

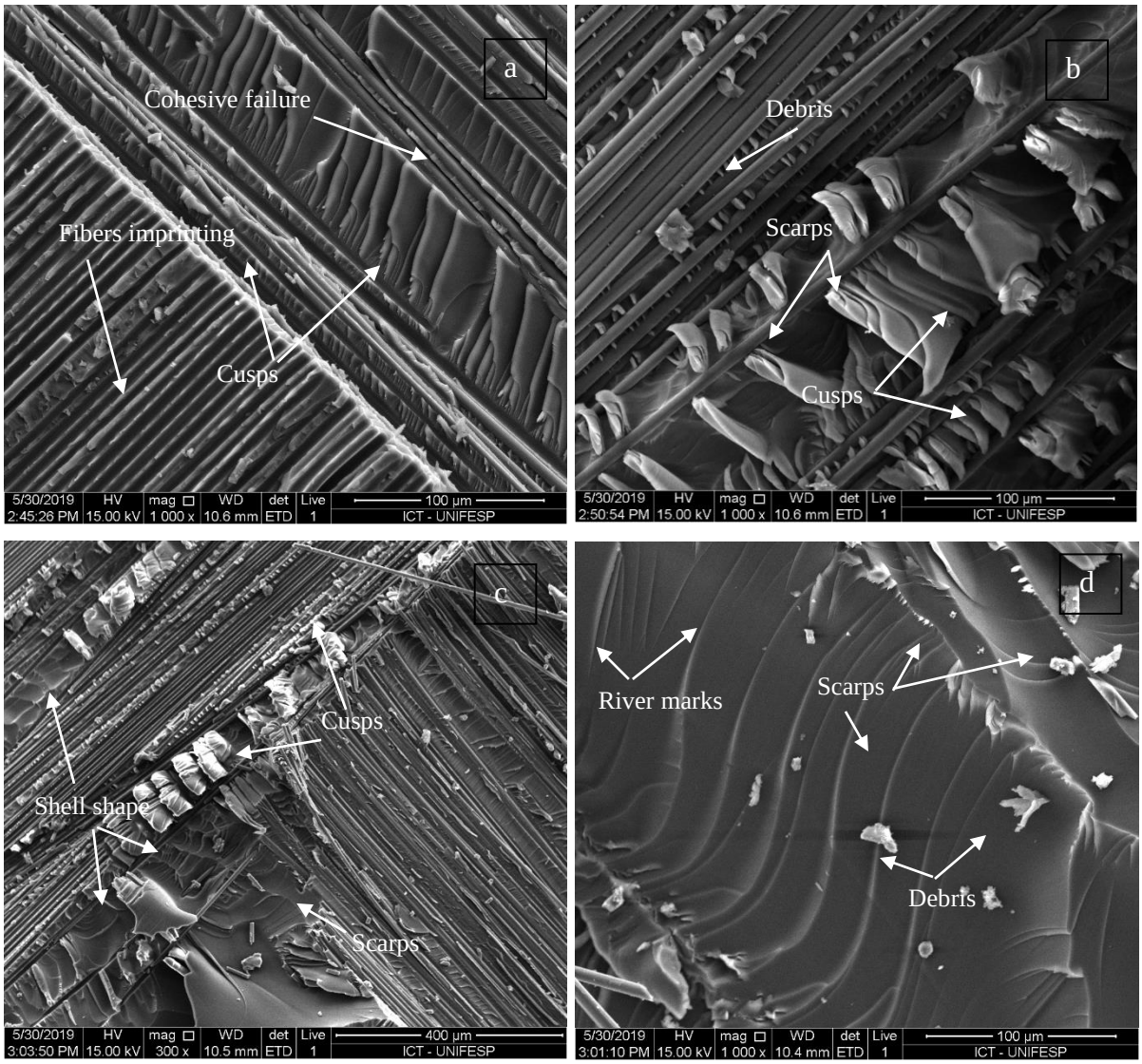

Fig 2.13 - SEM of fracture surfaces of CF/Epoxy composites

The thermoplastic composite has presented a higher resistance to crack propagation in the PC test and it is possible to notice that the cohesive failure did not occur for this type of material, indicating that the fractographic aspects founded are representative of pure shear. According to Greenhalgh, under mode II loading, the failure is predominately at the fiber/matrix interface with the presence of clean fiber tracks in the matrix-dominated face of the fracture surfaces. On the other hand, the cohesive failure occurs directly at the fiber/matrix interface and its main morphological feature is the presence of a thin layer of resin around the fibers [88]. The cohesive failure can be observed in some regions of Epoxy/ CF composites as shown in Figure 2.13a. Besides that, the failure propagation was observed in the interfacial region, and in all SEM images, it was possible to notice the fiber's striation showing a typical interfacial failure [60,86-89] as a result of a failure in the fiber/matrix interface.

Although interfacial failure is beneficial to the results of the interlaminar shear strength in Mode II, it is possible that the mechanical properties, in general, are somewhat improved by means of a specific treatment given previously to the surface of the fibers in order to promote the observation of the cohesive failure. In a study conducted by Bonfaida.Z et al (2015) it was observed that the properties significantly depend on the specific treatment applied previously to the fibers. In this case, a sizing in which it includes a chemical group with the ability to establish bonds with acrylic resins can increase its resistance [90]. Thus, a specific sizing compatible with the acrylic resin could have influenced the occurrence of cohesive failure, which could increase its resistance during the NPC test by means the matrix anchorage in the fibers.

2.5 Conclusion

Thermoplastic carbon fiber composite was manufactured with Elium® 150 and its behavior in Mode II interlaminar fracture was evaluated. The results were compared to traditional epoxy matrix carbon fiber composites by conducting experiments and further understanding the surface morphological fractographic aspects. The thermoplastic laminates showed a higher resistance to crack propagation. Although its failure occurs at lower energies in the NPC test (125,25 ± 11,46 J/m^2) compared to thermoset composite (195,10 ± 24,69 J/m^2), in the PC test it can resist up to 40% (214,22 ± 29,97 J/m^2) more than epoxy matrix composites (201,22 ± 58,47 $J/m^{2)}$. The performed analyses identified plastic deformations in matrix rich regions and was evidenced by Fig. 2.12c, this characteristic could be attributed to the viscoelastic behavior of the thermoplastic matrix. The pure mode II shear failure was identified in both laminates by the interfacial failure in the fiber/matrix interface region with the presence of fiber striations and by shear cusp aspects in the matrix fracture region. In general, the Elium® 150 composites presented greater resistance to Mode II interlaminar fracture than Epoxy-based composites and this value could have been higher using a specific sizing compatible with acrylic resin.

CHAPTER 3 : EFFECTS OF MOISTURE ABSORPTION ON MECHANICAL AND VISCOELASTIC PROPERTIES

Considering the Figure 1.1 this chapter investigated the effect of moisture on the tensile strength and in-plane shear of laminated composites. For this the results of a composite system based on a new thermoplastic Elium® 150 resin was compared to a traditional epoxy resin result. Both composites were fabricated via VARTM using a 0/90° plain weave carbon fiber fabric. Additional analysis based on design of experiments has analyzed the major influences of each parameter. Besides that, the unknown fractographic aspects of the fracture surfaces of both composites were also used as a complementary tool for the mechanical characterization.

3.1 Introduction

Polymer composites are materials widely used in various industrial sectors. Combining high strength and rigidity with low density, these materials considerably reduce the weight of structural components. In addition, composite materials not only have a very high static strength, but also high resistance to fatigue and corrosion [88,89].

The wide range of commercially available types of fibers and resins allow designers to match a wide variety of mechanical properties to a specific application. Thus, with the constant need for the light structure's development, advances in science and technology in several areas have contributed to the ever-increasing improvement in processing techniques and raw materials for the manufacture of polymeric composites [90,91]. However, when put into operation these materials can suffer degradation effects caused by external environmental agents such as humidity and temperature. In this case, because they are materials used most often in applications that require high structural

responsibility, it is important a better prediction of the long-term durability of composite materials with organic matrix [89-93].

In general, these factors may limit the application of composite materials, deteriorating their mechanical properties. Environmental effects caused by temperature and humidity may be reversible when the exposure time is short. However, when the exposure occurs for prolonged periods, the effects produced may be irreversible. In this case, the damages are mainly generated due to the water affinity by specific polar functional groups in matrices. In this case, destructive changes can occur in the fiber/matrix interface due to the physical-chemical interactions degradation between the resin and the interface [90-93].

In polymer composites, moisture penetrates the structure by diffusive or capillary mechanisms according to Fick's second law. As the diffusion process of moisture is highly temperature-dependent, it is assumed that the water tends to diffuse through the amorphous regions of the polymer. In this case, the hydrolysis occurs at a rate dependent on the crystallinity and molecular structure of the end-groups [94,95]. Thermosetting and thermoplastic polymers tend to behave differently when exposed to moisture conditions. However, in a general way, the moisture increase tends to weaken the mechanical properties of these materials and their combination with high temperatures may further aggravate this characteristic [96,97].

Thus, the moisture becomes a noxious condition to the composite, as it induces the appearance of severe mechanical and physicochemical polymer matrix alterations affecting the fiber/matrix interface. In this way, polymer chains can undergo a plasticization process, promoting a reduction in glass transition temperature and the weakening of the fiber/matrix interface thus increasing the internal stresses concentration in the composite material [98,99].

Unlike most traditional structural materials, whose mechanical behavior is assumed to be homogeneous and isotropic, mechanical properties of composite materials exhibit intrinsic statistical dependence. In particular, their strength properties are usually scattered due to their inhomogeneity and anisotropic characteristics and to the brittleness of the matrices and fibers [100]. An adequate and well-performed statistical analysis is fundamental so that the material behavior can be deeply understood and can characterize it [101].

Vauthier *et al.* (1998) analyzed the effects and interactions of hygrothermal aging on the fatigue behavior of a unidirectional glass/epoxy composite [102]. Several authors make use of statistical methods in composite materials in order to predict, characterize or optimize fatigue responses [103,104,105].

Some other authors evaluated the moisture on composite materials [106,107,108]. Yet few (or almost none) have gone into advanced statistical analysis, especially through the use of design-of-experiments techniques.

Moreover, the effect of moisture in resistance of composite materials can causes delamination and this is of fundamental importance in predicting their durability when exposed to aggressive environments [94,96,98,99]. In this context, the present work focus on evaluating the moisture and temperature effects on mechanical and viscoelastic properties of a new thermoplastic liquid resin reinforced with carbon fibers composites by comparison with a well-known epoxy system. Full factorial design and the analyses of variance (ANOVA) were performed to identify the effects of the moisture and temperature on mechanical strength under tensile and in-plane shear loading.

3.2 Experimental

Carbon fiber laminates were manufactured using a 0/90 ° plain weave fabric provided by SIGRATEX, SKDL 8051 model, with Grafil/Pyrofil TR50S and 6000

filaments (6k) per weft and warp mesh. Two arrangements were utilized to manufacture the composites. For the in-plane shear tests the fibers were positioned in the ±45 orientation and for the tensile strength, the laminates were made with 0/90 ° orientation.

The resin used is a low viscosity thermoplastic liquid acrylic resin commercially known by ELIUM® 150 supplied by ARKEMA. Its polymerization reaction is initiated by 0.8 % - 1.6 % peroxide called LUPEROX® 75, established based on the supplier's datasheet suggestion. Therefore, this work was selected with a basis the 1.6% value in the weighing of peroxide.

On the other hand, the thermosetting composites were manufactured using Araldite® LY 5052/Aradur® 5052 supplied by Huntsman. The manufactured composite laminates are composed of 8 layers of carbon fiber fabric. The number of layers was chosen so as to obtain plates with a thickness of ~4mm for composites. As the ELIUM® 150 is a liquid thermoplastic resin, both laminates were prepared by the VARTM process.

3.2.1 Hygrothermal conditioning

Hygrothermal conditioning was performed according to ASTM D5229. The samples were submerged in distilled water according Figure 3.1. For the evaluation of the effect of conditioning, the traveler samples and the specimens were exposed to a temperature of 65 °C for a period of eight weeks. The heating was done by a heating plate and the temperature was monitored daily by an infrared camera. The temperature was monitored by prior to the procedure for exposure to moisture, all specimens and follow-up samples were dried in an oven for an average of 48 hours at 60 ° C. After this drying step the follow-up samples were weighed in an analytical balance. From the data of mass gain obtained, it was possible to construct a gain graph with the average number of days.

Fig 3.1 - (A) samples under conditioning (b) Infrared camera measuring the water temperature

The moisture content absorbed by the material over the immersion time for each sample was calculated according to the mass obtained before exposure (W_i) and after exposure (W_b), according to Equation 1.

$$\%\, umidade = \left(\frac{W_i - W_b}{W_b}\right) x\, 100 \quad (1)$$

3.2.2 Mechanical characterization

The tensile strength and the in-plane shear (tensile test of a ± 45 ° laminate) tests were performed according to ASTM D3039-18 and ASTM D3518 respectively, in universal test equipment (Instron 8801) combined with an Advanced Video Extensometer (AVE). The elasticity modulus was calculated by Digital Image Correlation (DIC).

A total of 10 specimens of each test were tested, 5 specimens without hygrothermal conditioning and 5 specimens after the saturation period. The test speed adopted for the tests was 2 mm / min. Obtaining the deformations and, consequently, the shear modulus (G), was possible with the video strain gage positioned in the central region of the

samples, in the longitudinal and transversal to the loading application. The tests were performed in a universal servo-hydraulic testing machine, model 8801, Instron® brand, in which they were tested statically until failure. The in-plane shear strength and the shear modulus are calculated according to the equations 2, 3, 4.

$$\tau = \frac{F}{2.b.h} \quad (2)$$

$$G = \frac{\Delta\tau}{\Delta\gamma} \quad (3)$$

$$\gamma = \varepsilon_l + \varepsilon_t \quad (4)$$

Where τ is the shear strength (MPa), F is the force applied in (N), b and h are width and thickness measure in (mm), G is the shear modulus (GPa) and γ is the shear strain composed by the sum of the ε_l longitudinal strain and ε_t transversal strain given in (mm / mm).

3.2.3 Void contents determination

Three samples of each composite made were machined as Figure 3.2 . The samples were weighed on a precision balance from Shimadzu®, model AUW220D, and on the same The specific density of the composite was measured using the Archimedes. To obtain specific mass measurements by this method, it is necessary that in the balance a device is installed that can measure the dry mass of the composite and in then the specific mass is calculated with the sample submerged in water. Before the sample is placed in the water, the temperature and density of the water must be measured. These procedures are in accordance with ASTM D792 - 08. The samples were placed in separate baths of 40 mL of sulfuric acid heated to approximately 180°C for 1 hour and

30 minutes, then 70 mL was added of hydrogen peroxide. These steps were carried out according to Procedure B described in ASTM D3171 - 99.

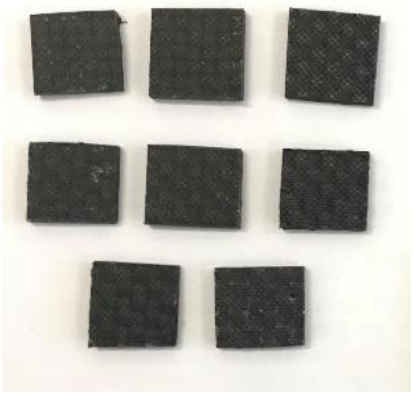

Fig 3.2 - Samples used for the voids content test

For the dissolution of the Elium matrix, the specimens were placed in a acetone solution. All the solutions with the samples were placed in analytical glass filters, installed in a Kitasato, and vacuum filtered. The fibers were washed three times with distilled water and once with acetone, to remove sulfur from sulfuric acid. Before weighing the fibers, they were taken to a greenhouse and the drying was carried out for 40 minutes at 100oC. After drying, the fibers were weighed and the fiber volume (Vf), the resin volume (Vr) and the voids contents (Vv) were determined based on equation 5, 6 e 7.

$$V_f = \frac{M_f.\ \rho_c.100}{M_i.\ \rho_r} \tag{5}$$

$$V_r = \frac{\left(M_i - M_f\right).\rho_c}{M_i.\ \rho_c} \tag{6}$$

$$V_v = 100 - (V_r + V_m) \tag{7}$$

3.2.4 Dynamical mechanical analysis (DMA)

Dynamic mechanical analysis is a thermal analysis technique that measures properties of a given material while it is deformed under periodic stress. Its principle of operation consists of applying a sinusoidal voltage and measuring the deformation corresponding wave, as well as in calculi of the phase difference between these two.

Polymers are viscoelastic materials, whose mechanical behavior exhibits characteristics of both solids and liquids, and for this reason the analysis via DMA is among the most used in these materials, being able to characterize them regarding the glass transition, secondary transitions, crystallinity, molecular weight / crosslinking, phase separation, aging, among others . dynamic-mechanical analysis is considered one of the most accurate techniques for measurement of the glass transition temperature (Tg). The Tg is usually identified in a simple way from the DMA results as the point at which the sharp decrease in the storage module E' occurs, this being a more conservative approach, or either from the de $tan\delta$ peak.

One of the reasons why the procedure for determining the Tg by the onset point of the E′ curve is adopted, is associated with the fact that this temperature is considered a limiting factor in the application of polymers. The onset point is associated with the start of movement of the molecules and the consequent softening of the polymeric structure while at the temperature $tan\delta$ peak, it is clear that the beginning of softening has already been exceeded, that is: it is observed at this temperature a substantial relaxation involving the increasing movement of polymeric chains.

In this work the dynamic mechanical analysis (DMA) was used to characterize the viscoelastic properties of the material using an equipment SEIKO SII EXSTAR 6000 (Figure 3.3), DMS 6100 with dual cantilever assembly and bending operation mode. A

heating rate of 5 °C/min, the operation frequencie was 1Hz, force of 4.000mN, the amplitude of 10μm and a temperature range of 25 °C – 200 °C was used.

Fig 3.3 - SEIKO SII EXSTAR 6000 equipament

3.2.5 Fractographic study

The scanning electron microscopy technique was used to observe the fracture surfaces obtained after mechanical tests and allowed the analysis of the interfacial region of the welding surface. The use of this technique is essential in fractographic studies, as it provides excellent resolution and a great depth of focus, allowing to elucidate the failure mechanisms prevalent in the laminates, as well as to identify the aspects of fractures.

The samples were metalized with a gold coating by a sputtering process (Quorum Q150RS plus model), making them conductive for Scanning Electron Microscope (SEM) analyses. This study was performed in a microscope model FEI INSPECT S50.

This technique was used to identify and characterize the different failure morphologies presented by conditioned and unconditioned composites.

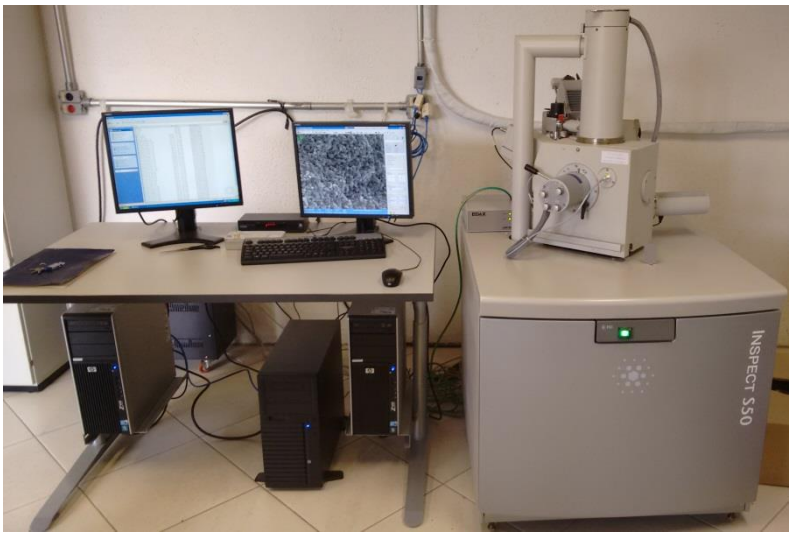

Fig 3.4 - MEV equipament

3.2.6 Full Factorial 2^k analysis

DOE (Design of Experiments) is an experimental planning methodology that combines mathematical and statistical techniques for the development of efficient, balanced and economical experimental arrangements, from which the experimenter can infer with a high level of confidence.

Mathematically, DOE combines the techniques of ANOVA (analysis of variance) 2-sample tests and Regression Analysis to create non-linear equations (response surfaces) that attempt to represent phenomena of interest, without mechanistic models, in a restricted region of interest.

Full Factorial Designs (FFD) are experimental combinations of factors, designed so that each factor (independent variable) is tested an equal number of times at each of its levels. In this way, FFD arrangements are balanced and orthogonal (the sum of the contrast signals is zero). The most common FFDs are base 2. In this type of

arrangement, the number of experiments required to generate a balanced arrangement is equal to $N = 2^k$, where *k* is the number of factors involved [109].

In this study, a complete factorial was performed so that it was possible to understand and prove quantitatively and influence of each parameter involved in the process. Table 3.1 shows the two factors studied, that is, the type of resin used and whether or not the material involved was involved.

Tab. 3.1 - Description of the factorial analysis considering 2 factors

Factor	Description	Lower level	Upper level
A	Resin type	Epoxy	Elium
B	Material conditioning	No	Yes

3.3 Results and Discussions

3.3.1 The influence of moisture in mechanical and viscoelastic properties

The physicochemical characteristics of certain polymer matrices, such as the degree of cross-linking/polymerization and molar mass distribution, allow fiber-reinforced composites to absorb moisture through the diffusion process. In this case, when combined with high temperatures, the moisture content tends to cause degradation of the material. Water absorption data are given in Figure 3.5. According to the graph of the mean values of water absorption, the thermosetting composites had a higher absorption percentage than the Elium® 150 resin-based composites. In addition, epoxy resin-based composites showed void volume values of 1.72 ± 0.29 % while thermoplastic composites showed 1.40 ± 0.36 % which may have influenced the percentage of water absorption of the thermosetting composites.

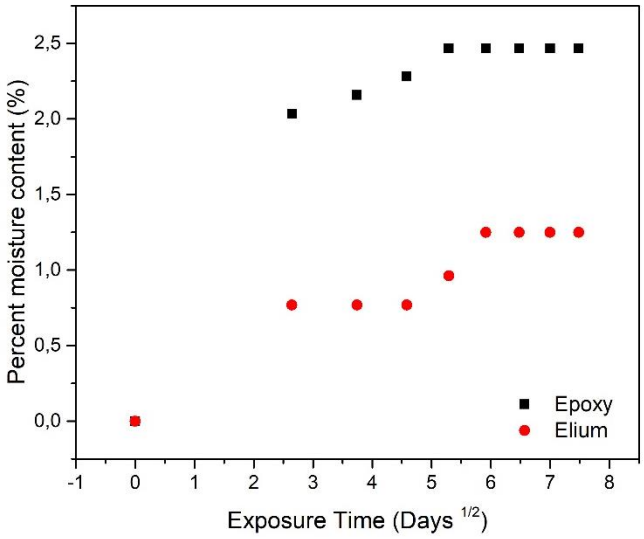

Fig 3.5 - Water absorption percentage od each composite material

In a general way, the water absorption and diffusion mechanism in polymeric materials are related to the free volume and the polymer–water affinity [97,110,111]. It is facilitated when the polymer molecule has clusters capable of forming hydrogen bonds causing. This phenomenon can cause a certain swelling of the material since the water molecules disrupt the interlinked hydrogen bonds and induce the plasticization of the polymer. On the other hand, another phenomenon can occur when the water absorption occurs without a swelling of the material, it is suggested that the water is accommodated within the free volume present between the polymer chains [110,111].

As the free volume is dependent on molecular packaging and is affected by crosslink density, it is expected that thermosetting polymers will absorb a greater amount of water as compared to thermoplastic polymers [94,95,97]. In epoxy resins a significant amount of free volume exists, plasticization occurs due to the disruption of Van der Waals bonds between the polymer chains of ethers, secondary amines, and hydroxyl groups. In this case, the epoxy-water affinity is relatively strong due to polar hydroxyl groups. However, polar water molecules can bind to the hydrogen bonds, thus interrupting the inter-hydrogen bonding of chains. On the other hand, polymers like

PMMA (polymethyl methacrylate) with ketone and imide groups are more resistant to hydrolysis because they are less polar, reducing their interaction with water [96]. In this case, the molecular structure is altered to adapt to the presence of moisture. These results are often observed as dimensional changes and reductions in Tg (Figure 3.6 and Table 3.2) [110,111].

Tab. 3.2 –Tg results of the composites

	E'	**Tanδ**
Elium 150 unconditioned	104 ± 1.01	126 ± 1.12
Elium 150 conditioned	94 ± 0.81	114 ± 0.31; 132.95 ± 0.45; 165.50 ± 0.23
Epoxy unconditioned	103.54 ± 0.33	115.12 ± 0.17
Epoxy conditioned	104.12 ± 0.73	114.73 ± 0.12

In order to evaluate the influence of water absorption on the mechanical properties of these materials, tensile strength and in-plane shear static tests were performed. The mean values of the mechanical properties of the conditioned and unconditioned samples for each material are shown in Table 3.3, which also includes the elasticity modulus values.

According to Table 3.3, it is possible to notice that the tensile strength properties were favored by the absorption of water. However, on the other hand, the in-plane shear properties presented a decrease in their values.

(Intentionally left blank)

Tab. 3.3 - Mechanical properties of the composites

	Tensile strength (MPa)	E (GPa)	In-plane shear (MPa)	E (GPa)
Elium 150 unconditioned	782.51 ± 50.80	57.47 ± 1.70	51.63 ± 2.61	2.91 ± 0.76
Elium 150 conditioned	804.92 ± 15.00	55.20 ± 2.29	42.30 ± 1.30	2.09 ± 0.69
Epoxy unconditioned	624.09 ± 50.17	55.65 ± 3.70	66.74 ± 2.16	5.66 ± 1.17
Epoxy conditioned	693.79 ± 11.73	53.33± 1.44	60.23 ± 1.57	4.17 ± 1.02

Between polymer chains, there is a considerable amount of intermolecular hydrogen bonding which contributes considerably to the physical characteristics of the polymer [112,113]. The presence of water at elevated levels inside the polymer can begin to disrupt its intermolecular bonding and thereby reduce the effectiveness of these interactions in maintaining the polymer structure [113].

This interruption could result in a temporary reduction of the rigidity of the material and increases deformation under the action of load. In this case, moisture can favor the formation of surface cracks and weakening the fiber/matrix interfacial adhesion [110,111,112]. Besides that, it is typically manifested by reductions in those properties which tend to be resin dominated, i.e., interlaminar properties, shear, compression, and also can affect the Glass Transition Temperature (Tg) [113,114].

On the other hand, for fiber-dependent properties, like the tensile test, the breakage of the intermolecular bonds interactions caused by plasticization in polymeric composites submitted to moisture may be beneficial proportioning high elongation at break, and better impact resistance [113]. In this way, plasticization tends to favor the

polymer softening providing a greater matrix plastic deformation, promoting a ductile fracture of the composite. The influence of moisture on viscoelastic properties was evaluated by dynamical mechanical analysis. The results for the storage modulus (E') and loss factor (Tanδ) are shown in Figure 3.2.

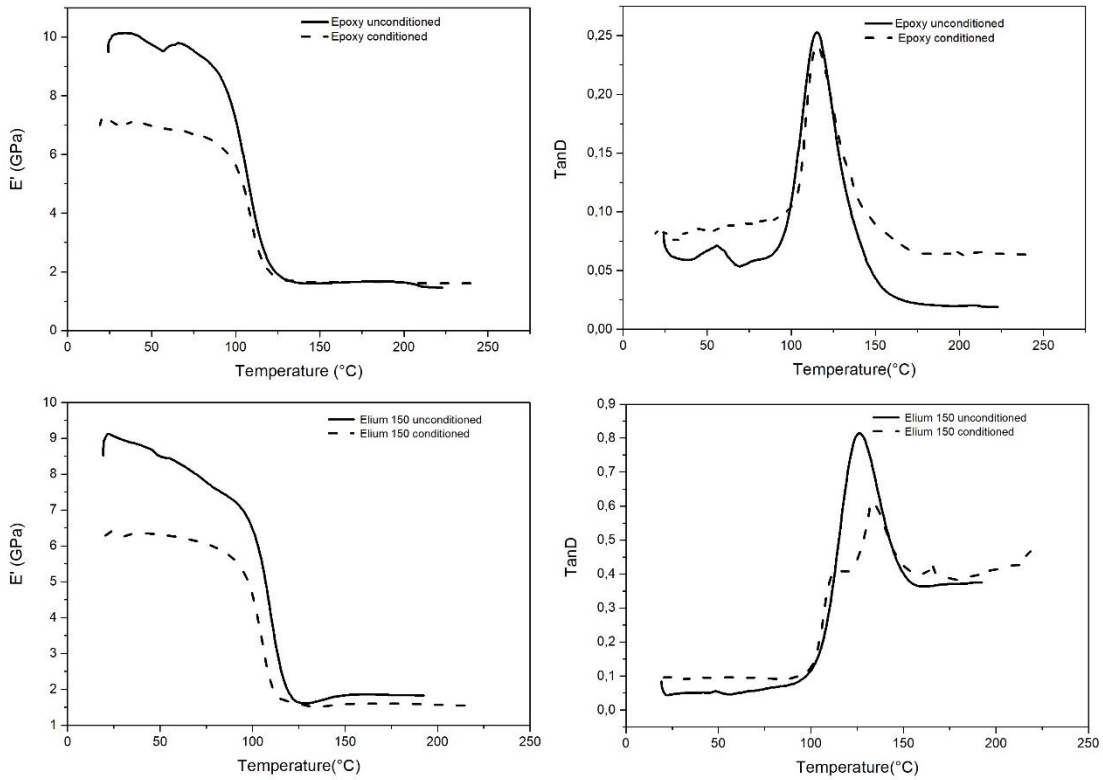

Fig 3.6 - Viscoelastic properties of composites

Considering that the increased moisture content induces a more plastic behavior of the material, weakening the intermolecular bonds, lower values of Tg are expected to be observed [112-117]. However, the weakening of the intermolecular bonds through plasticization favored the rearrange of the polymer chains in both composites. Although these differences were not as significant for the thermosetting composite as for the thermoplastic, this variation was somewhat a little more expressive.

Moisture also had a direct impact on Tanδ values. The tanδ peak was shifted to higher temperatures with an increase in moisture content but decreasing peak intensity.

The damping peak is associated with the partial loosening of the polymer structure, favoring the movement of lateral groups and small chain segments.

In the thermoplastic composite, it can be observed that the increase in moisture causes an increase in the amplitude of the tan δ curve due to the heterogeneity of the structure. This is due to the increase in the free volume between the monomer units, which in turn affects the polymerization reaction as well as the molecular and diffusion motions [115]. As Elium resin is made by block copolymers, the water absorption can promote a phase separation giving rise to a new peak and separation of the Tg, in this case, this phenomenon can be observed before the principal peak in Figure 3.6.

Therefore, low damping is observed in all conditioned composites, because there is little internal friction, already in the unconditioned composites the chains are more rigid and this implies high damping. Figure 3.7 shows typical images of the fracture region of CF/Elium 150 and CF/ Epoxy laminates after the tests.

(Intentionally left blank)

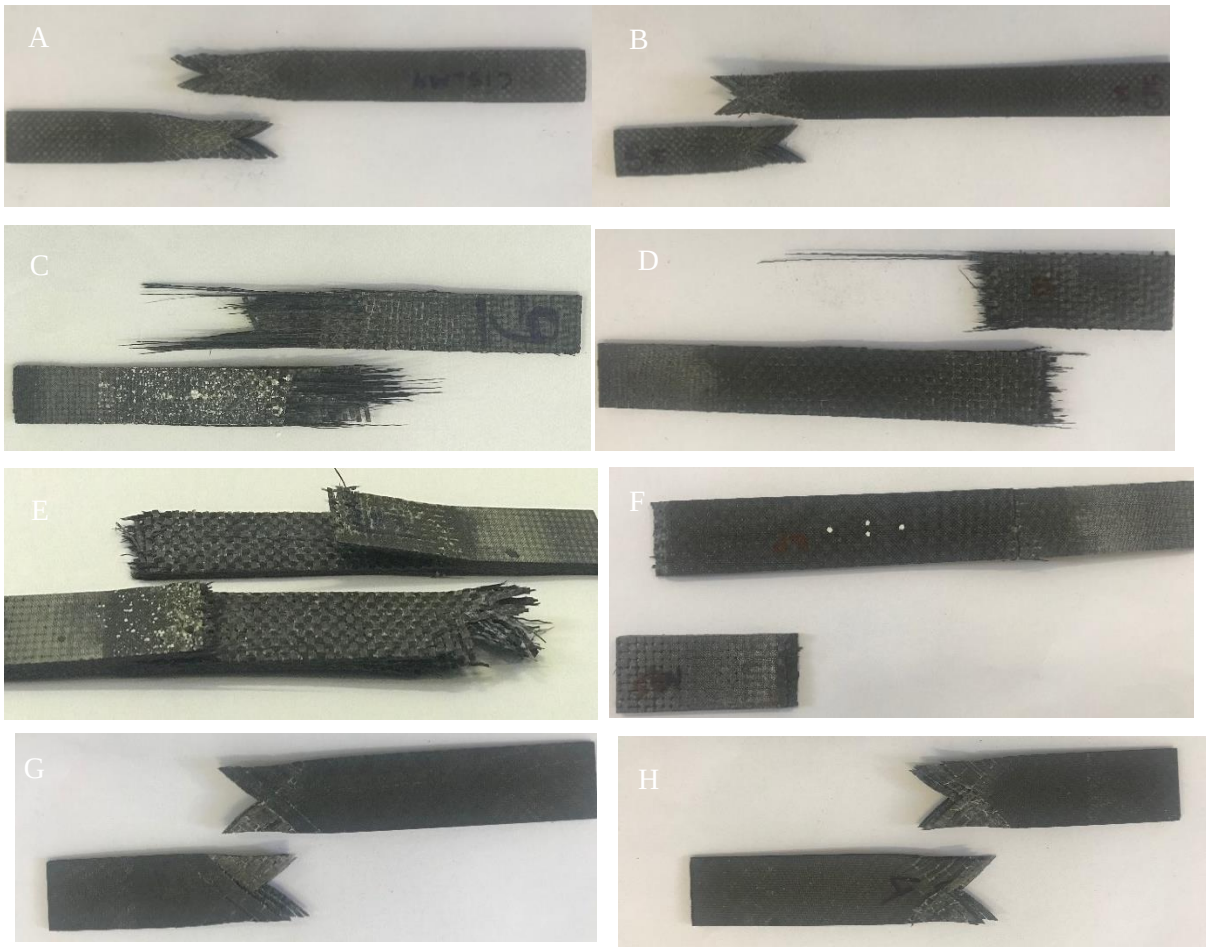

Fig 3.7 - Macroscopic images of fracture regions after mechanical tests. A- Elium conditioned (in-plane shear). B- Elium non-conditioned (in-plane shear). C- Elium conditioned (tensile strength). D- Elium non-conditioned (tensile strength). E- Epoxy conditioned

From the images of Figure 3.7, it is possible to notice the macroscopic differences in the fractographic surfaces. In this case, taking in account that the moisture can cause the matrix plasticization, it can be observed in the fracture aspects for tensile strength tests that the conditioned laminates presented more deformation in comparison to non-conditioned specimens.

As the moisture absorption in composites structures directly affects the fiber-matrix interfacial adhesion, weakening its interface, so the quality of this interface is extremely important for efficient load transference from the matrix to fibers [116]. Bradley *et al.*, studied the effect of moisture absorption on interfacial resistance in seven polymer composite systems for structural applications by subjecting them to continuous immersion in seawater. The authors observed a decrease in interfacial shear bond

strength and transverse tensile strength. This fact supports the hypothesis that moisture-induced degradation directly affects the integrity of the composite interface [117].

When subjected to tensile strength, failure in polymer composites is usually initiated from an external or internal defect (microvoids or defects in the fibers). In the close defect region, the damage develops slowly, and as the fracture propagates beyond this initial region, the propagation velocity increases. In this way, the accumulation of fracture energy causes it to propagate in different planes, producing a rougher surface (Fig 3.9 and 3.10)[31].

In addition, fractures may occur in planes other than the main fracture. In this case, the damage propagates, however, is contained in a more limited region, because the energy involved is insufficient to cause the composite to fail. Thus, in a given region, the fracture that occurs in a fiber (possibly by a defect), tends to propagate to the others through the points of contact between them. This process is called DAFFs (directly attributable fiber failures) and can be used in order to determine the direction of damage propagation in a particular region of the composite. Figure 3.8 presents an example of DAFFs observed on the fracture surfaces of each laminate. It is possible to observe the sequence of failing fibers, originating from a common fiber. In this, the origin of the failure occurs in the flat region of the fibers propagating later to other fibers or matrix that is in contact with the point of propagation [31]. As the damage energy can be different for each fiber, several directions are expected to be observed.

Other fractographic aspects as delamination and pull out are also observed in Figure 3.8. In this case, when the material is subjected to longitudinal tension, the failure starts as a transverse tension and changes progressively to the pulling and breaking of fibers, while the fracture moves, reducing the resistance to interfacial shear that occurs between fiber and matrix.

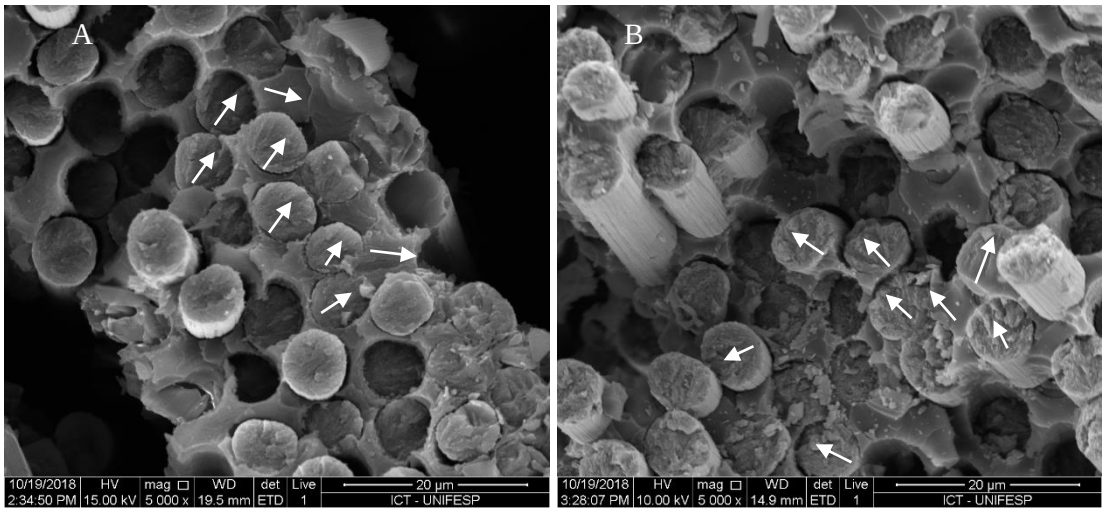

Fig 3.8 - DAFFs observed in the frature surface of CF/ Elium 150 (A) and CF/ Epoxy (B) laminates.

In general, the fractographic aspects observed in laminates with orientation 0/90°, are those that occur in the polymer matrix and were observed in both materials, such as river lines and escarps (Fig 3.9a). The river line marks are formed by several peers of unequal crack plans, which are directed to a single crack plane during the failure propagation. The crack growth is the direction in which the river line marks converges to the aspect of scarps. Besides this, aspects such as shear cusps are also observed (Fig. 3.9b). The cusps inclination indicates the direction of failure propagation and is related to shear movements during loading. For laminates with orientation ± 45°, the behavior is directly dependent on fiber/matrix interaction. In the case of strong adhesion, the fibers have their mobility restricted by the polymer matrix, failing due to the shear stresses in the plane. In this case, the fracture occurs in the matrix and leaves a thin layer on the fibers [118,31].

Figure 3.9a shows a good fiber/matrix interfacial adhesion, evidenced by the cohesive fracture of the polymeric matrix and the presence of ruptured fibers, which are covered by a thin layer of the polymeric matrix. These aspects highlight the presence of good interfacial adhesion. Thus, it is possible to assert that the failure also propagated near the fiber/matrix interface presenting fibers imprinting on the fracture surface. In

this case, in a poor interfacial fiber/matrix adhesion, which may be favored by the presence of moisture, separations between the fiber and the matrix may occur due to the limited mobility of the fibers [118,31-34].

Figure 3.9b shows the matrix plastic deformation between two fibers in the thermoplastic composite. The continuity of mechanical stress can lead to the polymer matrix rupture, resulting in the polymer deformation aspects on the fiber surface.

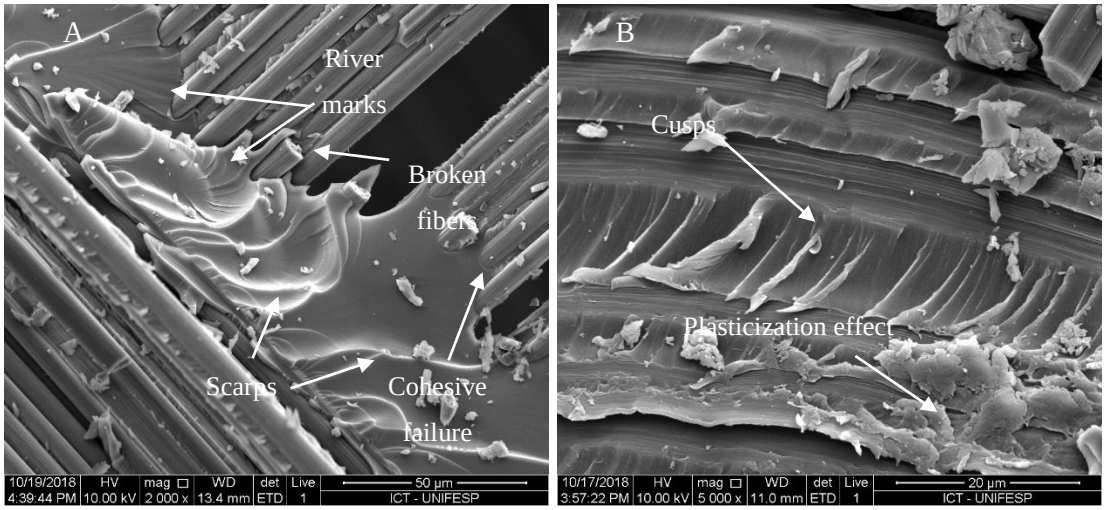

Fig 3.9 - Fracture aspects representatives of (A) the CF/Epoxy non-conditioned, (B) conditioned

The effects of water absorption in the composites can be observed in the images of Figure 3.9b and 3.10c, where it is possible to notice the presence of the mechanism of plasticization in both polymeric matrices.

In a general way, in the conditioned composites the failure propagation was observed in the interfacial region, and in all SEM images, it was possible to notice the fibers striation showing a typical interfacial failure [31-34] as a result of a failure in the fiber/matrix interface.

(Intentionally left blank)

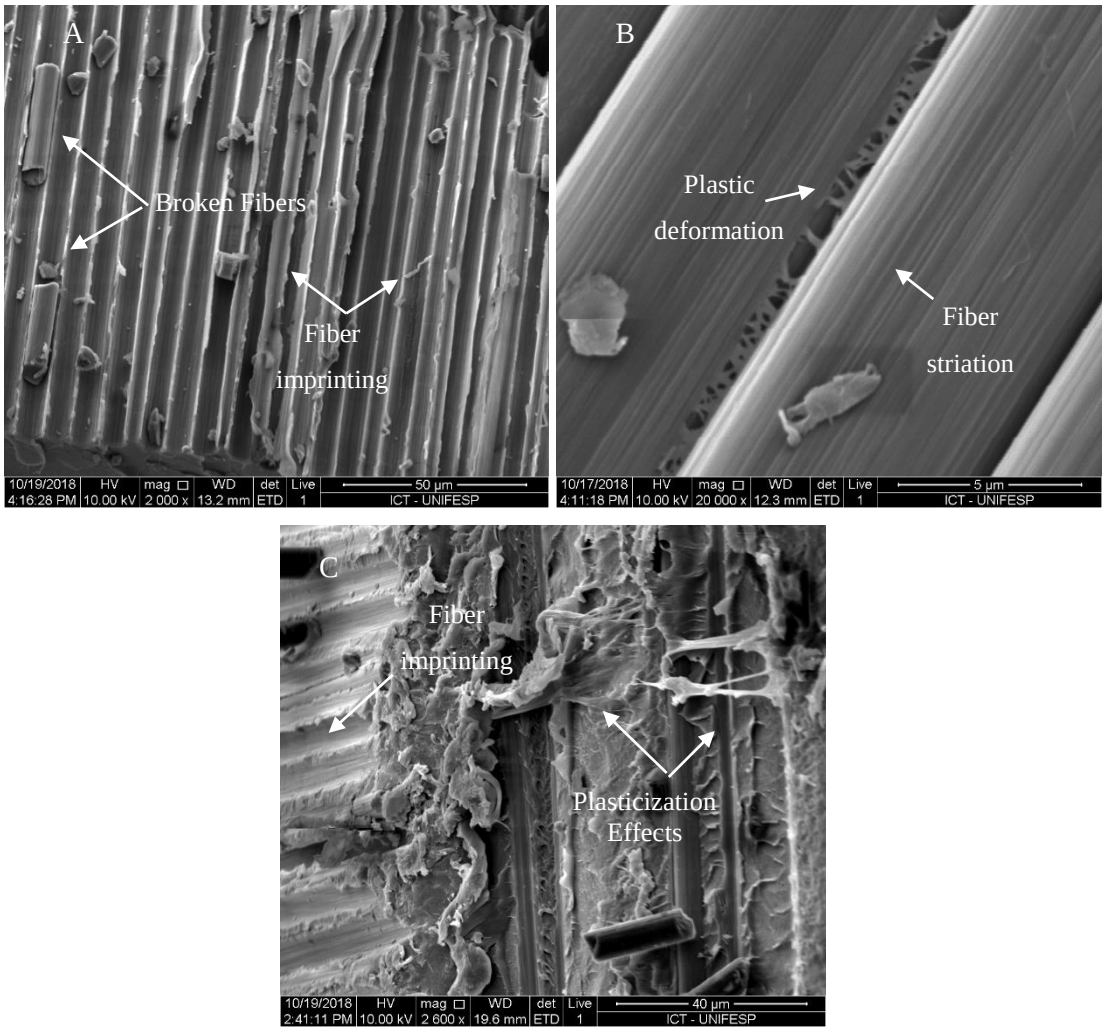

Fig 3.10 - Fracture aspects representatives (A,B),CF/Elium non-conditioned , (C) CF/Elium conditioned

3.3.2 Statistical evaluation of the influence of each condition on the response variables

Based on the study, a complete factorial arrangement was constructed. This arrangement consists of two factors and five replicates. The experimental planning is presented in Table 3.4 where the evaluated responses are also exposed. The responses in question are tensile and in-plane shear strength. The total planning then resulted in 20 evaluated specimens.

(Intentionally left blank)

Tab. 3.4 - Full factorial 2k analysis with 2 levels and 5 replicates

Experiment	Resin	Conditioning	Tensile stress (MPa)	In-Plane Shear stress (MPa)
1	epoxy	no	637.434	67.0400
2	elium	no	720.188	65.6308
3	epoxy	with	693.954	61.2700
4	elium	with	824.853	49.2941
5	epoxy	no	643.299	67.7000
6	elium	no	827.004	67.0449
7	epoxy	with	702.062	60.0800
8	elium	with	794.563	51.6634
9	epoxy	no	643.392	68.2600
10	elium	no	783.141	67.0412
11	epoxy	with	674.315	59.3100
12	elium	with	800.026	55.1687
13	epoxy	no	643.731	64.7500
14	elium	no	766.466	71.2080
15	epoxy	with	703.889	60.3200
16	elium	with	787.897	50.9823
17	epoxy	no	651.118	65.8700
18	elium	no	741.987	65.6308
19	epoxy	with	694.763	60.3100
20	elium	with	817.286	53.9007

Some important aspects can be observed from the planning done. First, Figures 3.11 and 3.12 exhibits Pareto charts for both tensile and in-plane shear responses evaluated. It can be observed that both resin and conditioning effects impact composite strength. However, there is no significant interaction (AB) in this response.

On the other hand, both factors A, B and the interaction of these two (AB) strongly impact the shear response (Figure 3.12). This is because the properties related to this test are directly dependent on the matrix, in this case, the crack can propagate in the fiber/matrix interface causing delamination in the material

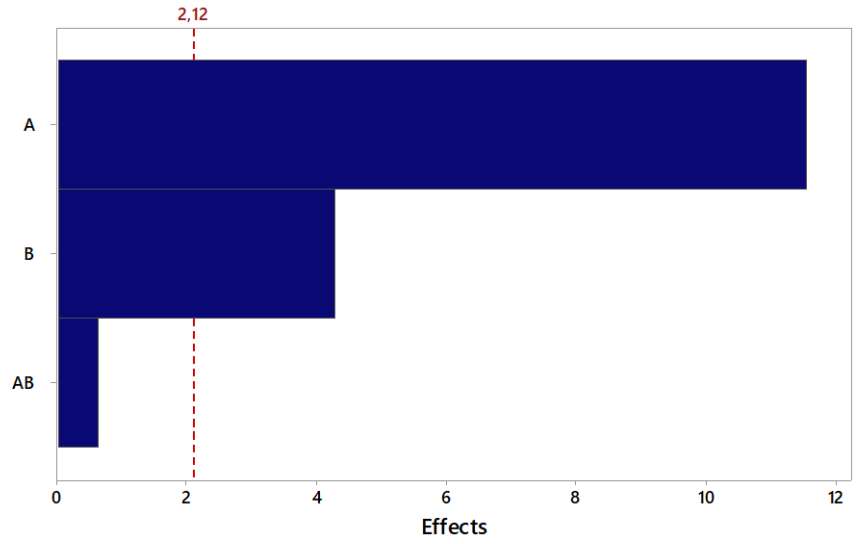

Fig 3.11 - Pareto Chart of Standardized Effects for tensile stress (terms A: Resin and B: Conditioning).

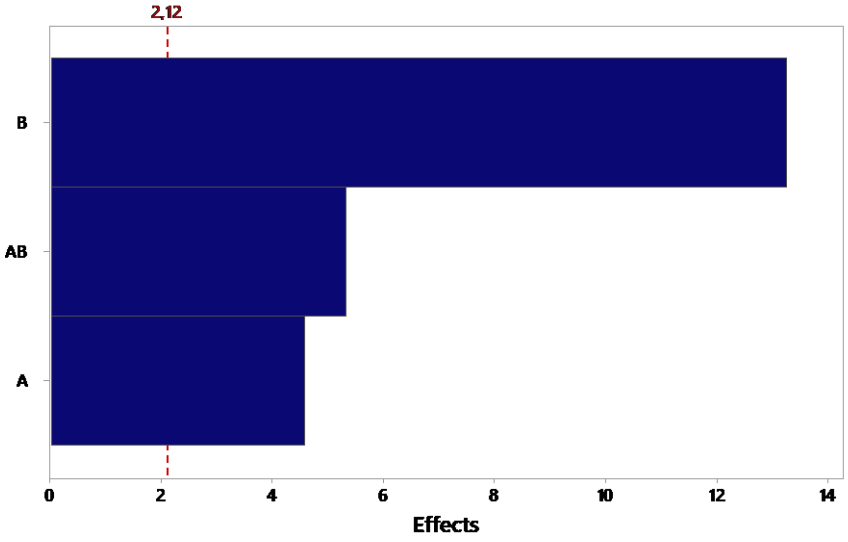

Fig 3.12 - Pareto Chart of Standardized Effects for shear stress (terms A: Resin and B: Conditioning).

In addition, Figures 3.13 and 3.14 exhibit the main effects of response factors. As already mentioned, it can be observed that the type of resin used strongly impacts the tensile strength of the material. However, the treatment condition does not have a great influence on this response.

On the other hand, it may be noted that the material conditioning positively impacts the in-plane shear strength of the laminate. However, the type of resin does not appear to have great influence.

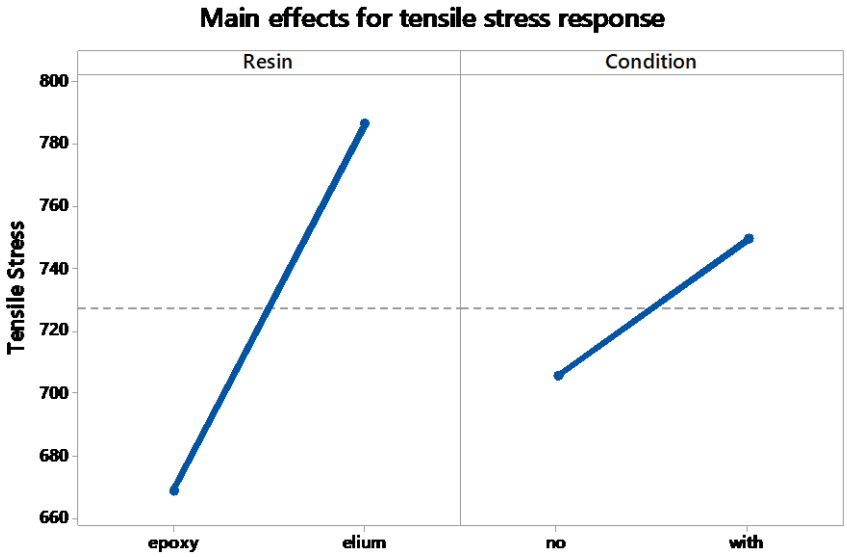

Fig 3.13 - Main effects results for tensile stress response.

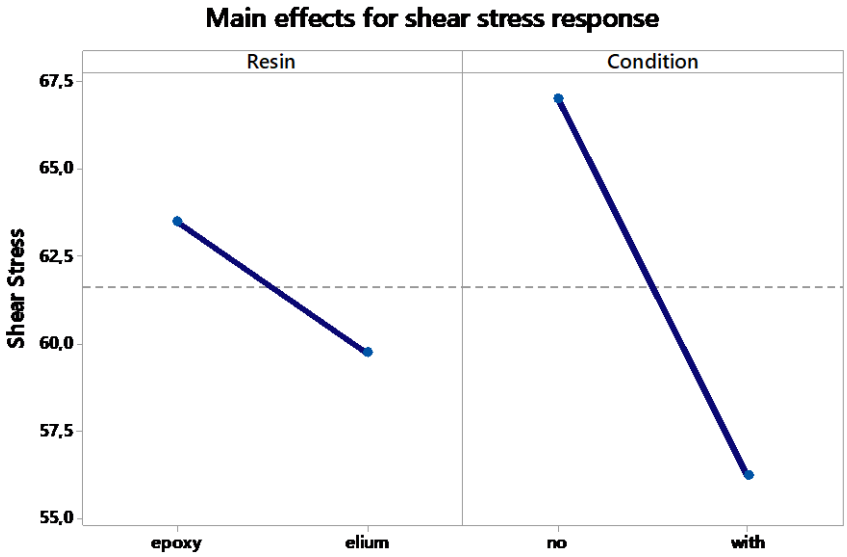

Fig 3.14 - Main effects results for shear stress response.

Finally, Figure 3.15 shows the data pooling results, i.e., dendrogram. By means of the result, one can observe the level of similarity of the variables involved in the process (the type of resin and whether or not there is conditioning). As already discussed from the foregoing results (Figure 3.7-10), it is clear that the resin type has a much more important role in the tensile strength of the material. On the other hand, it

can be observed through the dendrogram that the material conditioning positively impacts the in-plane shear strength.

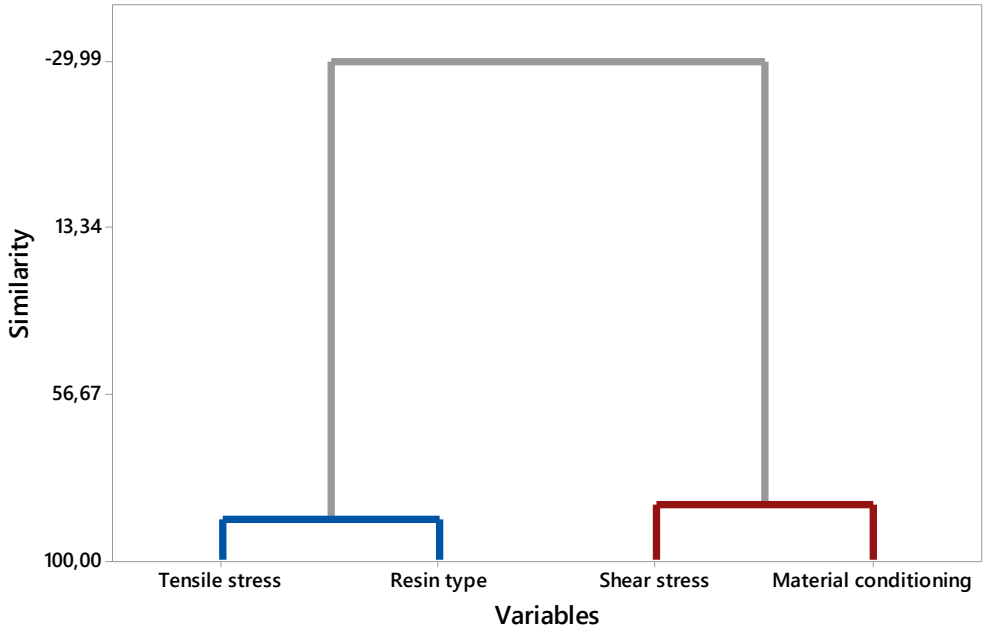

Fig 3.15 - Dendrogram results showing a similar level of all studied factors.

Then, knowing the impact of each variable in the process, one can then be able to obtain a fitting equation suitable for each evaluated response. Therefore, the goal was to obtain an optimal point, that is, a design vector composed of the factors studied in order to optimize (maximize) the responses (mechanical resistance).

Table 3.5 summarizes the overall result considering three optimization cases: i) optimization of tensile strength, ii) optimization of shear strength and iii) optimization of both resistances. For the 3 cases in question, Elium® 150 resin is obtained as optimum. In fact, this resin employed was superior to epoxy in both evaluated items. On the other hand, the material conditioning factor proved to be more interesting in terms of the tensile strength of the laminate. Overall, in multiobjective optimization, the use of Elium® 150 resin and the option of not conditioning the material are adequate.

Tab. 3.5 - Best configuration results considering the maximization of the multiple responses

Objective function	Factor A optimum	Factor B optimum
Maximize Tensile stress	Elium	With conditioning
Maximize Shear stress	Elium	Without conditioning
Maximize Tensile stress plus shear Stress	Elium	Without conditioning

3.4 Conclusion

Thermoplastic carbon fiber composite was manufactured with Elium ® 150 and its behavior in tensile strength and in-plane shear was evaluated with non-conditioned and conditioned specimens. The results were compared to traditional epoxy matrix carbon fiber composites by conducting experiments and further understanding the surface morphological fractographic aspects.

The thermoplastic laminates showed a higher tensile resistance and for the non-conditioned specimens with values 30 % higher in comparison to epoxy composites. For conditioned specimens, this difference was 14%. On the other hand, the in-plane shear properties were 30% higher for the thermosetting laminates for both conditions.

Although it is difficult to predict the impact of conditioning on the polymeric composite, it is possible to state that its effects are concentrated in the polymer matrix. For this reason, it was observed that when the mechanical behavior of the composite is dominated by the properties of the fibers, the influence is not so evident. However, in cases where the mechanical behavior is dominated by the properties of the matrix, such as in-plane shear, the effects are more pronounced.

Equally important, it was showed by the factorial analysis that the resin type has a much more important role in the tensile strength of the material. On the other hand, it

can be observed through the dendrogram that the material conditioning positively impacts the shear strength.

The performed analyses identified plastic deformations in matrix rich regions and the plasticization effects were evidenced by Fig. 3.9b and 3.10c. The pure tensile strength failure was identified in both laminates by the presence of pull out and broken fibers. Besides that, the interfacial failure evidenced by the presence of fiber striations shows that the moisture affected directly the fiber/matrix interface region.

CHAPTER 4 : PREDICTION OF TEMPERATURE-FREQUENCY-DEPENDENT MECHANICAL PROPERTIES USING ARTIFICIAL NEURAL NETWORKS

A considerable interest has been generated in recent years in the use of thermoplastic polymers as matrices in the manufacture of advanced composites that require high reliability during long-term operations. In this chapter, a new Elium® acrylic matrix developed by Arkema was studied to evaluate the accelerated test methodology based on time-temperature superposition principle. As shown in Figure 1.1 the artificial neural network has also been used to model the temperature-frequency dependence of dynamic mechanical over the wide range of temperatures and frequencies due to its complex non-linear behavior. And the long-term life prediction using master curves was used to confirm how this new material can be used considering the reference temperatures.

4.1 Introduction

The diversity of materials available for engineering applications is nowadays large in order to serve the diverse industry applications. Within this context, composites are an example of recognized interest in unconventional engineering materials. Composite materials obtained from the combination of thermoplastic or thermoset polymer matrices with fiber reinforcements have been widely used in industries due to their high performance associated with their low specific mass, with recognized advantages in terms of weight reduction, performance increase and costs reduction [120-123].

Within this scope, new materials have been developed to meet the demanding industry specifications. In this scenario, the acrylic resin Elium® 150 emerged as an advance in composites manufacture for structural applications. Because it is a liquid thermoplastic resin, its processing can be done by infusion, a technique previously

exclusive to thermosetting composites, allowing the production of large and rigid structural pieces with excellent tenacity [124]. However, under structural stress conditions, these materials can be exposed to a wide range of environmental conditions associated with various types of mechanical loading, which may cause irreversible damage to the material [60].

Thus, the durability prediction of composite material under stress becomes difficult because of the difficulty associated with short-duration tests in evaluating the effect of reducing properties over longer periods of time. In this context, the predictive analyzes of mechanical behavior over time are of extreme importance to guarantee the level of reliability of material during its service life.

One of the ways of evaluating the viscoelastic properties of polymer composites and their main transitions temperatures is the method that correlates the frequency with the viscoelastic properties, from the data obtained in DMA (Dynamic Mechanical Analysis). This analysis measures the modulus (stiffness) and damping (energy dissipation) as they are deformed under periodic stress providing quantitative information of these materials' performance [122,123,124-127].

A powerful means for the evaluation of polymers by DMA analysis is through the use of frequency multiplexing experiments. In this approach, the material is subjected to several different frequencies (usually 5 or more) in order to measure the frequency influence in time or mechanical behavior exhibited by the material. From the frequency multiplexing results in DMA, the time and temperature effects on a material can be established by the principle of time-temperature superposition. This allows the generation of master curves by which the acoustic or vibrational damping properties can be estimated [123, 126-128].

Artificial neural networks (ANN) have evolved as one of the promising artificial intelligence concepts used in real-world applications. As a powerful modeling method,

it has been applied to describe the complex phenomenon in a variety of materials related fields. Its recent applications include discovering new materials, describing the behavior of materials, structural design, and mechanical evaluation [129-134]. ANN is essentially a system that contains many simple and highly interconnected neurons that process information based on an architecture inspired by the structure of the cerebral cortex of the brain. ANN is used to derive a relationship between a set of input parameters and their output responses [135].

Sankar *et al.* studied the improvement of the material damping of glass fabric epoxy composites with particle rubber inclusions. It was observed that considerable enhancement in damping without a significant reduction in stiffness was related to lower particle size. An ANN-based prediction model was developed to predict these properties for a given frequency/temperature and particle size. The predicted values were very close to the experimental values with a maximum error of 5% [136].

The artificial neural network (ANN) technique with a feed-forward backpropagation algorithm was used by Burgaz *et al.* to examine the effect of clay composition and temperature on thermal stability, crystallinity and thermomechanical properties of poly(ethylene oxide)/clay nanocomposites. The simulated data found by ANN results confirm that nanocomposite's thermal stability increases with the decrease of enthalpy of melting and relative crystallinity. And the ANN technique was confirmed to be a useful mathematical tool in the thermal analysis of polymer/clay nanocomposites [137].

ANN model was developed by Ang *et al*. to predict the onset of failure of glass fiber reinforced epoxy composite pipes under multiaxial loadings. The developed ANN model used to input/output experimental data for training and classification. The results suggested that the ANN model can be extended to yield useful predictions of the onset of failure in composite pipes under a range of stress conditions [138].

Although many studies have been reported on the effects of temperature variation in dynamical analyses of composites materials, very few have been focused on the use of ANN as a technique to predict this value considering both temperature-frequency dependences. The work presented here assesses the potential of a long-term prediction of a new resin system with properties still little known developed for use in structural composites.

To the author's best knowledge, there are no (or very scarce) studies in the literature investigating the effects of multiplexed frequencies on viscoelastic properties of a Carbon fiber/ Elium® 150 composites using the ANN technique for temperature-frequencies inputs. Besides that, this paper investigates the dynamical response of frequency variation on long-term prediction in this new resin.

4.2 Experimental

This study was performed using a solid laminate produced by VARTM technology using Carbon fibers fabric reinforced ELIUM® 150 composites. Carbon fiber laminates were manufactured using a 0/90° plain weave fabric provided by SIGRATEX, SKDL 8051 model, with Grafil/Pyrofil TR50S and 6000 filaments (6k) per weft and warp mesh. The resin used is a low viscosity thermoplastic liquid acrylic resin commercially known by ELIUM® 150 supplied by ARKEMA. Therefore, in this work was selected with basis the 1.6% value in weigh of peroxide.

4.2.1 Dynamical mechanical analysis (DMA)

DMA analyses were performed to study the frequency and temperature influence on viscoelastic material properties, which is closely related to its mechanical performance, reflecting its structural behavior and can be used to characterize the secondary transitions chain length variations.

The tests were performed in a DMA SII SEIKO Exstar equipment, in air atmosphere using the dual cantilever assembly and bending operation mode. All tests were carried out in specimens with 45 mm long, 12 mm wide and 3mm thick. The temperature values ranged from ambient temperature to 200°C, at a heating rate of 5°C/min, and the maximum load of 4N.

The multiplex test was carried out at different frequencies (0.5,1,2, 5 and 10 Hz) in the synthetic oscillation mode. From the multiplex test, it was possible to plot the material master curve at different reference temperatures. The temperature of glass transition was measured by the 3 methods being: storage module onset (E') according to ASTM D 7028 (2007), loss module peak (E') and tan δ peak.

To determine the Tg for the construction of the master curves, the frequency was set at 1 Hz and was determined by storage module onset. The shift factors, a_T, was calculated based on the WLF (Williams–Landel–Ferry)[126] principle using Equation 1.

$$\log(a_T) = \frac{-C_1(T - T_r)}{C_2 + (T - T_r)} \quad (1)$$

where C_1 and C_2 are positive constants that depend on the material and on the reference temperature (T_r) and T is the Tg of the material.

4.2.2 Artificial Neural Networks

Artificial neural networks are computational systems, which simulate the microstructure (neurons) of a biological nervous system [128]. ANNs are composed of simple elements operating in parallel, i.e., ANNs are the simple clustering of the primitive artificial neurons. A neuron influences others' behavior through a weight. Each neuron simply computes a non-linear weighted sum of its inputs and transmits the result over its outgoing connections to other neurons.

In the training phase, the ANN system learns by adjusting the weights of the relative impact of inputs to outputs and trying many combinations of weights until a good fit to the training cases is obtained. It will be easier to understand if we draw an analogy between artificial neural networks and the standard technique of curve-fitting using polynomial functions. A polynomial can be regarded as a mapping from a single input variable to a single output variable. The coefficients in the polynomial are analogous to the weights in a neural network, and the determination of these coefficients (by minimizing a sum-of-squares error) corresponds to the process of network training. The network generally consists of several layers of neurons, namely the input layer, hidden layer or layers, and output layer. The input layer takes the input data and distributes them to the hidden layer(s) which do all the necessary computation and transmit the final results to the output layer.

Then, after several training sessions and ANN parameter modifications, the best configuration was found using 75 neurons in a single hidden layer. Figure 4.1 shows the network architecture built for the dynamic properties' prediction problem addressed in this paper. As can be seen, the temperature and frequency dependence was chosen. The hidden layer has the interconnection of artificial neurons. The output layer then provides information about the material properties of the carbon fiber/Elium® 150 specimens.

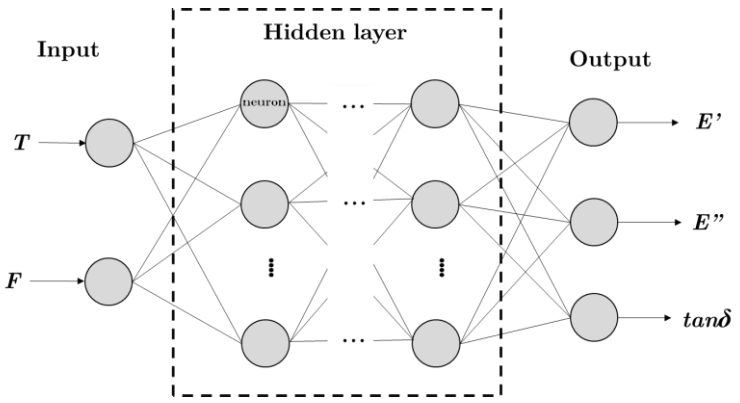

Fig 4.1 - ANN structure composed of 2 inputs, infinite hidden layers, and 3 outputs

In this work, no rule was established for choosing the optimal number of hidden layers and neurons for each layer, therefore they are decided by trial and error and the mean square error (MSE) is used to monitor the performance of ANN. While the error on the training set is driven to a very small value due to the powerful ANN learning process, a problem called over-fitting may arise, that is when new data is presented to the network the error is large. This is because the network has memorized the training examples, but it has not learned to generalize to new situations[127]. Then, after training and ANN parameter modifications, the best configuration found was found using 75 neurons in a single hidden layer as shown in Fig. 4.1 and Fig.4.2. A summary of the neural network training and testing parameter is provided in Table 1. The learning rule employed was Levenberg-Marguardt algorithm, and the gradient descent transfer function was incorporated into the network.

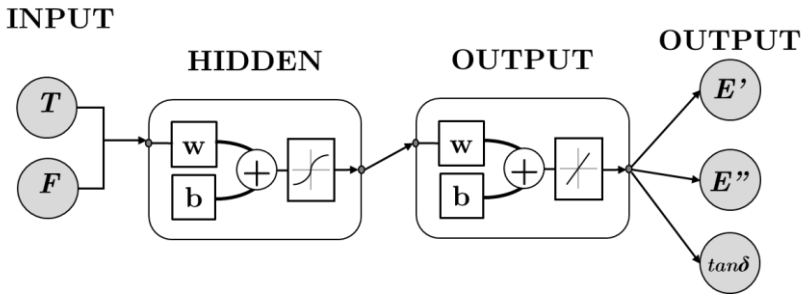

Fig 4.2 - ANN backpropagation structure.

Tab. 4.1 - Neural network parameters setup

Variable	Value
Training function	Levenberg-Marquardt
Activation function 1	Hyperbolic tangent sigmoid
Activation function 2	Linear transfer
Error (performance)	10^{-6}
Number of Neurons	75

Learning rate	0.02
Max. iterations	10000

4.3 Results and discussions

4.3.1 Accelerate damage effects on dynamic properties

The viscoelastic behavior of the CF/Elium® 150 laminate on multiplexed frequencies was performed using the dynamic-mechanical analysis technique. As the Elium® 150 is an amorphous material and show linear viscoelastic behavior, its relation at time and temperature are directly dependent on mechanical behavior, not only in the region above the glass transition temperature but also in the region below Tg. Therefore, as the viscoelastic properties of the polymer composites are directly influenced by the frequency and temperature, this behavior is related to the relaxation times of the material [121-125]. Figures 4.3, 4.4 and 4.5 show the influence of the frequency increase on the values of E', tanδ and E".

The analysis of the results of E'of Figure 4.3 and Table 4.2 shows that the frequency has a strong influence on the Tg of the laminates since its increase changes the value of the glass transition to higher temperatures. In this case, as there is a significant influence on the relaxation time, the higher the frequency, the greater the energy absorption by the polymer chains and the shorter the response time of the material [123-125, 129].

Tab. 4.2 - Tg values of CF/ Elium® 150 composite

Frequencies (Hz)	Tanδ	Tg E" (°C)	Tg E' (°C)
0.5	127.56	108.39	112.39

1	124.75	110.18	110.18
2	124.75	111.97	104.84
5	136.84	112.87	102.18
10	110.19	112.87	101.31

The storage modulus curve (E'), represented by Figure 1, shows a progressive decay indicative of a probable increase in the free volume (V_f), within the material[114,130]. At this moment, the first transitions γ and transition β can occur. These transitions are related to the relaxation of the lateral groups of the polymer chains and the movements of other small segments that are smaller than those involved in the displacements associated with Tg involving at least four carbon atoms. [114,131,144-146].

These secondary transitions can increase the glass transition with the increase of the frequency. As the Elium resin is based on poly (methyl methacrylate), this class of polymers tends to exhibit secondary transitions due to movements of the side groups. In this context, it can be explained the molecular motions responsible for the ductile behavior of some glassy polymers are probably associated with limited range motions of the major segments of the chain [114].

The progressive increase in temperature from ambient temperature causes the material expansion and consequently, the V_f continues to increase. In this case, the V_f tends to increase the bonding movements and the side chains and the localized groups of four to eight atoms of the main chain begin to have sufficient space to move and the material begins to develop some resistance. This transition is denominated as T_β and is not always so clearly defined and may be related to the Tg of a minor component in a mixture or a specific block in a block copolymer [114,125,128,142-145].

In the range between Tg and T_β, the material has the stiffness to withstand deformation and the flexibility not to shatter under tension. Thus, the decrease of the storage modulus is a consequence of a lower resistance of the material to the

deformation [123,142]. It is important to highlight that the thermal transitions only occur when the test frequency is equal to the frequency of segmental movement of the polymer chain. Therefore, an increase in the test frequency shifts the thermal transition to greater temperatures, since only then the polymer can achieve the same frequency of the assay (the temperature influences the mobility of the polymer chain and, consequently, the time related to its relaxation) [114]. In this case, it can be considered that there is a type of resonance that occurs between the frequency of forced vibration selected in the analysis and the frequency of the diffusion movement assigned to the main chain.

Thus, considering that higher frequencies favors the elastic behavior of the material, strengthening intermolecular bonds, it is expected that higher Tg values can be observed. In this case, the material undergoes molecular rearrangements in an attempt to minimize localized stress [123, 146].

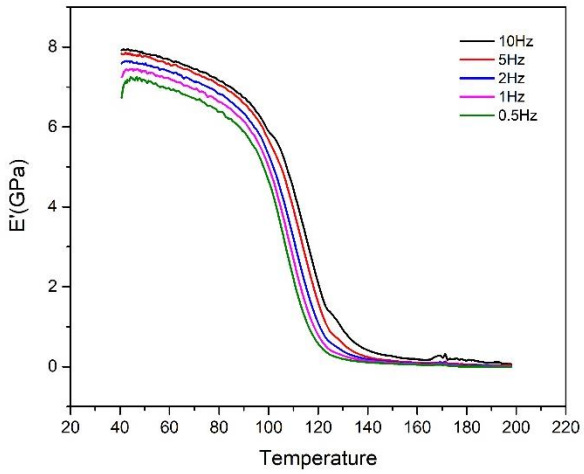

Fig 4.3 - DMA storage moduli (E') as a function of temperature (T) for CF/Elium150®composites in a multiplexed frequencies

In amorphous polymers, like poly (methyl methacrylate), it can be observed the appearance of a transition above Tg. This phenomenon is called T_{ll}, and is considered a liquid-liquid transition[125]. As above Tg the mobility tends to promote a greater structural reorganization in the material, the separation of phases can occur. In this way,

since the polymer used in this study is a block copolymer, it is intuitive that the second drop in the E' value, accentuated to high frequencies, can be related to the Tg of the copolymer. After this transition, the material enters the softening region.

Figure 4.4 shows the curves related to the loss modulus (E"), this magnitude is directly linked to the energy dissipation in heat form in the materials. In a way, the loss modulus is the result of something similar to friction losses. In the glass transition region, the molecular movements occur with greater difficulty due to the rearrangement of the molecules, which are described as molecular friction and dissipate a large part of the force. More energy is dissipated increasing the loss modulus. Less energy is stored because the molecules move with force [125,130,144,148]. Thus, high frequencies tend to cause a gradual increase in the number of intermolecular movements increasing the modulus of loss.

As shown in Figure 4.4, all curves of FC/Elium 150 composites exhibit well-defined peaks in E". However in higher frequencies is observed an enlargement of these peaks and could represent the Tg associated with the copolymer.

The Tg can also be identified as the peak value of tanδ or as the maximum of the loss modulus. It is important to note that these highs are not coincident. The maximum in tan δ is observed at a higher temperature than in E", and this occurs because the value of tanδ is associated with the ratio between E' and E" and both modules change in the transition region.

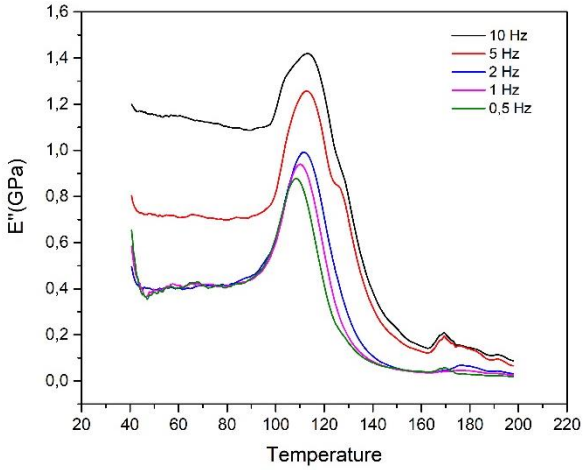

Fig 4.4 - DMA loss moduli ([E"]^') as a function of temperature (T) for CF/Elium150®composites in a multiplexed frequencies

The frequency also had a direct impact on tan δ values (Figure 4.5). The tanδ peak is shifted to higher temperatures with a frequency increase. The damping peak is associated with partial loosening of the polymer structure so that groups and small chain segments can move and also is indicative of the glass transition temperature.

The increase in frequency causes an increase in the tan δ curve due to the heterogeneity of the structure. This is due to the increase in the free volume between the monomeric units, which in turn affects the polymerization reaction as well as the molecular and diffusion motions [114,146,147].

Therefore, low damping is observed at low frequencies because there is little internal friction, already at high frequencies, the chains are more rigid, and this implies high damping.

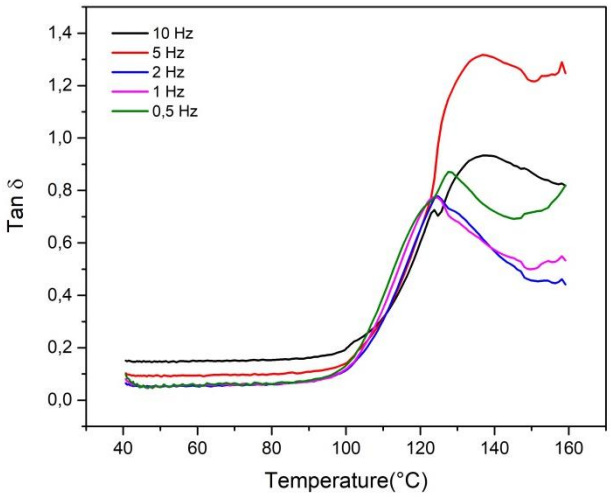

Fig 4.5 - DMA Tan δ as a function of temperature (T) for CF/Elium150®composites in a multiplexed frequency.

4.3.2 Prediction of dynamic mechanical properties using backpropagation ANN

The artificial neural network which has been developed in the present study was applied on Carbon Fiber/Elium® 5 specimens subject in DMA testing. In the training phase of the neural network, temperature and frequency were chosen as input variables with 920 values of input. The input was then preprocessed, that is, normalized in the range 0 to 1. This processing promotes a reduction in the level of uncertainty of the neural network. The output of the network is then targeted by obtaining the dynamic mechanical properties E', E" and tan(δ).

After performing the training phase, it can be verified that there were an excellent fit and regression results with experimental and trained data. The network was also trained with 1130 input data. The results showed that the application of the Levenberg-Marquardt/Hyperbolic tangent sigmoid/Linear transfer algorithm leads to a high predictive quality for the global training results. In this situation, Figure 4.6 shows the results for the training ANN phase considering a data-set corresponding to one single specimen.

It can be seen that the ANN showed a rapid rate of convergence in the early epochs. This can be explained by the characteristics of the data in question and by the correct use of the network parameters.

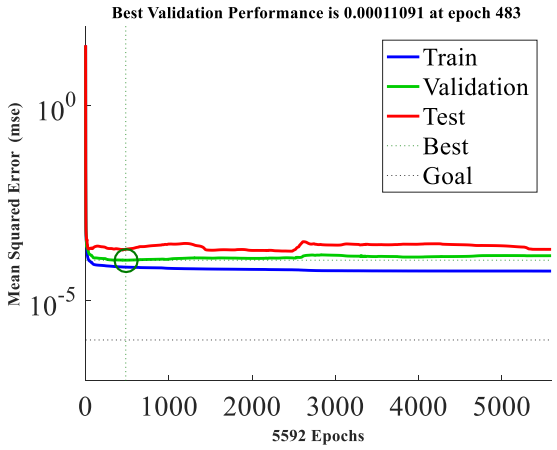

Fig 4.6 - ANN training phase results showing a 10-4 performance.

Equally important, Figure 4.7 shows the regression results in relation to the experimental data and the ANN adjustment. The excellent adjustment by means of the coefficient R^2 is clear (~1.00). This shows a relation of the physical phenomenon between input-output.

In the same way, the global error between the experimental data and those trained by ANN is shown in figure 4.8. The error was obtained by the absolute difference between the data, that is, $|E'_{experimental} - E'_{ANN}|$, $|E''_{experimental} - E''_{ANN}|$, and $|tan(\delta)_{experimental} - tan(\delta)_{ANN}|$. It can be seen a small difference for all output data E', E" and tanδ.

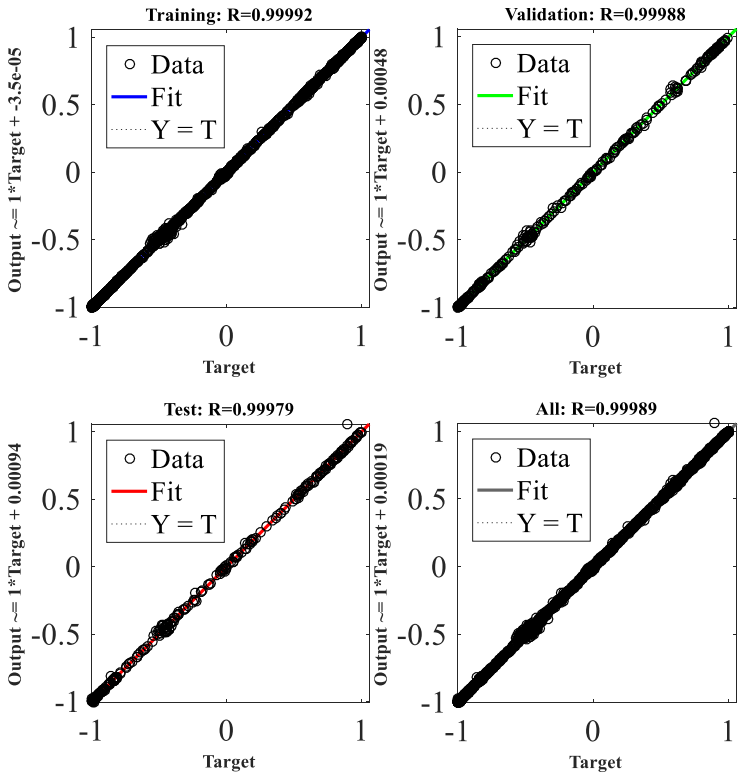

Fig 4.7 - ANN regression results showing a R^2 coefficient higher than 99%.

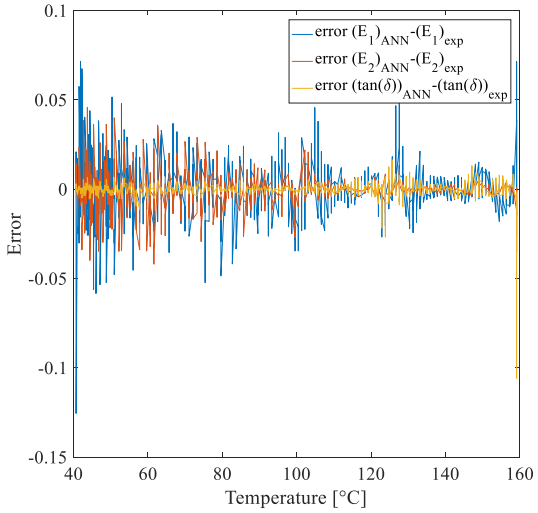

Fig 4.8 - Global difference between experimental and trained results for the dynamic mechanical properties.

Figures 4.9 to 4.11 show the general results of all outputs of the network built for the 3 outputs observed at a different frequency and test temperature. It is observed an expected and good performance of the obtained behavior. It is important to take into account the overfitting in the neural network training process. A very small performance

in training can affect the generalization of the network. It is observed that for E”, the network did not take into account the small oscillations in the temperature ranges from 40 to 100ºC.

Figure 4.9 shows the E 'values experimental and adjusted by training the network. It can be seen that the E’ data has a very well-defined pattern with an inflection temperature for all frequencies evaluated. This led to an excellent prediction result.

In almost the same way, Figure 4.10 shows the results for E”. In this case, the curve follows an intrinsic pattern, however, due to the experimental test some oscillations in E’ values up to 90°C are present. These variations (or experimental noises) contribute the network training has bypassed this problem these noises were well handled by ANN at this stage. A similar discussion can be made about the results of tan(δ) in Figure 4.11.

Figure 4.12 shows the E’ prediction results for unknown data from the neural network. It can be observed that the network was effective in predicting the behavior of E’. A small error was present as expected; however, the transition temperature can be determined efficiently by a small deviation.

Considering E", Figure 4.13 shows the results of the prediction. Similar to E’, an excellent temperature prediction was performed. There was an error concerning the value of module E " in the temperature range of 100 to 120 °C.

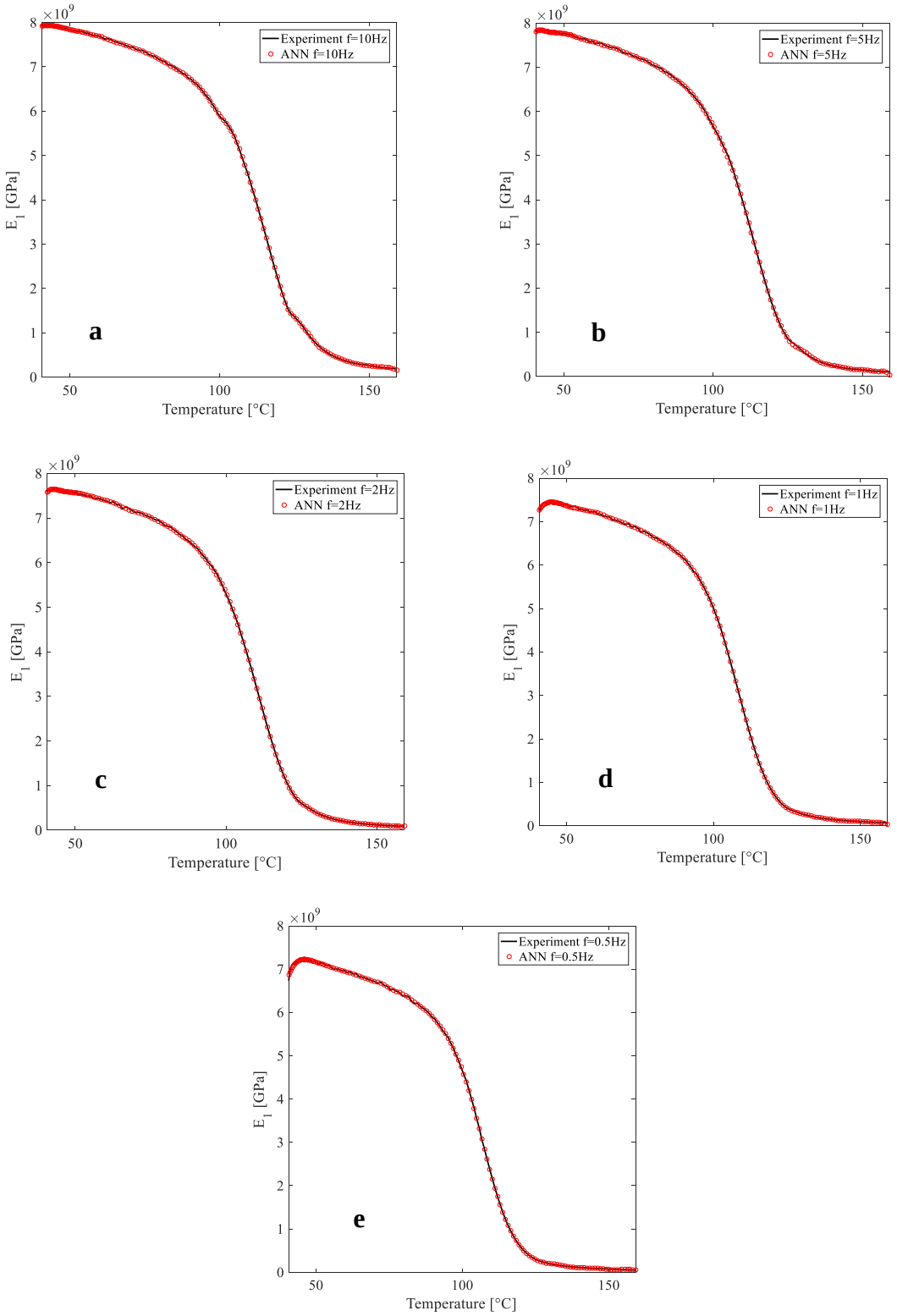

Fig 4.9 - Experimental and ANN Trained output results for E' for (a) 10 Hz, (b) 5Hz, (c) 2 Hz, (d) 1 Hz and (e) 0.5 Hz.

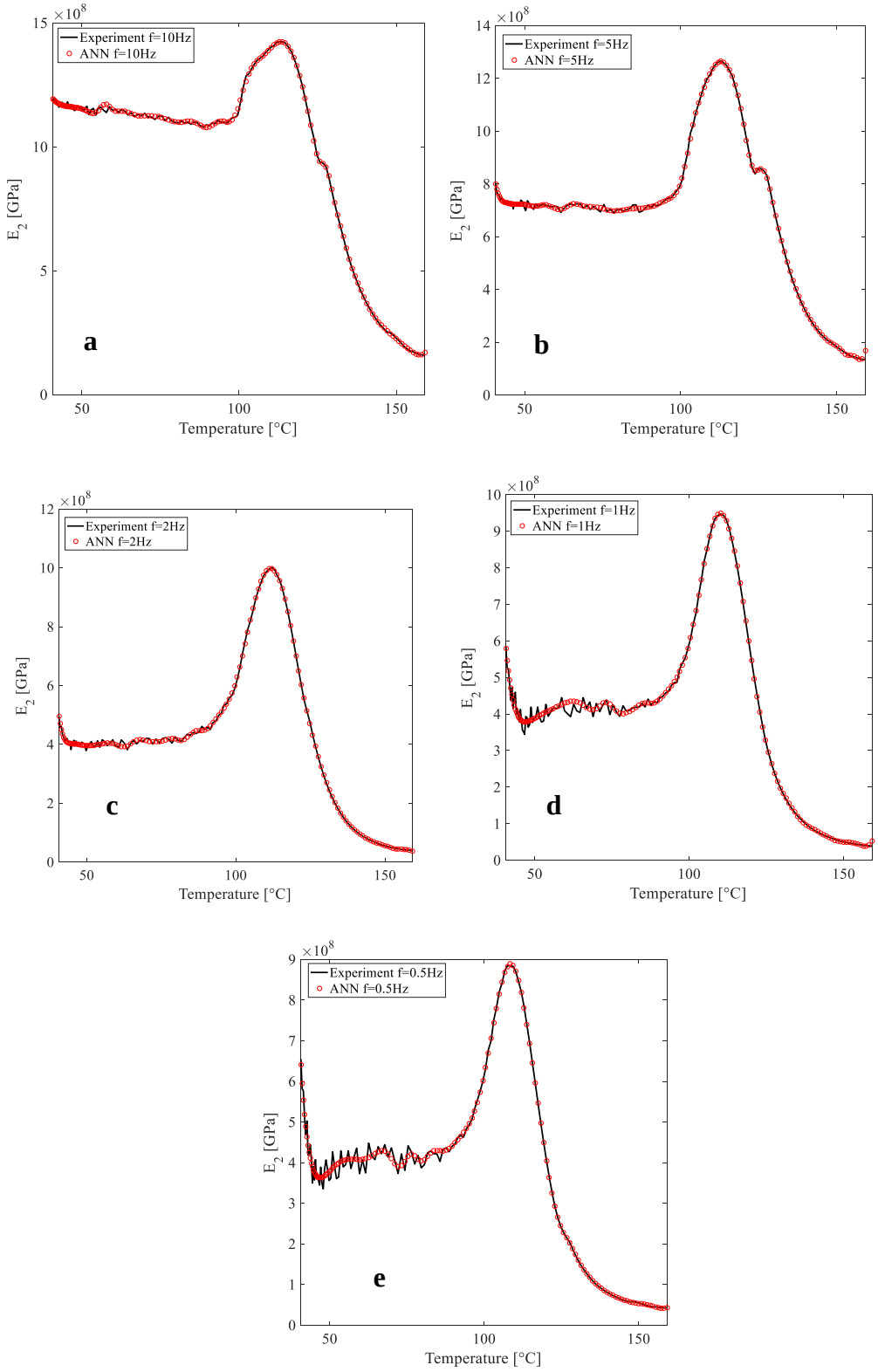

Fig 4.10 - Experimental and ANN Trained output results for E" for (a) 10 Hz, (b) 5Hz, (c) 2 Hz, (d) 1 Hz and (e) 0.5 Hz.

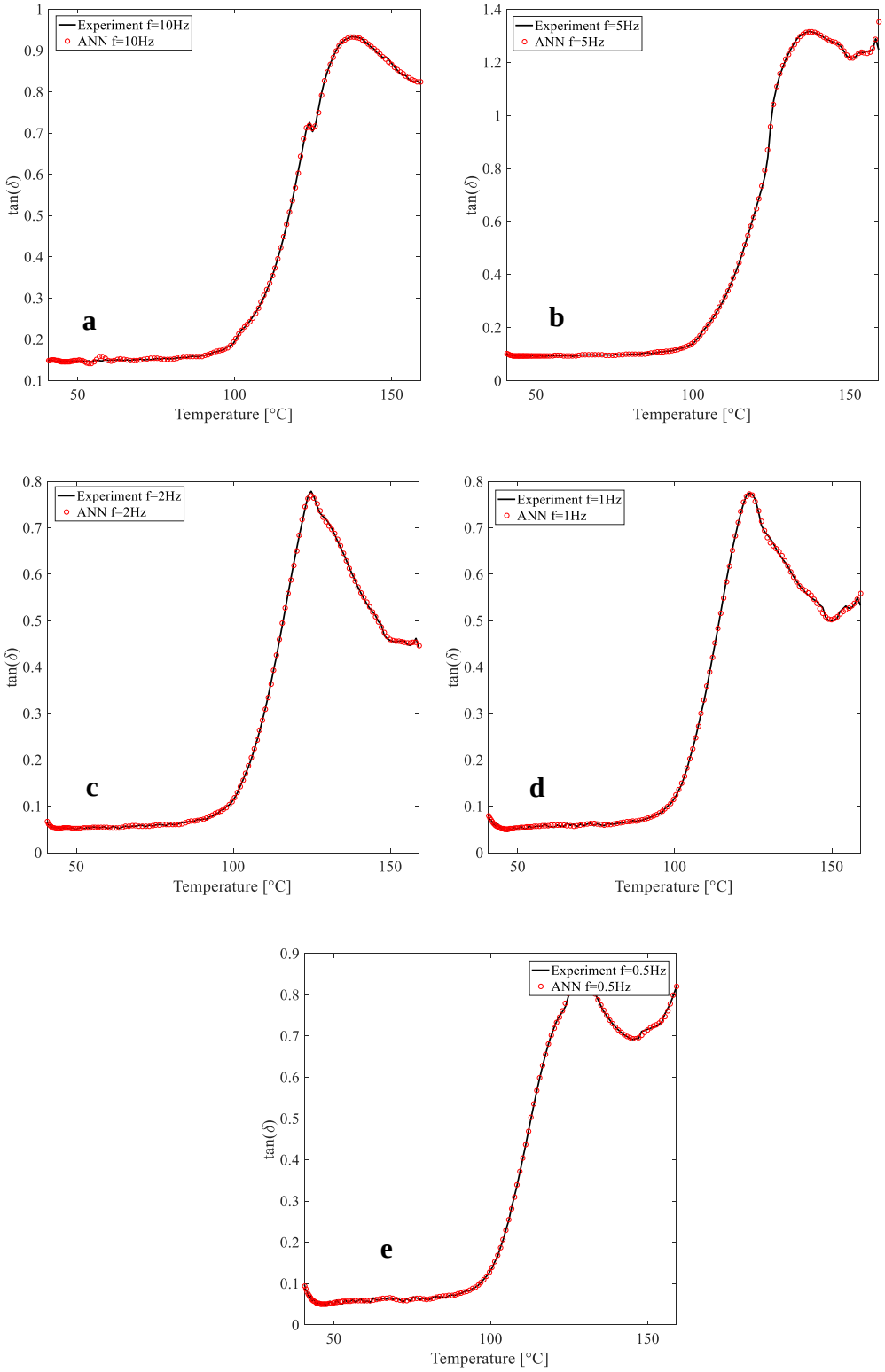

Fig 4.11 - Experimental and ANN Trained output results for tan(δ) for (a) 10 Hz, (b) 5Hz, (c) 2 Hz, (d) 1 Hz and (e) 0.5 Hz.

Finally, Figure 4.14 shows the prediction results for tanδ. Although the peak values were not so close, the network was able to predict with great efficiency the positive slope ramp around 100ºC for all 5 frequencies evaluated. For testing the network, a

completely new data set that does not belong to the training validation data was introduced. Figures 4.12 to 4.14 show the final result for the dynamic mechanical properties prediction considering non-trained data. It can be verified a satisfactory ANN-experimental prediction. The results showed that the application of the Levenberg-Marquardt algorithm leads to a high predictive quality.

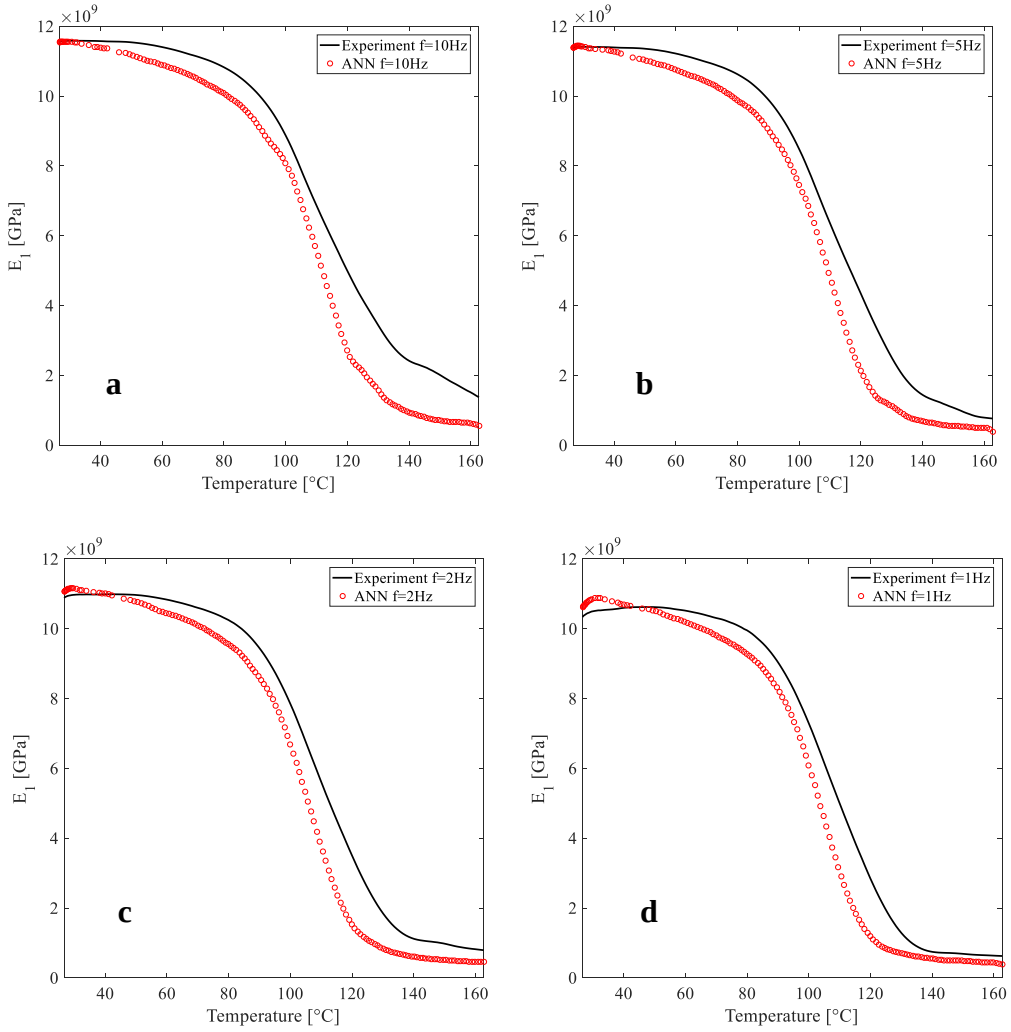

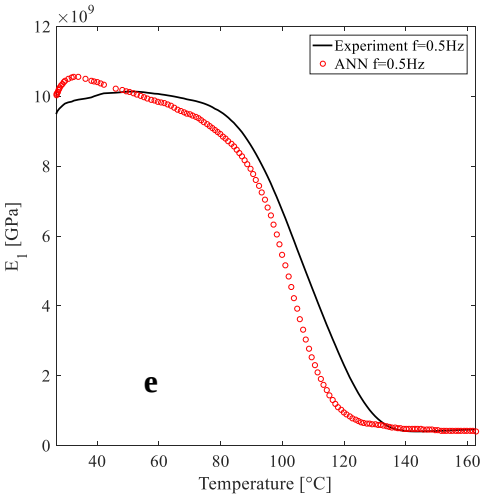

Fig 4.12 -Experimental and ANN output results for E' for (a) 10 Hz, (b) 5Hz, (c) 2 Hz, (d) 1 Hz and (e) 0.5 Hz considering non-trained experimental data

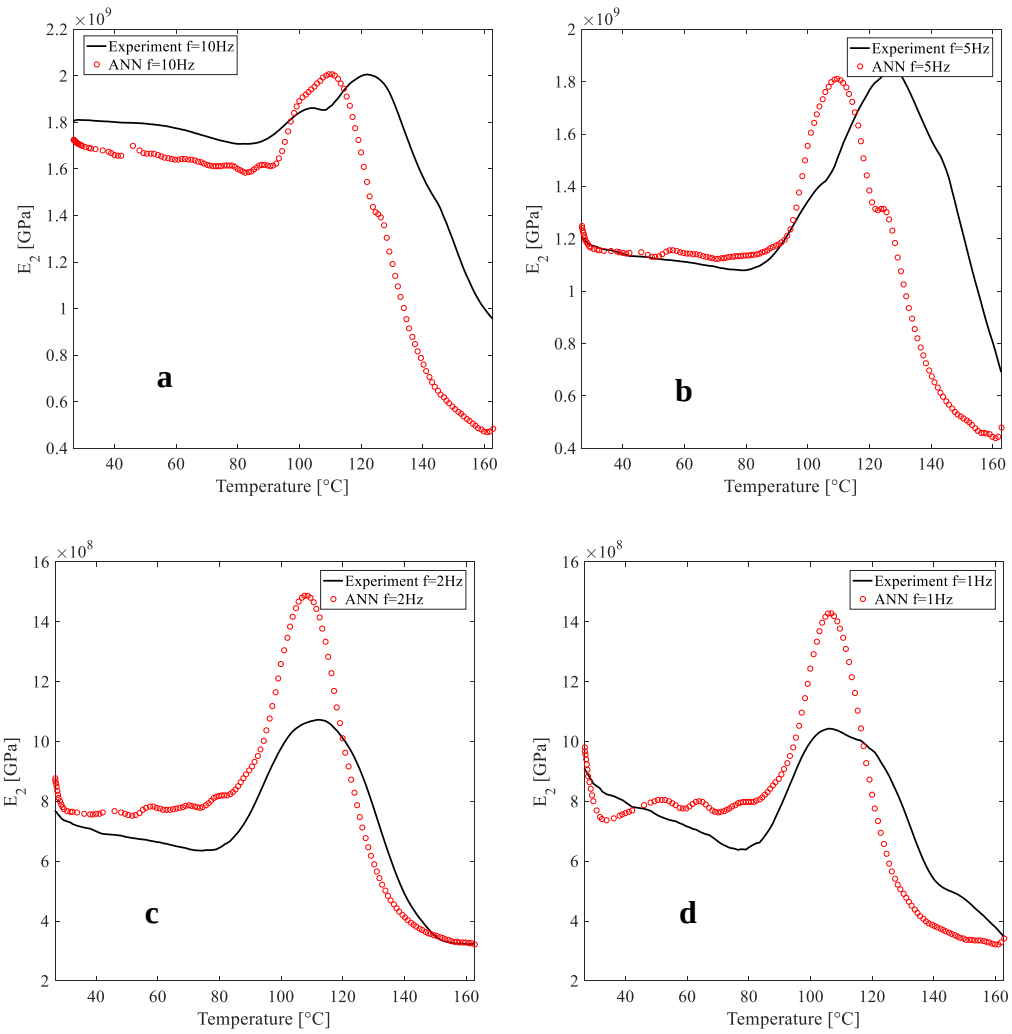

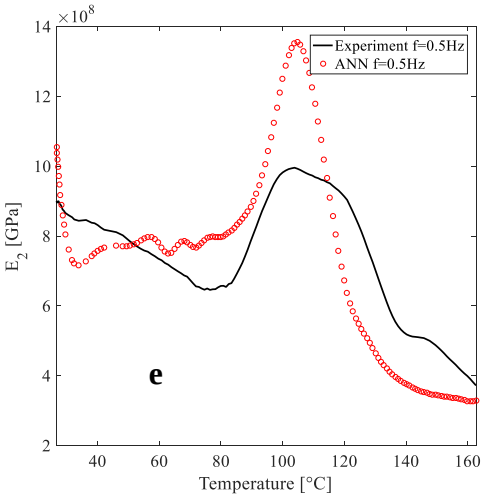

Fig 4.13 - Experimental and ANN output results for E" for (a) 10 Hz, (b) 5Hz, (c) 2 Hz, (d) 1 Hz and (e) 0.5 Hz considering non-trained experimental data.

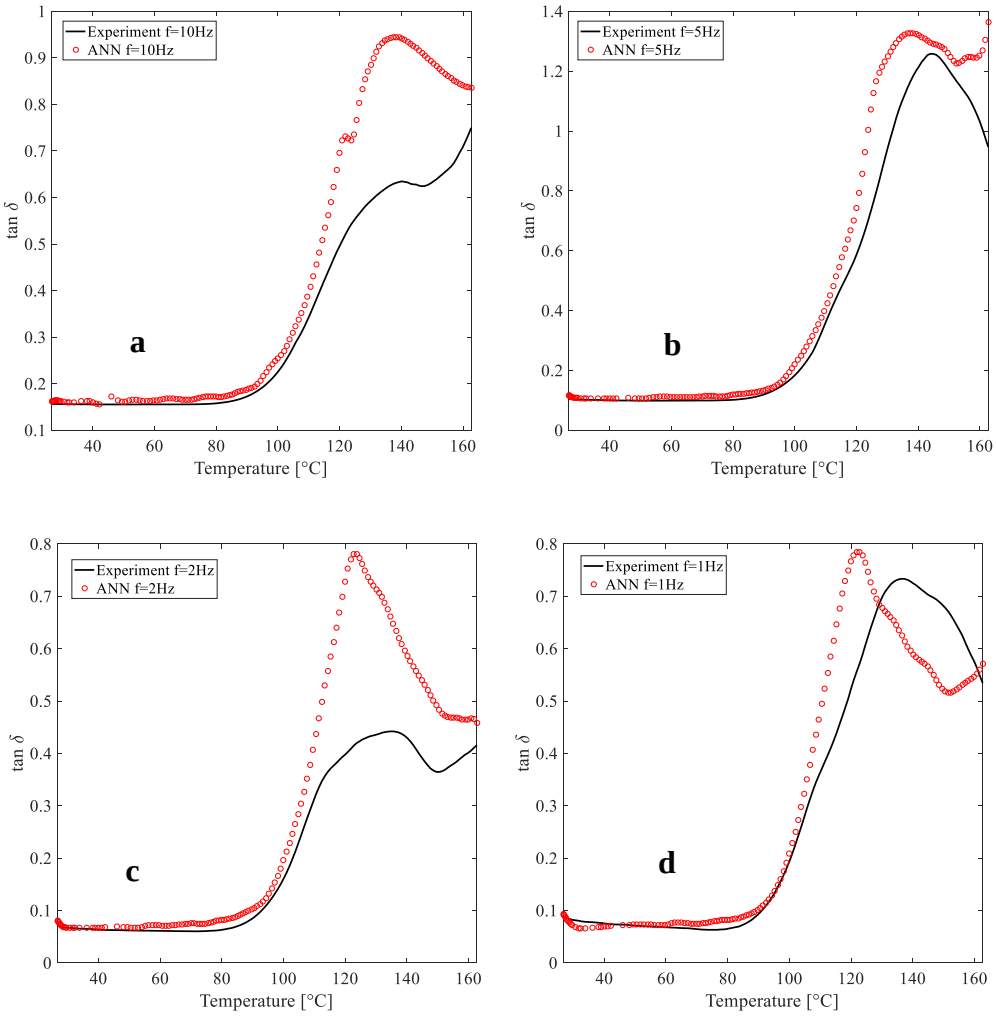

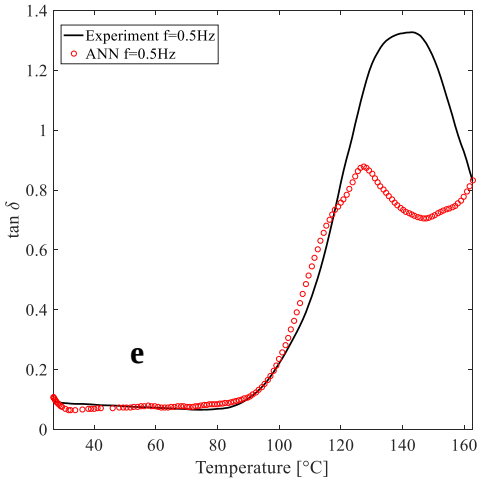

Fig 4.14 - Experimental and ANN output results for tan(δ) for (a) 10 Hz, (b) 5Hz, (c) 2 Hz, (d) 1 Hz and (e) 0.5 Hz considering non-trained experimental data.

4.3.3 Master curve construction based on the time-temperature superposition principle

Measured dynamic modulus data at multiple temperatures and frequencies were used to construct a single master curve at different reference temperatures to predict the time-dependent behavior of the composite. From the multiplexed frequencies test, it is possible to predict the time-temperature equivalence that would normally require measurements over many months or years [122,123]. Additionally, this method can be utilized to calculate the activation energy for sub-Tg and α-relaxation processes.

Based on the WLF principle and using the equation 1, it was possible to obtain the temperature shift factors, a_T, at chosen reference temperatures (considering C1 = 7 and C2 = 82 and Tg = 112 ° C). The software provides an automated procedure of best fit for determining the values of the constants WLF, C1, and C2 used to generate the master curves. Since the shift factor reflects the atomic mobility associated with the configurational rearrangements in the material, the temperature dependence of the shift factors in Figure 4.15a has a linear relationship with temperature. In this case, temperatures below the Tg tend to favor better material performance.

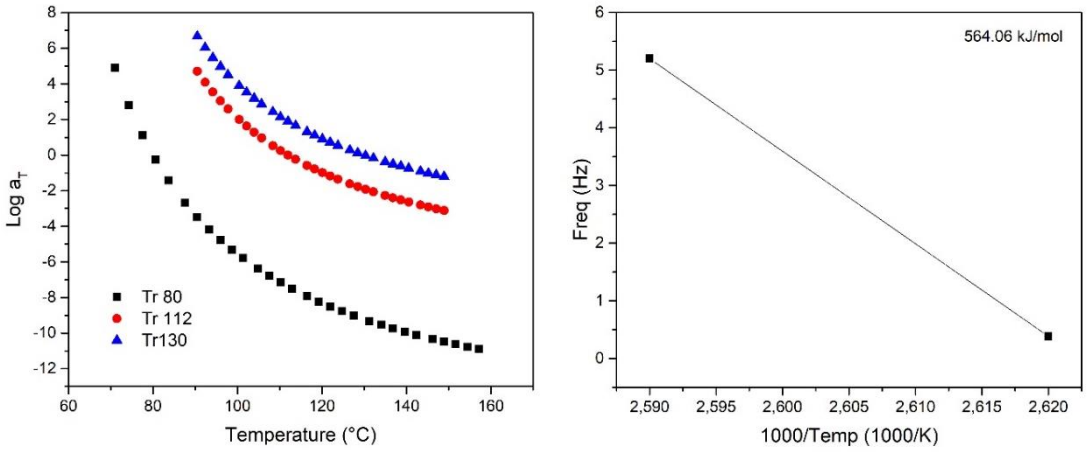

(a) (b)

Fig 4.15 - Shift factors plot from WLF-fit (a) and Activation energy at Tg of CF/ Elium® 150 composites (b).

The two data points present by the activation energy was calculated from E" a plot using Arrhenius equation directly in the software of DMA test and the graph is shown in Figure 4.15. The Arrhenius parameter is usually extracted from the shift factor graph and can express the dependence of relaxation processes. Over a limited frequency range, the response is linear and the slope of the best-fit line yields the apparent activation energy. The value of the activation energy, in this case, provides information on chain densities and on the particular nature of the relaxation transition in terms of its assignment based on molecular rotations[114,126].

From the plot of activation energy in Figure 4.15b based on glass transition temperatures at different frequencies, the activation energy required to reach the relaxation was 564.06 kJ / mol. This higher relaxation temperature can likely be attributed to the transition related to α-relaxation. In addition, it may be related to the fiber-matrix load transfer efficiency, decreasing the mobility of the polymer chain due to a lower diffusion distance atom [122,114,126]. As discussed, the interfacial adhesion observed for the results presented in the fractographic analysis may be related to the high activation energy value found.

The master curves obtained from the relaxation tests at multiplexed frequencies for three different reference temperatures (80, 112 and 130 °C) are shown in Figure 4.16. In this study, the Tg adopted as a reference (112°C) was determined by the tangent of the storage module (E') curve, in a preliminary dynamic test at 1Hz, because it is considered the most conservative way to determine this magnitude.

In Figure 4.16 it was observed that, for the reference temperature (T_f) of 80°C, the time for polymer relaxation occurs at $10^{6.93}$ s. For a reference temperature equal to Tg (112°C), the relaxation time was $10^{1.27}$ s and finally, at a temperature above Tg, about 130°C, the relaxation time was $10^{-2,35}$s, showing how the temperature can influence in the material relaxation. In this way, its applicability in the ambient temperature could increase the useful life of CF/Elium® 150 composites in several years. However, it is important to notice that the constants obtained above Tg are not useful to predict the response of the polymer to structural applications, which must necessarily operate at temperatures below Tg.

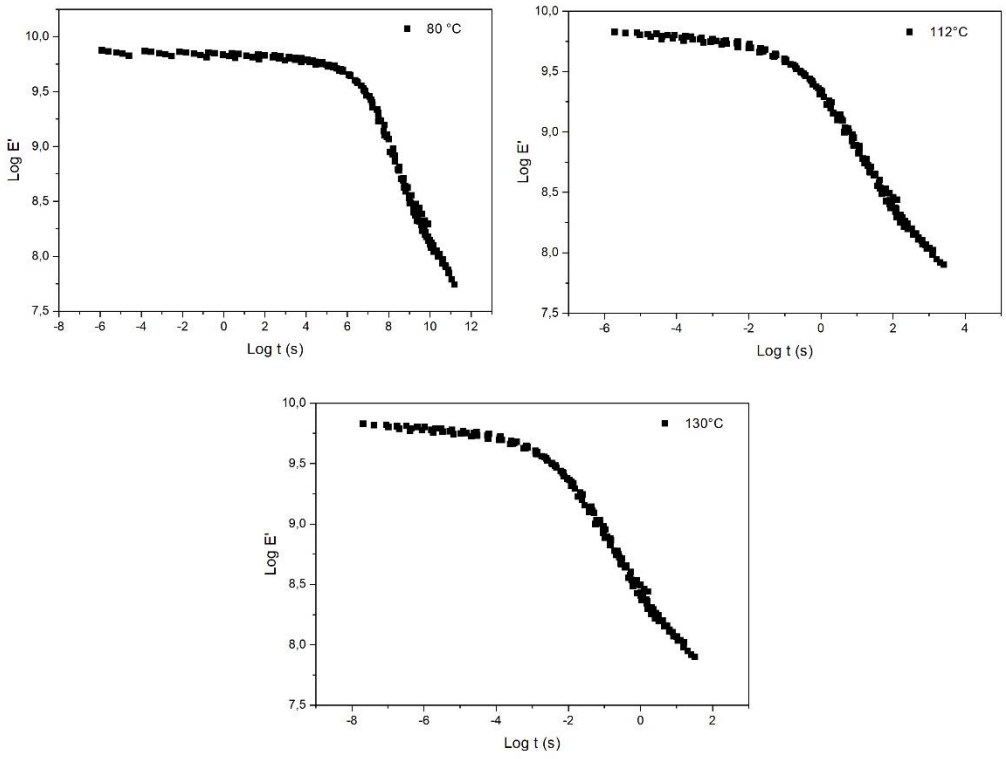

Fig 4.16 - Master curves generated at various reference temperatures

4.4 Conclusion

In this paper, the evaluation of the multiplexed frequencies and long-term life prediction of a new polymer composite was evaluated. It was observed that the Tg is strongly influenced by the frequency, is related to the free volume favored by polymer chains movement. The E' values above Tg were high and tan δ peak became broader. The great mobility above Tg promoted a greater structural reorganization in the material, and the phases separation could be observed in E" peak at high frequencies.

ANN technique has been used to model the temperature-frequency dependence of dynamic mechanical properties over the range of temperatures and frequencies. The variations of the storage modulus, loss modulus and damping factor with temperature, obtained from the dynamic mechanical analysis tests across transition temperatures in variable frequencies testing have been modeled by the back-propagation artificial neural network. An excellent agreement between the modeled and experimental data has been found over the entire investigated temperature and frequency interval. The predictive abilities of ANN models can also be used in the development of new carbon fiber/ Elium® 150 with desired dynamic mechanical properties.

A master curve was constructed for the storage modulus of composites based on the time-temperature superposition principle. The analysis shows that as the reference temperature increases, there is a decay in the material relaxation time. The activation energy value was 564.06 kJ/mol, representing the α-relaxation and can be related to a lower diffusion distance atom.

Considering acoustic or vibrational damping purposes, the master curves for this material was very informative to estimate its performance over a wide spectrum of frequencies during which the material relaxes.

CHAPTER 5 : GENERAL CONCLUSIONS

This study consisted of the investigation of laminate composites based on acrylic resins in order to compare them to well-known epoxy-based composites subject to different loading conditions. Analyses of the mechanical properties of the composites allowed the understanding of the effect of both types of matrix to fracture toughness, damage tolerance, and strength. Besides that, the effect of moisture on the tensile strength and in-plane shear of the laminated composites were analyzed. All these investigations were supported by the fractographic study of the fracture surfaces. Finally, this work investigates the effects of multiplexed frequencies on the viscoelastic properties of a Carbon fiber/ Elium® 150 composites by dynamical mechanical analyses. The response of frequency variation was used in the long-term life prediction and the ANN technique was used to support the results of the temperature-frequencies inputs.

The main conclusions of this study are as follows:

- the matrices presented different and comparable behaviors in the G_{IIc} values;
- the average G_{IIc} values for the Elium® 150 / carbon fiber composites in the NPC test were 36% lower than the values found for the thermosetting composites;
- it was possible to notice an increase in GIIc values in general for both materials;
- the epoxy-based composite presented a small change (3%) in the GIIc between the non precracked (NPC) sample and the precracked (PC). In the Elium® 150 composites, this variation was 41%;
- the thermoplastic laminate fail at lower energies compared to thermosetting laminate (NPC test), but during the crack propagation (PC test), the thermoplastic matrix exhibits a higher resistance to crack propagation;

- the pure mode II shear failure was identified in both laminates by the interfacial failure in the fiber/matrix interface region with the presence of fiber striations and by shear cusp aspects in the matrix fracture region;
- It was observed that the thermosets composites absorbed a greater amount of water as compared to thermoplastic polymers;
- the tensile strength properties were favored by the absorption of water, However, on the other hand, the in-plane shear properties presented a decrease in their values. This occurred probably because in the fiber-dependent properties, like the tensile test, the breakage of the intermolecular bonds interactions caused by plasticization in polymeric composites. In this way, plasticization tends to favor the polymer softening providing a greater matrix plastic deformation, promoting a ductile fracture of the composite;
- the tanδ peak was shifted to higher temperatures with an increase in moisture content but decreasing peak intensity;
- the fractographic aspects observed in laminates with orientation 0/90° are those that occur in the polymer matrix and were observed in both materials, such as river lines and escarps;
- both resin and conditioning effects impact composite strength. However, there is no significant interaction (AB) in this response;
- the type of resin used strongly impacts the tensile strength of the material. However, the treatment condition does not have a great influence on this response. In the other hand, the material conditioning positively impacts the in-plane shear strength but the type of resin does not appear to have great influence;
- considering three optimization cases: i) optimization of tensile strength, ii) optimization of shear strength and iii) optimization of both resistances, Elium®

150 resin is obtained as optimum and was superior to epoxy in both evaluated items;

- the frequency had a strong influence on Tg of the laminates;
- the heterogeneity of the structure promoted an increase in the tan δ curve as a frequency causes an increase in the free volume between the monomeric units, which in turn affects the polymerization reaction as well as the molecular and diffusion motions;
- the E', E" and tanδ data have a very well-defined pattern with an inflection temperature for all frequencies evaluated. This led to an excellent prediction in the ANN result and it was observed that the network was effective in predicting its behavior. A small error was present as expected;
- the master curve analysis showed that as the reference temperature increases, there is a decay in the material relaxation time.

All of these findings showed the complexity that involves the study of new material and also that several characteristics can affect the mechanical properties of the structures significantly. How it was seen in this work the type of test, the arrangement of the reinforcements, the effects of frequency and humidity are very sensitive parameters and can alter the mechanical performance of the composites significantly.

For example, as both materials were manufactured by VARTM, problems in the process step can promote the appearance of voids and it can induce the degradation of the mechanical properties and the service life of the structure. However, optimum manufacture allows a noticeable improvement of these same properties with a considerable enhancement of the damage tolerance.

This thesis focused on what was above described, as well as to help identify some of the damaging behavior of these materials in comparison to epoxy-based composites. There is still much to be done in order to the acrylic composites to reach the

same level of understanding about their mechanical behavior than the epoxy-based laminated composites. And a lot of studies start to be published. If there was a hierarchy of perspectives to be done, all the mechanical study of this type of composite structure should be placed at the top of the list.

In this context, as part of a complementary work developed by the author, an in-depth study of the self-heating method using multi-instrumentation through non-destructive methods is being developed. This method is an adequate tool to predict as quickly as possible the fatigue resistance limit of this type of material and will spread the knowledge in this area.

Finally, in a general way, this work presented an attempt to formulate documentation that can be used as a database for in-depth knowledge of this type of material. The findings and observations presented in this thesis will serve to foster an understanding of acrylic matrices in continuous fiber-reinforced composite applications. Such knowledge is essential for highlighting applications where acrylic-based composite may most effectively be employed and may provide guidance on necessary performance-enhancing modifications.

PUBLICATIONS

The publications resulting out of this thesis work are listed below:

- Barbosa, L. C. M.; Bortoluzzi, Daniel Brighenti ; Ancelotti Junior, A. C. Analysis of fracture toughness in mode II and fractographic study of composites based on Elium® 150 thermoplastic matrix. **Composites Part B-Engineering**, v. 175, p. 107082-107092, 2019.

  Impact factor: 6.86

- Barbosa, Lorena Cristina Miranda; Santos, Monique ; Oliveira, Thiago Luiz Lara ; Gomes, Guilherme Ferreira ; Ancelotti Junior, Antonio Carlos . Effects of moisture absorption on mechanical and viscoelastic properties in liquid thermoplastic resin/carbon fiber composites. **Polymer Engineering and Science (Online)**, v. 58, p. 1548, 2019.

  Impact factor: 1.92

- Barbosa, Lorena Cristina Miranda; Gomes, Guilherme ; Junior, Antonio Carlos Ancelotti . Prediction of temperature-frequency-dependent mechanical properties of composites based on thermoplastic liquid resin reinforced with carbon fibers using artificial neural networks. **International Journal of Advanced Manufacturing Technology (Internet),** v. 105, p. 2543-2556, 2019.

  Impact factor: 2.49

Submitted papers

- Barbosa, Lorena Cristina Miranda; Duque, Gabriel Roberto Vieira; Ancelotti Junior, Antonio Carlos. Mechanical behavior analysis of a bio-composite based on liquid thermoplastic resin reinforced with Jute fibers. Submitted to

Mechanical of materials – Journals – Elsevier (Paper under revision by the authors)

Conference papers

Oct'18 - ***Brazilian Congress of Engineering and Materials Science***- BARBOSA, L. C. M.; BORTOLUZZI, D. B. ; OLIVEIRA, T. L. L. ; RAPONI, O. A. ; Ancelotti Junior,A.C . Efeito do condicionamento higrotérmico nas propriedades mecânicas e viscoelásticas de compósitos termoplásticos à base de resina termoplástica líquida/fibras de carbono.

Oct'18 - ***Brazilian Congress of Engineering and Materials Science***- SANTOS, M. P. ; BARBOSA, L. C. M. ; OLIVEIRA, T. L. L. ; Ancelotti Junior,A.C . Efeito do condicionamento higrotérmico nas propriedades de cisalhamento no plano de compósitos termoplásticos à base de resina ELIUM 150/ fibras de carbono.

Oct'18 - ***Brazilian Congress of Engineering and Materials Science***- DUQUE, G. R.V. ; BARBOSA, L. C. M. ; Ancelotti Junior,A.C . Estudo e caracterização de compósitos a base de resina termoplástica líquida reforçados com fibras de sisal.

Oct'17 - ***Carbon Congress*** - BARBOSA, L. C. M.; RAPONI, O. A. ; BORTOLUZZI, D. B. ; BENEDETTO, R. M. ; Ancelotti Junior,A.C . Caracterização de compósitos termoplásticos de resina acrílica/fibras de carbono fabricados via VARTM. 2017

FURTHER WORKS

As suggestion for further works the main suggestions were:

- The construction of a numerical model in order to optimizing the parameters to enhance the mechanical performance of these structures;
- Improve the model by neural networks proposed in this work by means the adjustment of the network parameters;
- Construction of the master curve by ANN;
- Application of Elium resin in composites reinforced with natural fibers found in the region, such as jute, banana and etc.

REFERENCES

[1] Franco, L. A. L.; Graça, M. L. A.; Silva, F. S. Fractography analysis and fatigue of thermoplastic composite laminates at different environmental conditions. Materials Science and Engineering A, v. 488, p. 505-513, 2008.

[2] Costa, G. G. Avaliação da Influência dos Ciclos Térmicos nas Propriedades dos Compósitos Termoplásticos de PPS e PEI com Fibras de Carbono e Vidro Conformados por Prensagem a Quente. 2006. Master thesis - Instituto Tecnológico de Aeronáutica, São José dos Campos, 2006.

[3] Paiva, J. M. F.; Mayer, S.; Rezende, M. C. Danos por impacto de baixa energia em compósitos de carbono/epóxi de uso aeronáutico. In: Congresso brasileiro de polímeros, 7 Anais... [S.1.: s.n.]. CD-ROM. Belo Horizonte, 2003.

[4] Yilmaz,T.; Sinmazçelik,T. Bearing strength of pin-connected polymer composites subjected to dynamic loading. Polymer Composites. V. 31,p. 25-31, 2010.

[5] Yousefpour, A.; Hojjati, M.; Immarigeon, J.P. Fusion bonding/welding of thermoplastic composites. Journal of Thermoplastic Composite Materials, v. 17, n. 4, p. 303–341, 1 jul. 2004.

[6] B. C. Jin, X. Li, R. Mier, A. Pun, S. Joshi, and S. Nutt, “Parametric modeling , higher order FEA and experimental investigation of hat-stiffened composite panels,” Compos. Struct., vol. 128, pp. 207–220, 2015.

[7] M. R. Wisnom, “The role of delamination in failure of fibre-reinforced composites,” Phil. Trans. R. Soc. A, vol. 370, pp. 1850–1870, 2012.

[8] Faria, M. C. M.; Cioffi, M. O. H.; Botelho, E. C. Análise do Efeito Higrotérmico no Comportamento em Fadiga de Compósitos de PPS/Fibras de Carbono. Polímeros, vol. 22, n. 1, p. 7-12, 2012.

[9] Rezende, M. C; Botelho, E. C. O uso de compósitos estruturais na indústria aeroespacial. Polímeros: Ciência e tecnologia. v. 10, n. 2, 2000.

[10] Rezende, M. C. ; Costa, M. L.; Botelho, E. C., Compósitos Estruturais - Tecnologia e Prática, 1ª ed. São Paulo: Artliber,2011.

[11] Costa, A. P. d., Botelho, E. C., Costa, M. L., Narita, N. E. & Tarpani, J. R. A Review of Welding Technologies for Thermoplastic Composites in Aerospace Applications. Journal of Aerospace Technology and Management 4, 255-265 (2012).

[12] Liu, Y., Farnsworth, M. & Tiwari, A. A review of optimisation techniques used in the composite recycling area: State-of-the-art and steps towards a research agenda. Journal of Cleaner Production 140, 1775-1781,

[13] van Rijswijk, K. & Bersee, H. E. N. Reactive processing of textile fiber-reinforced thermoplastic composites – An overview. *Composites Part A: Applied Science and Manufacturing* 38, 666-681, doi:https://doi.org/10.1016/j.compositesa.2006.05.007 (2007).

[14] H. Helms, U. Lambrecht, The potential contribution of light-weighting to reduce transport energy consumption, Int. J. Life Cycle Assess. 12 (2006) 58–64,

[15] Bender, D., Schuster, J. & Heider, D. Flow rate control during vacuum-assisted resin transfer molding (VARTM) processing. *Compos. Sci. Technol.* 66, 2265-2271,

[16] P. Ó Máirtín, P. McDonnell, M. Connor, R. Eder, C.M. Ó Brádaigh, Process investigation of a liquid PA-12/carbon fibre moulding system, Compos. Part A 32 (2001) 915–923.

[17] K. Van Rijswijk, J.J.E. Teuwen, H.E.N. Bersee, A. Beukers, Textile fiber-reinforced anionic polyamide-6 composites. Part I: the vacuum infusion process, Compos. Part A Appl. Sci. Manuf. 40 (2008) 1–10,

[18] S. Pillay, U.K. Vaidya, G.M. Janowski, Effects of moisture and UV exposure on liquid molded carbon fabric reinforced nylon 6 composite laminates, Compos. Sci. Technol. 69 (2009) 839–846

[19] S.M. Coll, A.M. Murtagh, C.M. Ó Brádaigh, Resin film infusion of cyclic pBT composites: a fundamental study, in: Proc. SAMPE Eur. 25th Int. Jubil. Conf., Paris, 2004.

[20] H. Parton, I. Verpoest, In situ polymerization of thermoplastic composites based on cyclic oligomers, Polym. Compos. 26 (2005) 60–65.

[21] C. Yan, L. Liu, Y. Zhu, H. Xu, D. Liu, Properties of polymerized cyclic butylene terephthalate and its composites via ring-opening polymerization, J. Thermoplast. Compos. Mater. 31 (2018) 181–201,

[22] C.M. Ó Brádaigh, A. Doyle, D. Doyle, P. Feerick, Electrically-heated ceramic composite

tooling for out-of-autoclave manufacturing of large composite structures, SAMPE J. 47 (2011) 6–14

[23] A. Doyle, P. Feerick, P. Mallon, C. Ó Brádaigh, D. Doyle, A heated mould for moulding polymeric composites, a method for making such mould and its use, European Patent EP (2012)

[24] G. Gardiner, Thermoplastic Wind Blades: To be or not? 2012 https://www. compositesworld.c

[25] ARKEMA. The innovative resins for thermoplastic composites. 2014.

[26] ARKEMA,Innovative Chemistry - Elium® for RTM.2014a. AVAIABLE IN: http://www.arkema.com/en/products/product-finder/product-viewer/elium-for-rtm.

[27] C. Baley, M. Lan, A. Bourmaud, A. Le Duigou, Compressive and tensile behaviour of unidirectional composites reinforced by natural fibres: influence of fibres (flax and jute), matrix and fibre volume fraction, Mater. Today Commun. 16 (2018) 300–306,

[28] A. Aronica, D. Fossati, Effects of Resin and Processing on Mechanical Properties of Carbon Fibre Composites, Politecnico di Milano, 2015 Master's Thesis.

[29] T. Pini, F. Caimmi, F. Briatico-Vangosa, R. Frassine, M. Rink, Fracture initiation and propagation in unidirectional CF composites based on thermoplastic acrylic resins, Eng. Fract. Mech. 184 (2017) 51–58,

[30] T. Pini, F. Briatico-Vangosa, R. Frassine, M. Rink, Matrix toughness transfer and fibre bridging laws in acrylic resin based CF composites, Eng. Fract. Mech. 203 (2018) 115–125,

[31] T. Pini, F. Briatico-Vangosa, R. Frassine, M. Rink, Time dependent fracture behaviour of a carbon fibre composite based on a (rubber toughened) acrylic polymer, Procedia Struct. Integr. 2 (2016) 253–260,

[32] A. Aronica, D. Fossati, Mechanical Properties of Carbon Fiber Composite Materials, Politecnico di Milano, 2014 [Master's Thesis].

[33] A. Monti, A. El Mahi, Z. Jendli, L. Guillaumat, Mechanical behaviour and damage mechanisms analysis of a flax-fibre reinforced composite by acoustic emission, Compos. Part A Appl. Sci. Manuf. 90 (2016) 100–110,

[34] P. Davies, M. Arhant, Fatigue behaviour of acrylic matrix composites: influence of seawater, Appl. Compos. Mater. (2018) 1–12

[35] A. Chilali, W. Zouari, M. Assarar, H. Kebir, R. Ayad, Analysis of the mechanical behaviour of flax and glass fabrics-reinforced thermoplastic and thermoset resins, J. Reinf. Plast. Compos. 35 (2016) 1217–1232,

[36] S.K. Bhudolia, P. Perrotey, S.C. Joshi, Optimizing polymer infusion process for thin ply textile composites with novel matrix system, Materials (Basel) 10 (2017)

[37] M.R. Boumbimba, M. Coulibaly, A. Khabouchi, G. Kinvi-Dossou, N. Bonfoh, P. Gerard, Glass fibres reinforced acrylic thermoplastic resin-based tri-block copolymers composites: low velocity impact response at various temperatures, Compos. Struct. 160 (2017) 939–951

[38] S.K. Bhudolia, S.C. Joshi, Low-velocity impact response of carbon fibre composites with novel liquid methylmethacrylate thermoplastic matrix, Compos. Struct. 203 (2018) 696–708

[39] G. Kinvi-Dossou, R. Matadi Boumbimba, N. Bonfoh, S. Garzon-Hernandez, D. GarciaGonzalez, P. Gerard, A. Arias, Innovative acrylic thermoplastic composites versus conventional composites: improving the impact performances, Compos. Struct. 217 (2019) 1–13,

[40] W. Obande, D. Ray, C.M. Ó Brádaigh, Viscoelastic and drop-weight impact properties of an acrylic-matrix composite and a conventional thermoset composite – a comparative study, Mater. Lett. 238 (2019) 38–41

[41] S.K. Bhudolia, P. Perrotey, S.C. Joshi, Mode I fracture toughness and fractographic investigation of carbon fibre composites with liquid methylmethacrylate thermoplastic matrix, Compos. Part B Eng. 134 (2018) 246–253, https://doi.org/10.1016/j. compositesb.2017.09.057.

[42] M. Haggui, A. El Mahi, Z. Jendli, A. Akrout, M. Haddar, Damage analysis of flax fibre/ elium composite under static and fatigue testing, in: M. Haddar, F. Chaari, A. Benamara, M. Chouchane, C. Karra, N. Aifaoui (Eds.), Des. Model. Mech. Syst, Springer International Publishing, Cham 2018, pp. 681–691.

[43] M. Haggui, A. El Mahi, Z. Jendli, A. Akrout, M. Haddar, Static and fatigue characterization of flax fiber reinforced thermoplastic composites by acoustic emission, Appl. Acoust. 147 (2019) 100–110,

[44] P. Davies, Environmental degradation of composites for marine structures: new materials and new applications, Philos. Trans. R. Soc. A Math. Phys. Eng. Sci. 374 (2016) 1–14

[45] P. Davies, P.-Y. Le Gac, M. Le Gall, M. Arhant, Marine ageing behaviour of new environmentally friendly composites, in: P. Davies, Y.D.S. Rajapakse (Eds.), Durab. Compos. a Mar. Environ, vol. 2, Springer International Publishing, Cham 2018, pp. 225–237,

[46] L. Freund, V. Bouchart, H. Perrin, P. Chevrier, Hydrothermal aging of natural fibers composite: determination of diffusivity parameters, ECCM17 - 17th Eur. Conf. Compos. Mater, 2016.

[47] A. Chilali, W. Zouari, M. Assarar, H. Kebir, R. Ayad, Effect of water ageing on the loadunload cyclic behaviour of flax fibre-reinforced thermoplastic and thermosetting composites, Compos. Struct. 183 (2017) 309–319

[48] A. Chilali, M. Assarar, W. Zouari, H. Kebir, R. Ayad, Effect of geometric dimensions and fibre orientation on 3D moisture diffusion in flax fibre reinforced thermoplastic and thermosetting composites, Compos. Part A Appl. Sci. Manuf. 95 (2017) 75–86,

[49] J. Beguinel, J.-F. Gérard, F. Lortie, P. Gérard, J. Maupetit, New continuous fiber reinforced thermoplastic composites: an analysis of interfacial adhesion from the micro scale to the macro scale, 20th Int. Conf. Compos. Mater, 2015.

[50] Z. Boufaida, L. Farge, S. André, Y. Meshaka, Influence of the fiber/matrix strength on the mechanical properties of a glass fiber/thermoplastic-matrix plain weave fabric composite, Compos. Part A Appl. Sci. Manuf. 75 (2015) 28–38.

[51] T. Pini, F. Briatico-Vangosa, R. Frassine, M. Rink, Fracture toughness of acrylic resins: viscoelastic effects and deformation mechanisms, Polym. Eng. Sci. 58 (2018) 369–376,

[52] T. Pini, Fracture Behaviour of Thermoplastic Acrylic Resins and Their Relevant Unidirectional Carbon Fibre Composites: Rate and Temperature Effects, Politecnico di Milano, 2017 [Doctoral Thesis].

[53] M. Haggui, Z. Jendli, A. Akrout, A. El Mahi, Damage identification in flax fibre composite with thermoplastic matrix under quasi-static loading, Int. Conf. Adv. Mater. Mech. Manuf 2016, pp. 1–4.

[54] M. Haggui, A. El Mahi, Z. Jendli, A. Akrout, Damage characterization of flax fibre composite using linear and nonlinear vibration resonant techniques, 26th Annu. Int. Conf. Compos. Eng, 2018

[55] Q. Lin, M. Ferriol, M. Cochez, H. Vahabi, C. Vagner, Continuous fiber-reinforced thermoplastic composites: influence of processing on fire retardant properties, Fire Mater 41 (2017) 646–653,

[56] S.K. Bhudolia, P. Perrotey, S.C. Joshi, Enhanced vibration damping and dynamic mechanical characteristics of composites with novel pseudo-thermoset matrix system, Compos. Struct. 179 (2017) 502–513,

[57] G. Fredi, A. Dorigato, A. Pegoretti, Novel reactive thermoplastic resin as a matrix for laminates containing phase change microcapsules, Polym. Compos. (2019)

[58] T. Lorriot, J. El Yagoubi, J. Fourel, F. Tison, Non-conventional glass fiber NCF composites with thermoset and thermoplastic matrices, 20th Int. Conf. Compos. Mater., Copenhagen, 2015

[59] R.E. Murray, D. Penumadu, D. Cousins, R. Beach, D. Snowberg, D. Berry, Y. Suzuki, A. Stebner, Manufacturing and flexural characterization of infusion-reacted thermoplastic wind turbine blade subcomponents, Appl. Compos. Mater. 27 (2019) 1–17

[60] Cândido GM, Donadon MV, Almeida SFM, Rezende MC. Fractografia de Compósito Estrutural Aeronáutico Submetido ao Ensaio de Tenacidade à Fratura Interlaminar em Modo II. Polim.: Cienc. Tecnol 2014; 24; 65-71.

[61] Hojo M, Kageyama K, Tanaka K. Prestandardization study on mode I interlaminar fracture toughness test for CFRP in Japan. Composites 1995;26:243–55.

[62] Borowski E, Soliman E, Kandil UF, Taha MR. Interlaminar fracture toughness of CFRP laminates incorporating multi-walled carbon nanotubes. Polym. 2015;7:1020–45.

[63] Matsuda S, Hojo M, Ochiai S. Mesoscopic fracture mechanism of mode II delamination fatigue crack propagation in interlayer-toughened CFRP. JSME Int J Ser A 1997;40:423–9.

[64] Carlsson LA, Aksoy A. Analysis of interleaved end-notched flexure specimen for measuring mode II fracture toughness. Int J Fract 1991;52:67–77.

[65] Gillespie Jr JW, Carlsson LA, Pipes RB. Finite element analysis of the end notched flexure specimen for measuring mode II fracture toughness. Compos Sci Technol 1986;27:177–97.

[66] Carlsson LA, Aksoy A. Crack tip yield zone estimates in mode II interlaminar fracture of interleaved composites. Eng Fract Mech 1991;39:525–34.

[67] Benzeggagh ML, Kenane M. Measurement of mixed-mode delamination fracture toughness of unidirectional glass/epoxy composites with mixedmode bending apparatus. Compos Sci Technol 1996;56:439–49.

[68] Qian.X, Kravchenko.O.G, Pedrazzoli.D, Manas-Zloczower.I. Effect of polycarbonate film surface morphology and oxygen plasma treatment on mode I and II

fracture toughness of interleaved composite laminates. Composites Part:A 2018; 2015, 138-149.

[69] Salpekar SA, O'Brien TK, Shivakumar KN. Analysis of local delaminations caused by angle ply matrix cracks. J Compos Mater 1996;30(4):418–40.

[70] Raghu Panduranga , Kunigal Shivakumar. Mode-II total fatigue life model for unidirectional IM7/8552 carbon/epoxy composite laminate. Int. J. Fatigue 2017;94;97–109

[71] Sela N, Ishai O. Interlaminar fracture toughness and toughening of laminated composite materials: a review. Composites 1989;20:423–35.

[72] Goodsell J, Pagano NJ, Kravchenko OG, Pipes RB. Interlaminar stresses in composite laminates subjected to anticlastic bending. J Appl Mech 2013;80:041020-7.

[73] Yasaee M, Killock C, Hartley JW, Bond IP. Control of compressive fatigue delamination propagation of impact damaged composites using discrete thermoplastic interleaves. Appl Compos Mater 2015;22:559–72.

[74] Gillespie Jr JW, Carlsson LA, Smiley AJ. Rate-dependent mode I interlaminar crack growth mechanisms in graphite/epoxy and graphite/PEEK. Compos Sci Technol 1987;28:1–15.

[75] Roberts, John D. and Caserio, Marjorie C. (1977) *Basic Principles of Organic Chemistry, second edition.* W. A. Benjamin, Inc. , Menlo Park, CA.

[76] Chawla, K. K; Meyers, M. A. (2009) Mechanical Behavior of Materials. Ed. Cambridge University Press.

[77] Friedrich K, Gogeva T, Fakirov S. Thermoplastic impregnated fiber bundles: manufacturing of laminates and fracture mechanics characterization. Compos Sci Technol 1988;33(2):97-120.

[78] Hunston DL, Moulton RJ, Johnston NJ, Bascom WD. Matrix resin effects in composite delamination - mode I fracture aspects. American Society for Testing and Materials 1987; 74-94.

[79] Hinkley JA. Interface effects in interlaminar fracture of thermoplastic composites. J Reinf Plast Compos 1990;9(5):470-6.

[80] Kim KY, Ye L. Interlaminar fracture toughness of CF/PEI composites at elevated temperatures: roles of matrix toughness and fibre/matrix adhesion. Compos Part a-Applied Sci Manuf 2004;35(4):477-87.

[81] Bortoluzzi DB, Gomes GF, Hirayama D. *et al.* Development of a 3D reinforcement by tufting in carbon fiber/epoxy composites. Int J Adv Manuf Technol (2018). https://doi.org/10.1007/s00170-018-2764-5

[82] Bhudolia SK , Perrotey P, Joshi SC. Enhanced vibration damping and dynamic mechanical characteristics of composites with novel pseudo-thermoset matrix system. Comp. Struc 2017; 179; 502–513

[83] Bhudolia SK, Perrotey P, Joshi SC. Mode I fracture toughness and fractographic investigation of carbon fibre composites with liquid Methylmethacrylate thermoplastic matrix. Composites: Part B 2018;134:246-53.

[84] Pini, T, Briatico- Vangosa F, Frassine R, Rink M. Time dependent fracture behaviour of a carbon fiber composite based on a (rubber toughened) acrylic polymer.

Structural Integrity Procedia 2016; 2; 253-260. 21st European Conference on Fracture, ECF21, 20-24, Catania, Italy

[85] Barbosa, L.C.M.; Souza, S.D.B.; Botelho, E.C.; Candido, G.M.; Rezende, M.C.; Fractographic study of welded joints of carbon fiber/PPS composites tested in lap shear. Engineering Failure Analysis, v.93, p. 172-182, 2018.

[86] Greenhalgh, E. S. *Failure Analysis and Fractography of Polymer Composites*. Woodhead Publishing Limited, Cambridge.2009

[87] Purslow, D. Matrix fractography of fibre-reinforced thermoplastics, Part 1. Peel failures. *Composites* 1987;18;5;365–374.

[88] Z. Boufaida, L. Farge , S. André , Y. Meshaka. Influence of the fiber/matrix strength on the mechanical properties of a glass fiber/thermoplastic-matrix plain weave fabric composite. Composites: Part A 2015;75;28–38

[89] Pini T, Caimmi F, Briatico-Vangosa F, Frassine R, Rink M. Fracture initiation and propagation in unidirectional CF composites based on thermoplastic acrylic resins. Eng Fract Mech. 2017; 184; 51-58.

[90] F. Taheri-Behrooz, M. Esmkhani, A. Yaghoobi-Chatroodi, S.M. Ghoreishi. Out-of-plane shear properties of glass/epoxy composites enhanced with carbon-nanofibers. Polymer Testing 55 (2016) 278e286.

[91] Njuguna, Lightweight composite structures in transport (design, manufacturing, analysis and Performance), first ed., Woodhead Publishing,2016.

[92] Wolff, E.G. Moisture effects on polymer matrix composites. SAMPE Journal, v.29, n.3, may/jun., p.11-19,1993.

[93] Hygrothermal effects on the tensile strength of carbon/epoxy laminates with molded edges. Materials research, v.3, n.2, p.11-17, 2000.

[94] Abd El-baky, M., & Attia, M. (2018). Water absorption effect on the in-plane shear properties of jute–glass–carbon-reinforced composites using Iosipescu test. Journal of Composite Materials.

[95] Cheour, K, Assarar, M, Scida, D Effect of water ageing on the mechanical and damping properties of flax-fibre reinforced composite materials. Comp Struct 2016; 152: 259–266.

[96] Pierre Gilormini*, Jacques Verdu. On the role of hydrogen bonding on water absorption in polymers. Polymer 142 (2018) 164e169

[97] Enns, J. B. and Gillham, J. K. (1983), Effect of the extent of cure on the modulus, glass transition, water absorptio, and density of an amine-cured epoxy. J. Appl. Polym. Sci., 28: 2831-2846.

[98] D.W. Van Krevelen, P.J. Hoftyzer, Properties of Polymers. Their Correlation with Chemical Structure. Their Numerical Estimation and Prediction from Additive Group Contributions, 4th ed., Elsevier, Amsterdam, 2009.

[99] Frisch, H. L. (1970), “Diffusion in polymers” edited by J. Crank and G. S. Park, Academic Press, London and New York, 1968; 452 pg. J. Appl. Polym. Sci., 14: 1657-1657.

[100] Gupta, V. B., Drzal, L. T. and Rich, M. J. (1985), The physical basis of moisture transport in a cured epoxy resin system. J. Appl. Polym. Sci., 30: 4467-4493

[101] A. Tcharkhtchi, P.Y. Bronnec, J. Verdu, Water absorption characteristics of diglycidylether of butane diole3,5-diethyl-2,4-diaminotoluene networks, Polymer 41 (2000) 5777e5785.

[102] Barbero, E., Fernández-Sáez, J., & Navarro, C. (2000). Statistical analysis of the mechanical properties of composite materials. Composites Part B: Engineering, 31(5), 375-381.

[103] Lemon, G. H., Norton, J. M., & Waddoups, M. E. (1980). Statistical Analysis Methods for Characterizing Composite Materials. In Fibrous Composites in Structural Design (pp. 733-759). Springer, Boston, MA.

[104] Vauthier, E., Abry, J. C., Bailliez, T., & Chateauminois, A. (1998). Interactions between hygrothermal ageing and fatigue damage in unidirectional glass/epoxy composites. Composites Science and Technology, 58(5), 687-692.

[105] Phoenix, S. L. (2000). Modeling the statistical lifetime of glass fiber/polymer matrix composites in tension. Composite structures, 48(1-3), 19-29.

[106] Kawai, M., & Yano, K. (2016). Anisomorphic constant fatigue life diagrams of constant probability of failure and prediction of P–S–N curves for unidirectional carbon/epoxy laminates. International Journal of Fatigue, 83, 323-334.

[107] de Souza, A., Gomes, G. F., Peres, E. P., Isaías, J. C., & Ancelotti, A. C. (2019). A numerical-experimental evaluation of the fatigue strain limits of CFRP subjected to dynamic compression loads. The International Journal of Advanced Manufacturing Technology, 1-19.

[108] Athijayamani, A., Thiruchitrambalam, M., Natarajan, U., & Pazhanivel, B. (2009). Effect of moisture absorption on the mechanical properties of randomly

oriented natural fibers/polyester hybrid composite. Materials Science and Engineering: A, 517(1-2), 344-353.

[109] Fernandes, R. L., De Moura, M. F. S. F., & Moreira, R. D. F. (2016). Effect of moisture on pure mode I and II fracture behaviour of composite bonded joints. International Journal of Adhesion and Adhesives, 68, 30-38.

[110] Eftekhari, M., & Fatemi, A. (2016). Tensile behavior of thermoplastic composites including temperature, moisture, and hygrothermal effects. Polymer Testing, 51, 151-164.

[111] Montgomery, D. C. (2017). Design and analysis of experiments. John wiley & sons

[112] Wel, van der, G. K., & Adan, O. C. G. (1999). Moisture in organic coatings - a review. Progress in Organic Coatings, 37(1-2), 1-14.

[113] Vanlandingham, M. R., Eduljee, R. F. and Gillespie, J. W. (1999), Moisture diffusion in epoxy systems. J. Appl. Polym. Sci., 71: 787-798.

[114] Menard KP. Dynamic mechanical analysis: a practical introduction. CRC press, 2008.

[115] T. Hatakeyama and F. X. Quinn, `Thermal Analysis Fundamentals and Applications to Polymer Science', John Wiley and Sons, Chichester, UK, 1994.

[116] A. Apicella, in `International Encyclopedia of Composites', ed. S. M. Lee, VCH, New York, 1990, vol. 2, pp. 46.

[117] Raponi OA, Barbosa LCM, Souza BR, Junior ACA. Study of the influence of initiator content in the polymerization reaction of thermoplastic liquid resin for advanced composite manufacturing. Adv Polym Technol. 2018;37:3579–3587.

[118] Barbosa, L.C.M.; Souza, S.D.B.; Botelho, E.C.; Candido, G.M.; Rezende, M.C.; Fractographic study of welded joints of carbon fiber/PPS composites tested in lap shear. Engineering Failure Analysis, v.93, p. 172-182, 2018.

[119] Bradley,W.L.; Grant,T.S. The effect of the moisture absorption on the interfacial strength of polymeric matrix composites. Journal of Materials Science, 1995, v.30, 5537-5542.

[120] Rezende MC, Costa ML, Botelho EC. Compósitos estruturais: tecnologia e prática. São Paulo: Artlibre Editora, 2011. 396p.

[121] Marshall AC. Composite structures in homebuilt sport aircraft. In: International sample symposium and exhibition, 32., 1987. Tokyo. Proceedings. Covina: SAMPE, 1510-1518 .

[122] Ferry JA. Viscoelastic properties of polymers. 3rd ed. New York: John Wiley 1980. 672p.

[123] Feng J, Guo Z. Temperature-frequency-dependent mechanical properties model of epoxy resin and its composites. Composites: Part B, 2016 , 85,161-169.

[124] Rouleau L, Deu JF,Legay A, Le Lay F. Application of Kramers–Kronig relations to time–temperature superposition for viscoelastic materials. Mech. Mater, 2013, 65, 66-75.

[125] Cassu SN, Felisberti MI. Comportamento dinâmico-mecânico e relaxações em polímeros e blendas poliméricas. Quim. Nova 2005, 28, 2, 255-263.

[126] Williams ML, Landel RF, Ferry JD. The Temperature Dependence of Relaxation Mechanisms in Amorphous Polymers and Other Glass-forming Liquids J. Amer. Chem. Soc.1955, 77, 3701.

[127] Idicula M, Malhotra SK, Joseph K, Thomas S. Dynamic mechanical analysis of randomly oriented intimately mixed short banana/sisal hybrid fibre reinforced polyester composites. Compos Sci Technol 2005;65:1077–1087.

[128] Zhang, Z., Friedrich, K., Artificial Neural Networks Applied to Polymer Composites: A Review, 2003 Compos Sci and technol, v. 63, pp. 2029-44.

[129] Goh, A.T.C., Back-propagation Neural Networks for Modeling Complex Systems, Artificial Intelligence in Engineering,1995, v. 9, pp. 143-51.

[130] Yang, H.J., Roe, B.P., Zhu, J., "Studies of Stability and Robustness for Artificial Neural Networks and Boosted Decision Trees", Nuclear Instruments and Methods in Physics Research Section A: Accelerators, Spectrometers, Detectors and Associated Equipment, 2007 v. 574, n. 2, pp. 342-9.

[131] Xu, X. and Gupta, N. Artificial Neural Network Approach to Predict the Elastic Modulus from Dynamic Mechanical Analysis Results. Adv. Theory Simul.,2019 :2: 1800131

[132] Zhang, Z., Klein, P., & Friedrich, K. Dynamic mechanical properties of PTFE based short carbon fibre reinforced composites: experiment and artificial neural network prediction. Compos Sci and Technol, 2002: 62(7-8), 1001–1009.

[133] Kopal, I.; Harničárová, M.; Valíček, J.; Kušnerová, M. Modeling the Temperature Dependence of Dynamic Mechanical Properties and Visco-Elastic Behavior of Thermoplastic Polyurethane Using Artificial Neural Network. Polymers 2017, 9, 519.

[134] Altinkok, N. Use of Artificial Neural Network for Prediction of Mechanical Properties of α-Al2O3 Particulate-reinforced Al–Si10Mg Alloy Composites Prepared by using Stir Casting Process. Journal of Composite Materials, 2006; 40(9), 779–796.

[135] Farhanaa N.I.E, Abdul Majida M.S., Paulraja M.P., Ahmadhilmib E., Fakhzana M.N., Gibson A.G..A novel vibration based non-destructive testing for predicting glassfibre/matrix volume fraction in composites using a neural networkmodel. Composites structures, 2016, 144, 96-107.

[136] Ihesiulor, O. K., Shankar, K., Zhang, Z., & Ray, T. Delamination detection with error and noise polluted natural frequencies using computational intelligence concepts. Composites Part B: Engineering,2014; 56, 906-925.

[137] H. Ravi Sankar , R.R. Srikant , P. Vamsi Krishna , V. Bhujanga Rao, P. Bangaru Babu. Estimation of the dynamic properties of epoxy glass fabric composites with natural rubber particle inclusions. International Journal of Automotive and Mechanical Engineering (IJAME), 2013, 7, 968-980.

[138] Engin Burgaz , Mehmet Yazici , Murat Kapusuz , Sevim Hamamci Alisir , Hakan Ozcanb Prediction of thermal stability, crystallinity and thermomechanical properties of poly(ethylene oxide)/clay nanocomposites with artificial neural networks. Thermochimica Acta, 2014, 575, 159-166.

[139] Ang J.Y., Abdul Majid M.S., Mohd Nor A., Yaacob S., Ridzuan M.J.M. First-ply failure prediction of glass/epoxy composite pipes using an artificial neural network model. Composites structures, 2018, 200, 579-588.

[140] Zhang, Z., Shankar, K., Ray, T., Morozov, E. V., & Tahtali, M. Vibration-based inverse algorithms for detection of delamination in composites. Compos Struct, 2013 102, 226-236.

[141] Chen L, Chiu TC, Chen TC, Chung MH, Yang PF, Lai YS. Using DMA to simultaneously acquire Young's relaxation modulus and time-dependent Poisson's ratio of a viscoelastic material. Procedia Eng. 2014, 79, 153 – 159.

[142] Heijboer, J. Secondary loss peaks in glassy amorphous polymers. J. Polym. Mater. 1977,6: 11-37.

[143] Boyer RF. Dependence of mechanical properties on molecular motion in polymers. Polym. Eng. Sci. 1968; 8: 161.

[144] Raponi OA, Barbosa LCM, Souza BR, Junior ACA. Study of the influence of initiator content in the polymerization reaction of a thermoplastic liquid resin for advanced composite manufacturing. Adv Polym Technol. 2018;37:3579–3587.

[145] Oysaed H. Dynamic mechanical properties of multiphase acrylic systems. J. Biomed. Mater. Res. 1990: 24: 1037-1048.

[146] Pothan LA, Oommen, Z, Thomas, S. Dynamic mechanical analysis of banana fiber reinforced polyester composites. Compos. Sci. Technol., 2003, 63, 2, 283-293.

[147] Rana D, Mounach, H, Halary, JL. *et al.* J. Differences in mechanical behavior between alternating and random styrene-methyl methacrylate copolymers. Mater Sci 2005, 40, 943.